



12-2011

Improvements in Multi-tool Surveying Efficiency for Archaeological Geophysics

Caitlyn Marie Williams
cwilli94@utk.edu

Follow this and additional works at: https://trace.tennessee.edu/utk_gradthes



Part of the [Archaeological Anthropology Commons](#), [Geographic Information Sciences Commons](#), and the [Geophysics and Seismology Commons](#)

Recommended Citation

Williams, Caitlyn Marie, "Improvements in Multi-tool Surveying Efficiency for Archaeological Geophysics. " Master's Thesis, University of Tennessee, 2011.
https://trace.tennessee.edu/utk_gradthes/1106

This Thesis is brought to you for free and open access by the Graduate School at TRACE: Tennessee Research and Creative Exchange. It has been accepted for inclusion in Masters Theses by an authorized administrator of TRACE: Tennessee Research and Creative Exchange. For more information, please contact trace@utk.edu.

To the Graduate Council:

I am submitting herewith a thesis written by Caitlyn Marie Williams entitled "Improvements in Multi-tool Surveying Efficiency for Archaeological Geophysics." I have examined the final electronic copy of this thesis for form and content and recommend that it be accepted in partial fulfillment of the requirements for the degree of Master of Science, with a major in Geology.

Gregory S. Baker, Major Professor

We have read this thesis and recommend its acceptance:

Devon Burr, Josh Emery

Accepted for the Council:

Carolyn R. Hodges

Vice Provost and Dean of the Graduate School

(Original signatures are on file with official student records.)

Improvements in Multi-tool Surveying Efficiency for Archaeological Geophysics

A Thesis Presented for the Master's Degree
The University of Tennessee, Knoxville

Caitlyn Marie Williams
December 2011

Copyright © by Caitlyn Marie Williams

All rights reserved.

Dedication

This thesis is dedicated to my grandfather, Dr. John H. Olive PhD, who constantly reminded me that 'data' is plural and that all problems can be solved in twenty-five words or less.

And for Mr. Dennis Jordan, who helped to foster my love for geology.

Acknowledgements

Primarily, I want to thank my entire committee for providing support and encouragement throughout this entire process. I want to also thank Dr. Greg Baker for taking me on as a student and giving me a second chance to really show what I am capable of. The upshot is that he taught me to really be proud of my work and to never submit anything that was sub-par. I want to also thank Dr. Brad Ault for all of his help on the archaeological aspects of this project. He really could give Harrison Ford a run for his money in the role of Indiana Jones.

I also want to thank Frank Garrod, the WSBA Archaeological Society, and the Cypriot Department of Antiquities for hosting us while in Cyprus and for letting the team survey on their turf. Also thanks to the British Royal Air Force for the wonderful accommodations. I want to also thank my field assistants, Rachel Storniolo and Christian Hunkus for their invaluable operation of the GPR, as it became quickly apparent that I cannot walk in a straight line. I want to also thank Mr. Brown, without whom, the mornings would have been torture.

Finally I want to thank my family for all the love and support during this process. I really could not have finished without you!

Abstract

Conventional archaeological excavation methods are, by design, extremely invasive and result in study areas being irrevocably altered for the sake of research. For this reason, near-surface geophysical techniques have been incorporated into archaeological investigations to promote enhanced site integrity. The objectives of this research are twofold. The first objective is to perform the first geophysical survey at an active archaeological site in Cyprus and to demonstrate the geophysical techniques that worked well in the area. The second objective is to develop an improved data management workflow that allows for near real-time feedback to archaeologists while in the field and to test its viability at a control site in Knoxville, Tennessee.

The first objective has been accomplished by performing a geophysical survey using ground penetrating radar (GPR) and magnetic methods at an active archaeological site in Cyprus. Sites were chosen by an on-site archaeologist, and a total of fifty-two 10 m by 10 m grids were surveyed. Upon processing these data, magnetic methods produced better data, as many rectilinear structures were found in these data. As none of these data have yet been ground-truthed, due to the strict permitting rules, we base the success of this research on the fact that the structures found in the subsurface have similar dimensions and orientations to many surface features.

The second objective has been accomplished by first collecting GPR and magnetic data at a control site in Knoxville, Tennessee, where targets had previously been buried and their locations accurately recorded. Out of 24 objects, 15 were detected in these data. Images of the data were later imported into Google Earth, and error was calculated between the actual locations of the target versus the interpreted locations. This research was deemed a success as the error calculated was smaller than an average archaeologist's square used for excavation. This new

data management methodology was applied retroactively to the data collected in Cyprus in order to provide the consulting archaeologist with more accurate spatial positioning data to be used at a later date to aid in obtaining excavation permits for the site.

Table of Contents

Chapter

| | |
|---|----|
| 1. Introduction | 1 |
| 1.1 Motivation | 2 |
| 1.2 Objective | 3 |
| 1.3 Previous Investigations | 5 |
| 1.3.1 Viability of Geophysical Methods in Archaeology | 5 |
| 1.3.2 The Usage of Google Earth as a GIS Platform | 8 |
| 1.4 Hypotheses | 10 |
| 2. Geophysical Techniques | 11 |
| 2.1 Ground Penetrating Radar (GPR) | 12 |
| 2.2 Magnetic Gradiometry | 15 |
| 2.3 Differential Global Positioning System | 18 |
| 2.4 Data Processing | 18 |
| 2.5 Error | 19 |
| 2.5.1 Positioning Error | 19 |
| 2.5.2 Instrument Related Error | 22 |
| 3. A Multi-tool Geophysical Investigation of the Dreamer's Bay Ancient Roman Port, Akrotiri Peninsula, Cyprus | 24 |
| 3.1 Introduction | 26 |
| 3.1.1 Motivation | 26 |
| 3.1.2 Objective I | 27 |
| 3.1.3 Hypothesis I | 27 |
| 3.2 Geophysical Techniques | 27 |
| 3.2.1 GPR | 27 |
| 3.2.2 Magnetic Gradiometry | 28 |
| 3.3 Case Study – Akrotiri Peninsula, Cyprus | 29 |
| 3.3.1 Site Description | 29 |
| 3.3.1.1 Geographic Setting | 30 |
| 3.3.1.2 Archaeological History | 33 |
| 3.3.2 Data Acquisition | 35 |
| 3.3.2.1 Dreamer's Bay Site | 35 |
| 3.3.2.1.1 Magnetic Gradiometer | 37 |
| 3.3.2.1.2 GPR | 38 |
| 3.3.2.1.3 GPS | 39 |
| 3.3.2.2 St. Mark's | 39 |
| 3.3.2.2.1 Magnetic Gradiometer | 40 |
| 3.3.2.2.2 GPR | 40 |
| 3.3.2.2.3 GPS | 41 |

| | |
|--|----|
| 3.3.3 Data Processing | 41 |
| 3.3.3.1 Dreamer's Bay | 42 |
| 3.3.3.1.1 GPR Data | 42 |
| 3.3.3.1.2 Gradiometer Data | 43 |
| 3.3.3.1.3 GPS Data | 45 |
| 3.3.3.2 St. Mark's | 45 |
| 3.3.3.2.1 GPR Data | 45 |
| 3.3.3.2.2 Gradiometer Data | 46 |
| 3.3.3.2.3 GPS Data | 47 |
| 3.3.4 Results | 47 |
| 3.3.4.1 Dreamer's Bay | 50 |
| 3.3.4.1.1 GPR Data | 50 |
| 3.3.4.1.2 Gradiometry Data | 51 |
| 3.3.4.2 St. Mark's | 51 |
| 3.3.4.2.1 GPR Data | 51 |
| 3.3.4.2.2 Gradiometry Data | 51 |
| 3.4 Discussion | 61 |
| 4. Enhancing Usability of Near-Surface Geophysical Data in Archaeological Surveys via Google Earth | 66 |
| 4.1 Introduction | 69 |
| 4.1.1 Motivation | 69 |
| 4.1.2 Objective II | 71 |
| 4.1.3 Hypothesis II | 71 |
| 4.2 Test Study I – B4 Plot, Knoxville, Tennessee | 71 |
| 4.2.1 Site Background | 72 |
| 4.2.2 Methodology | 74 |
| 4.2.2.1 Geophysical Techniques | 74 |
| 4.2.2.2 Data Collection | 75 |
| 4.2.2.3 Data Processing | 76 |
| 4.2.3 Geophysical Results | 76 |
| 4.2.3.1 GPR | 77 |
| 4.2.3.2 Gradiometry | 77 |
| 4.3 Incorporating Google Earth with Near Surface Geophysical Data | 77 |
| 4.3.1 GPR Data | 82 |
| 4.3.2 Gradiometer Data | 83 |
| 4.4 Test Study II – Akrotiri Peninsula, Cyprus | 86 |
| 4.4.1 Importing Cyprus Data to Google Earth | 86 |
| 4.4.1.1 Dreamer's Bay | 87 |
| 4.4.1.1.1 Magnetic Data | 87 |
| 4.4.1.1.2 GPR Results | 87 |
| 4.4.1.2 St. Mark's | 94 |
| 4.4.1.2.1 Magnetic Data | 94 |
| 4.4.1.2.2 GPR Data | 94 |
| 4.4.1.3 Geoarchaeological Maps | 94 |

| | |
|--------------------|-----|
| 4.5 Discussion | 103 |
| 5. Conclusions | 108 |
| List of References | 111 |
| Appendix A | 115 |
| Vita | 120 |

List of Figures

| | |
|---|----|
| Figure 1.1. Map of the island of Cyprus with a placemark indicating the location of the Akrotiri Peninsula..... | 4 |
| Figure 2.1. Cross section of a typical reflection ray path from the transmitter to the receiver (modified after Baker et al., 2007), where Φ_1 is the critical angle and ϵ_1 and ϵ_2 are different permittivity values for the material..... | 13 |
| Figure 2.2. A photo of the Pulse EKKO Pro Smart Cart System being used in the field..... | 14 |
| Figure 2.3. a) Shows the magnetic field created by a bar magnet. By replacing the image of the magnet with a globe (b), a diagram is created which demonstrates the magnetic field of the Earth..... | 15 |
| Figure 2.4. A photo of the Bartington Grad 601-2 being used in the field. Sensors located at the top and bottom of each arm of the instrument measure the magnetic field and the gradient is calculated as the difference between the two measurements..... | 18 |
| Figure 2.5. Schematic representation of in-line and cross-line error relative to the instrument survey direction, shown with dashed lines. The red line indicated the in-line error in the Y-direction, while the purple line indicates the cross-line error in the X-direction. Note that figure is not to scale..... | 21 |
| Figure 3.1. a) Google Earth image of the island of Cyprus with the area of interest located in the white rectangle. b) The location of the modern cities of Akrotiri and Kourion in relation to the sites at St. Mark's and Dreamer's Bay. The city of Kourion has been made famous by the spectacular archaeological remains discovered there..... | 31 |
| Figure 3.2. Artist's rendition of what the Akrotiri Peninsula might have looked like during the Roman period (4 th to 7 th century CE)..... | 32 |
| Figure 3.3. Photo of previously mapped warehouse structures at Dreamer's Bay..... | 34 |
| Figure 3.4. Photo inside the alleged catacombs located at the St. Mark's site..... | 34 |
| Figure 3.5. Schematic of the survey area showing the survey area geometry and the number of each grid as assigned by the Bartington 601-2..... | 36 |

| | |
|--|----|
| Figure 3.6. Survey design for the Bartington 601-2 with the solid bars representing the width of the instrument and the gray circles representing the operator. The dashed lines show the path of each sensor on either side of the instrument while the solid lines show the path walked by the operator. The first transect is walked 0.5 m from the origin in the X-direction. The subsequent transect is walked with 0.5 m spacing from the first. All remaining transects have 2.0 m spacing..... | 37 |
| Figure 3.7. Schematic of the survey area at St. Mark's. Grid numbers were assigned automatically with the Bartington Grad 601-2..... | 40 |
| Figure 3.8. Figure illustrating the error inherent in the data collected in Cyprus in 2010. The red line indicates in-line error, the purple line indicates the cross-line error, and the black, dashed rectangle represents the total error of any given point in the survey. Blue diagonal lines represent subsurface, linear features. As transects were run at a 45° angle to the anticipated orientation of features, we can calculate the error in the survey..... | 49 |
| Figure 3.9. a) Uninterpreted GPR data for the northern portion of Dreamer's Bay. Data were collected with the 100 MHz antenna with 8 transects running in an east-west direction. b) Uninterpreted GPR data collected with the 100 MHz antenna in the southern portion of the site at Dreamer's Bay. Transects were run in a north-south direction..... | 53 |
| Feature 3.10. The solid black lines in these photos are interpreted linear features. The black polygons with the cross-hatching are wider features. a) GPR data for the northern portion of Dreamer's Bay. Data was collected with the 100 MHz antenna with eight transects running in an east-west direction. Linear features representing possible subsurface building remains are highlighted in black. b) GPR data collected with the 100 MHz antenna in the southern portion of the site at Dreamer's Bay. Transects were run in a north-south direction. Linear features are highlighted in black..... | 54 |
| Figure 3.11. a) Uninterpreted magnetic data collected at Dreamer's Bay in the northern portion of the survey area. b) Uninterpreted magnetic data collected at Dreamer's Bay in the southern portion of the survey area..... | 55 |
| Figure 3.12. The solid red lines are interpreted linear features. a) Magnetic data collected at Dreamer's Bay in the northern portion of the survey area. Linear features located in the subsurface are highlighted in the data. The strong dipoles located on the northeastern portion of the data are the result of historic metal debris as this location was used for the British Air Force during World War II. b) Magnetic data collected at Dreamer's Bay in the southern portion of the survey area. A possible structure is highlighted in the data. This site lies directly south of a known warehouse at the surface..... | 56 |
| Figure 3.13. a) Uninterpreted GPR data collected with the 100 MHz antenna at St. Mark's in the northern portion of the survey area. b) Uninterpreted GPR data collected with the 100 MHz antenna in the southern portion of the survey area at St. Mark's..... | 57 |

| | |
|---|----|
| Figure 3.14. Black lines are interpreted linear features, while the circles indicate a distinct target. a) GPR data collected with the 100 MHz antenna at St. Mark's in the northern portion of the survey area. Linear features shown in the data are interpreted to be the remains of religious buildings. b) GPR data collected with the 100 MHz antenna in the southern portion of the survey area at St. Mark's. The fatter lines indicate where two linear features have been interpreted to be very close together. This was done arbitrarily to enhance the aesthetics of the data. Linear features in the data are again interpreted to be more ecclesiastical structures..... | 58 |
| Figure 3.15. a) Uninterpreted magnetic gradiometry data collected at St. Mark's in the northern portion of the survey area. b) Uninterpreted gradiometer data collected in the southern portion of the St. Mark's survey area..... | 59 |
| Figure 3.16. Solid red lines are interpreted linear features, while the dashed red lines are the locations of assumed features. Red circles indicate discrete targets. a) Magnetic gradiometry data collected at St. Mark's in the northern portion of the survey area. Linear features in the data are likely building remnants in the subsurface. b) Gradiometer data collected in the southern portion of the St. Mark's survey area. Again, structural remains are highlighted in the data..... | 60 |
| Figure 4.1. Diagram showing the conventional workflow for geophysical data acquisition at an archaeological site. The disconnect in geoarchaeological surveying often occurs with the last three steps of the workflow; commonly a long time lapse in completing the final two steps makes data less effective..... | 70 |
| Figure 4.2. a) Google Earth image showing the location of the B4 Plot in relation to the University of Tennessee main campus in Knoxville, Tennessee. b) Photo taken of the B4 Plot, looking to the south. The fenced-in hydrogeology station can be seen on the right-hand side of this photograph..... | 73 |
| Figure 4.3. Image of the survey geometry for GPR data collection at the B4 Plot. Note the zig-zag pattern in which the data were collected and the shorter transects run around the fenced-in area..... | 75 |
| Figure 4.4. Images of the GPR data collected at the B4 Plot. a) Uninterpreted GPR data. The two horizontal lines in the center of the data image are attributed to problems with the transmitting antenna. The dark blue rectangle is representative of the fenced-in area where no data were collected. b) Targets are circled in yellow on the interpreted data..... | 78 |
| Figure 4.5. Image of the magnetic data collected at the B4 Plot. a) The uninterpreted magnetic data. b) Possible targets are circled in yellow. The green rectangle in the lower left of the photo is the location of the fenced-in area where no data were collected..... | 79 |
| Figure 4.6. Placemarks added to the Google Earth satellite image delineating the survey boundary at the B4 Plot..... | 80 |

| | |
|--|----|
| Figure 4.7. Georeferenced image of GPR data displayed in Google Earth. Targets are identified by white placemarks. Distance was measured between these and the actual location of targets and then error was calculated..... | 84 |
| Figure 4.8. Georeferenced image of magnetic data collected at the B4 Plot and displayed in Google Earth. Yellow placemarks indicate the location of possible targets..... | 85 |
| Figure 4.9. Magnetic gradiometry data for the site at Dreamer’s Bay. Black and white dipoles that show up in the data were interpreted to be metallic debris at the surface from historic military operations. The features of interest are the light gray linear features seen in the southeast portions of the data. Each small square represents a minor grid and is 10 m by 10 m..... | 89 |
| Figure 4.10. Magnetic data from Dreamer’s Bay with features highlighted using the path tool in Google Earth. The solid red lines are interpreted linear features. Each small square represents a minor grid and is 10 m by 10 m..... | 90 |
| Figure 4.11. Uninterpreted GPR data collected at Dreamer’s Bay with the 100 MHz antenna. Data were accurately georeferenced in Google Earth using GPS data collected at the site..... | 91 |
| Figure 4.12. Interpreted GPR data collected with the 100 MHz antenna at Dreamer’s Bay. Linear features are highlighted using the path tool in Google Earth. Black lines indicate interpreted linear features. GPR data show fewer features than the magnetic data as the survey area was smaller and depth of penetration was poor..... | 92 |
| Figure 4.13. Google Earth image displaying the geometry of features found in both data sets. Transparency of the GPR data was set to 40% in order to be able to see both sets of data. All features seen in the data are interpreted to be real, however, we can hypothesize that features detected by the magnetometer are walls while those detected by the GPR are trenches..... | 93 |
| Figure 4.14. Uninterpreted magnetic gradiometry data collected at St. Mark’s. Data were accurately georeferenced using GPR coordinates taken after surveying. Features are interpreted to be the light grey lines which appear in the data. Each square represents a minor grid and is 10 m by 10 m..... | 96 |
| Figure 4.15. Interpreted magnetic data collected at St. Mark’s. Interpretations were added with both the path and the placemark tool. The solid red lines indicate linear, subsurface features and the dashed red lines are more subtle features. Linear subsurface features appear in the data as lighter grey areas, and are interpreted to be the remnants of buildings. Each square represents a minor grid and is 10 m by 10 m..... | 97 |
| Figure 4.16. GPR data collected with the 100 MHz antenna at St. Mark’s. Maximum depth of penetration was 1.5 m..... | 98 |

| | |
|--|-----|
| Figure 4.17. Interpreted GPR data for St. Mark's shows fewer subsurface features than the magnetic data. Black lines are interpreted linear features in the subsurface. Thicker lines indicate two linear features which were located very close together. Black circles encompass potential features which are not linear. Depth to features ranges from 0.75 m to 1.0 m..... | 99 |
| Figure 4.18. Google Earth image displaying the geometry of features found in both data sets. Transparency of the GPR data was set to 40% in order to be able to see both sets of data. All features seen in the data are interpreted to be real, however, we can hypothesize that features detected by the magnetometer are walls while those detected by the GPR are trenches..... | 100 |
| Figure 4.19. Map of Dreamer's Bay with subsurface features appearing on the surface. This map is useful to archaeologists in order to develop excavation plans..... | 101 |
| Figure 4.20. Map of subsurface features at St. Mark's. This map provides spatial data about features to archaeologists and aids in excavation plans..... | 102 |
| Figure 4.21. Diagram showing the new data management workflow developed at the B4 Plot in Tennessee. The first six steps of the workflow remain unchanged, as the focus of this research was expediting data processing and interpretation. Changes were made to the final steps of the workflow in order to provide archaeologists with a more useful final product..... | 104 |
| Figure A-1. Additional GPR data collected at Dreamer's Bay with the 200 MHz antenna. The depth of this slice is from 0.100 to 0.225 m. Velocity was calculated to be 0.060 m/ns and the slicing interval was 0.1515 m. The dark red, linear feature in the northern part of these data is a man-made historic rail that was used to wheel artillery onto a cement pad during World War II..... | 116 |
| Figure A-2. GPR data collected at Dreamer's Bay with the 100 MHz antenna in the northern part of the survey area. This data slice represents a depth from 0.250 to 0.500 m. The picked velocity was 0.07 m/ns and the slice interval was 0.200 m. No discernable features were interpreted in this data set..... | 117 |
| Figure A-3. GPR data collected with the 200 MHz antenna in the northern portion of St. Mark's. This slice represents a depth of 2.600 to 2.700 m. Velocity was calculated to be 0.150 m/ns and the slice interval was set to 0.100 m for the maximum resolution. No features were able to be interpreted in these data..... | 118 |
| Figure A-4. GPR data collected with the 200 MHz antenna in the southern portion of the survey area in St. Mark's. The depth slice for these data is from 0.630 to 0.730 m. The picked velocity for these data was 0.300 m/ns and the depth slice interval was 0.1449 m..... | 119 |

List of Tables

| | |
|--|----|
| Table 2.1. Table describing the different types of error applicable when using the GPR..... | 23 |
| Table 2.2. Table describing the different types of error applicable with using the magnetic gradiometer..... | 23 |
| Table 3.1. Velocities and depth slice picks for data are shown for each survey location at Dreamer's Bay..... | 43 |
| Table 3.2. Picked velocity and depth slices for GPR data collected at St. Mark's..... | 46 |
| Table 3.3. Criteria for geophysical interpretation. All interpretations made had to have at least two of these attributes..... | 48 |

1. Introduction

Specimen destruction is a negative by-product of most scientific research. In particular, archaeology is one field of science where an entire site may be compromised for the sake of research. Traditional archaeological excavation methods involve trowels, shovels, and on occasion, heavy machinery (e.g., Wynn, 1986), and while the artifacts may or may not be damaged, the surrounding soil is disturbed, compromising site context integrity. Thus, many modern archaeologists incorporate near-surface geophysical surveys in their research as a non-invasive tool for locating subsurface archaeological features with minimal compromising of site integrity (e.g. Baker and Ambrose, 2007 and Hesse, 1999).

1.1 Motivation

One drawback to using near-surface geophysics is that it is rarely a smooth process and can utilize significant resources (e.g. funds and field personnel). Generally, once a site of interest has been identified by archaeologists, a geophysicist will be called on-site to execute a geophysical survey. Data acquisition can take anywhere from a few hours to a few weeks depending on the size of the site, desired resolution, and how many methods are used. Once data are collected they must be uploaded onto a computer, run through processing software, and then displayed in such a way that the data can be easily interpreted and used by archaeologists. It is in this step that there is disconnect between the geophysicist and the archaeologist. The geophysicist is traditionally concerned with the survey design and the geophysical data collected while the archaeologist plans to use the data to develop excavation plans. Data need to be in a format where they are immediately applicable and useful to both fields.

Within the last decade there has been little change in archaeogeophysics (the field of applying geophysics to archaeological studies, except with respect to improvements in

instrumentation. There have been studies that outline ways to expedite geophysical surveys.; however, researchers have mainly focused on streamlining data collection in multi-parametric surveys (Hesse, 1999) and the quantitative integration of the data (Piro et al., 2000). Despite the attempts to simplify the process, there remain three primary problems with archaeogeophysical investigations: 1) limitations imposed by time and funding, 2) difficulty displaying data in a usable format, and 3) bridging the gap between geophysical data and archaeological usability.

1.2 Objectives

The objectives of this project are to 1) perform the first geophysical survey at an active archaeological site in Cyprus and to assess the geophysical techniques that work well in this area (we will refer to this as Objective I) and 2) to develop an improved data management workflow that will allow for near real-time data interpretation and to test the workflow's effectiveness at a control site (Objective II). To accomplish these tasks, data have been collected at an archaeological site on the island of Cyprus (Figure 1.1) using two separate geophysical techniques, and a workflow has been developed based on that experience for efficient usage of the data that that was later tested at a control site in Knoxville, Tennessee. Six different aspects of geoarchaeological surveying were taken into account during the creation of the workflow: data acquisition, processing, interpretation, display, sharing, and the application of results in the field.

Data acquisition encompasses the delineation of the survey area as well as the literal collecting of geophysical data. In this case, data were collected using two separate geophysical techniques: ground penetrating radar (GPR), and magnetic gradiometry (discussed in Chapter 2).



Figure 1.1. Map of the island of Cyprus with a placemark indicating the location of the Akrotiri Peninsula.

Data processing involves downloading raw data from equipment and manipulating them using various software packages so that they can be used. Once processing occurs, data are interpreted and displayed in a way that allows for subsurface features to be identified and highlighted. When working on a multi-disciplinary project, an important aspect is the ability to quickly share data with many different users having different budgets, knowledge bases and computer equipment.

Data integration with some form of geographic information system (GIS) software is required for the display and sharing of data that is cheap (or free), widely available, and easy to use. All of this work culminates in the practical application of data, which is the most important of the six pieces of the workflow, as data prove to be useless unless they can be successfully applied by the archaeologist to the problem at hand.

1.3 Previous Investigations

1.3.1 Viability of Geophysical Methods in Archaeology

A variety of studies have been conducted that utilize near-surface geophysics for archaeological purposes (e.g. Sternberg and McGill, 1995; Karastathis et al., 2001). Most often, surveys are conducted in areas where there are known archaeological artifacts, and the geophysical surveys are performed to supplement information already known about the site or highlight the extent of artifacts. A number of successful studies have been conducted that utilize GPR, magnetics, or a combination of the two. The geophysical data have been subsequently ground truthed in many surveys, which further proves the usefulness of these techniques in the field. While geophysical techniques are versatile in their range of applications, for archaeology

they are most commonly used for the discovery of relatively large artifacts or structures. For example, a study done by Yalciner and others (2009) was looking specifically for remains of buildings at the site of Nysa in western Turkey. Past excavations in the area had revealed a number of major ancient buildings which had been identified by archaeologists as theatres, amphitheatres, a library and a number of shops. The geophysical method of choice was GPR due to its ease of use and portability. A total of 22 GPR profiles were collected using 250 and 500 MHz antennae. Processing of the data revealed the existence of buried walls approximately 50 m west of what archaeologists believed to be a city boundary. Excavations were later done that confirmed the results obtained from the GPR.

As another example, a more recent study done by Sandweiss and others (2010) was aimed at using GPR to provide some insight on a structure at a site named Los Morteros located along the coast of northern Peru. The site consists of an elliptical mound approximately 225 m by 200 m, and 14.5 m tall at its highest point. What had previously been thought to be a sand-draped, bedrock-cored landform by researchers was thought by some archaeologists to be a man-made feature. GPR was used to examine the mound's interior structure (Grasmueck et al., 2004). The technique also allowed for rapid data collection in challenging terrain. Four radar profiles were collected using the lower frequency 100 MHz antenna in order to maximize penetration. Results from the geophysical survey support the interpretation of the structure as man-made and not a naturally occurring feature as previously suspected as the internal stratigraphy does not support the interpretation of the feature as a large, relict dune.

Numerous studies have also been conducted using magnetics as a tool for archaeological prospecting. One such study was done by Odah and others (2005) to locate buried remains near the Zoser pyramid in Giza, Egypt. They used a magnetic gradiometer to detect ancient remains

of structures built of mud-brick near the pyramid. A fluxgate gradiometer was used because it had been successfully used in the past by other researchers at sites in Egypt to locate buried mud-brick features. A survey area of 100 m by 100 m was broken down into 50 grids and each was surveyed with the gradiometer. Using this method, they were able to locate many interconnected tomb structures near the pyramid. The study was deemed a success and researchers were able to confirm the efficiency of magnetic surveying methods at archaeological sites.

Another similar survey was conducted by Abdallatif and others (2010) at a different location in Giza, Egypt. Again, a fluxgate magnetic gradiometer was used to locate four mud-brick structures associated with the nearby Pyramid of Amenemhat II. The survey area was 340 m by 200 m. It was broken down into smaller 20 m by 20 m grids for ease of surveying. As this was the first geophysical survey done in this area, researchers did not know what to expect as far as results, but the gradiometer was chosen as it had previous success working in arid environments. After the completion of the survey, excavation of the area was able to confirm the presence of building remains located with the gradiometer.

Sometimes it is beneficial to combine geophysical surveying techniques, especially when conditions at a site are unknown. An example of this benefit is highlighted by the work done by Chianese and others (2010) when they conducted a survey using both GPR and magnetic methods at a site in southern Italy. The main objective of their research was to identify buried structures at the Rossano di Vaglio ancient sanctuary in the Basilicata Region in Southern Italy. From both GPR and magnetic data, geophysicists were able to provide archaeologists with information about the boundaries of the site and subsequently compare geophysical data to archaeological data once the site was excavated.

Another example would be the work done by Kamei and others (2002) at the Kharga Oasis in Egypt. They integrated GPR and magnetic surveying to look for artifacts and extensions of structures that had previously been mapped. Survey area for the GPR was 40 m by 80 m and the survey was completed with the 400 MHz antenna for the best resolution. For the magnetic surveys, two different magnetometers were used on an area 20 m by 40 m. As a whole, the study was considered a success as scientists were able to efficiently integrate data from all three instruments to obtain results.

1.3.2 The Usage of Google Earth as a GIS Platform

Google Earth was released in June 2005, and since then has attracted many scientific users due to its ability to view landscapes in fairly realistic three dimensions. Not only is it an easy program for the everyday user, but advantages soon become apparent for its use in the scientific community. Experts can communicate science via this new platform and make it relevant and engaging to the general public (Sheppard and Cizek, 2009). One way that Google Earth makes data more engaging is the fact that it uses the Earth itself as an organization system for digital information (Butler, 2006). This type of program, once envisioned by Vice President of the United States, Al Gore, is called a virtual globe and is defined as a computer program allowing users to browse and search data projected on a cartographic representation of the Earth in various scales and projections (De Paor and Whitmeyer, 2011).

Aerial photography and satellite imagery are well established tools for archaeological site prospection, but data can be difficult to manipulate and expensive to acquire. Google Earth provides much of these data for free. Other benefits include the fact that: a) specialist GIS software is not required, b) data are pre-processed and georeferenced, and c) images are updated by Google, Inc. as soon as new data become available, typically twice a month (Beck, 2006).

Google Earth constructs a picture of the surface of the planet by downloading satellite data from a remote server (Lisle, 2006) and it is on this background that any genre of data can be plotted. Google Earth has applications for many types of sciences, from the earth sciences to the life sciences. In the earth sciences, it has been used for research in geochemistry, geophysics, mapping, and in geoscience education programs.

Google Earth uses a programming language called Keyhole Markup Language (KML), and while using Google Earth does not require a working knowledge of KML, it is a versatile programming language that enables the user to customize their Google Earth experience. Essentially, KML is a human-readable language composed of text and punctuation that can be created in any basic text editor and then saved and viewed in Google Earth. It is a 3D system that incorporates latitude, longitude, and altitude as opposed to x, y, and z coordinates. KML is widely supported by a variety of applications including NASA WorldWind, ESRI ArcGIS Explorer, Google Earth, Google Maps, and many other similar GIS-type programs (Wernecke, 2009). Thus, a file created in Google Earth can be viewed by a variety of other platforms which makes it a user-friendly and easily transferable way to display data.

A study done by Wright and others (2009) shows how Google Earth can be used to visualize changes through time. Specifically they were looking at visualizing the evolution of volcanic gas plumes. Using small, inexpensive ultraviolet spectrometers deployed in an automated network on Mt. Etna in Sicily, they measured volcanic sulfur dioxide (SO₂) changes at high frequency. The volcano is well-suited to these types of experiments as it continuously emits SO₂, during both quiescent and eruptive periods. Data were collected from a network of five scanning spectrometers positioned around the volcano. A 2D rendering of the gas plume was made based on measurements taken by two networks at a time. The 2D images were

imported into Google Earth to create a 3D snapshot of the image. Displaying a series of 3D plume reconstructions in quick succession allows for an animated time evolution of plume movement. These short clips can be used with other data to hypothesize about the plume's trajectory and thus create a possible warning system for those that live on the flanks of the volcano.

It is also possible to display some geophysical models in a virtual globe by using different coding languages. In a study done by De Paor and Whitmeyer (2011), geologic maps were turned into super-overlays and georeferenced onto Google Earth. A super-overlay is a collection of ground overlays that cover an entire region and are maintained in a special hierarchy that facilitates efficient processing (Wernecke, 2009). The authors investigated how to make applicable geologic icons as well as control data clutter and reveal pertinent data in layers. While the focus of this study was surface geologic data, they did briefly investigate how to integrate subsurface data, specifically 3D geophysical “beach balls” to represent earthquake focal mechanisms. De Paor and Whitmeyer (2011) did not address the idea of displaying planar subsurface data (e.g. a map of the subsurface) in Google Earth or how to glean additional data from those already presented.

1.4 Hypotheses

Hypothesis I is that near-surface geophysics can be used successfully to locate previously unmapped subsurface features at archaeological sites in Cyprus. Hypothesis II is that the effectiveness and efficiency of multi-tool, near-surface geophysical surveys for archaeological applications can be improved by displaying data with accurate GPS coordinates using a virtual globe.

2. Geophysical Techniques

2.1 Ground Penetrating Radar (GPR)

Ground penetrating radar (GPR) utilizes propagating electromagnetic (EM) waves to detect boundaries over which changes in dielectric properties of the shallow sub-surface exist. Propagation velocity of EM waves is determined by the dielectric permittivity contrasts between the background material and target. Dielectric permittivity dictates the ability of a material to store and then transmit EM energy when an electromagnetic field is imposed on the material (Baker et al., 2007).

Generally, a GPR unit consists of a transmitting and receiving antenna. Minimum antenna separation is dictated by antenna length. If spacing between antennae is too small, receiver electronics may be overloaded by the transmitting signal, resulting in data loss. In this investigation a 100 MHz antenna and a 200 MHz antenna were used and length of each antenna was 1.0 m and 0.5 m, respectively.

Transmitting antennae radiate an EM pulse that propagates into the subsurface, and subsequently scatters off interfaces or point sources. Both types of scattering are caused by a contrast in dielectric permittivity. Reflected/scattered energy that travels back to the surface is collected by the receiving antenna, and is recorded in terms of the amplitude of returned energy through time. The amount of time it takes for this wave to travel to an interface and back to the surface is called travel time, and is used to calculate propagation velocity and subsequently depth within the material. The attenuation of the propagating wave is dependent on the magnetic permeability and the electrical conductivity of the material. Magnetic permeability is defined as the ability of the material to become magnetized when an EM field is imposed on the material (Baker et al., 2007), while electrical conductivity is a measure of the movement of charge carriers in response to an applied electric field (Knight, 2005). Higher magnetic permeability of

a material will increase signal attenuation during propagation, and thus produce poorer quality data while reducing the penetration depth. Materials with high electrical conductivity also generally attenuate EM signals and will produce poor GPR data and/or shallow depth of penetration (Baker et al., 2007).

A generalized ray path shown in Figure 2.1 illustrates a ray travelling to an interface and subsequently reflecting back to the surface at the incident angle, Φ_1 . A wave traveling through the subsurface will encounter a boundary or objects with different electromagnetic properties than the surrounding material (i.e., wet versus dry sand, or for archaeological purposes a stone wall versus surrounding sediment). The part of the wave that interacts with the object will change direction by scattering. The type of scattering expected in most types of surveys is spectral reflection scattering. Spectral scattering is based on the law of reflection, where the angle of incidence is equal to the

angle of reflection (Baker et al., 2007). Some energy will not reflect at the interface and instead refracts through the interface to an underlying layer. The refracted energy will continue downward until it encounters another interface with different EM properties. At this interface, some energy will again be scattered while some will be transmitted through the interface. This pattern continues until the signal has been completely attenuated.

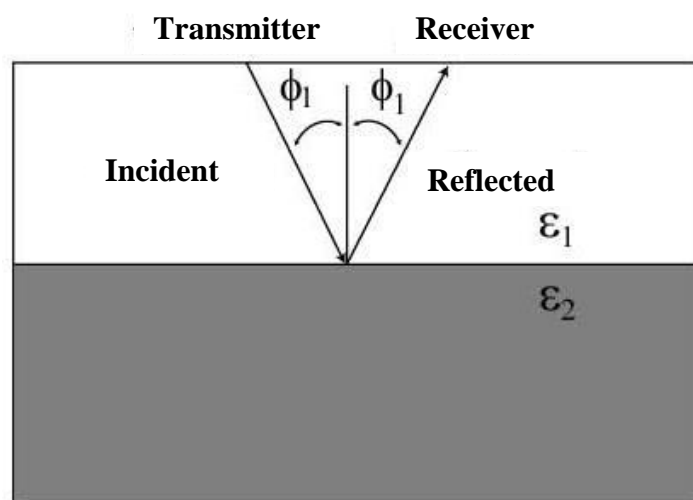


Figure 2.1. Cross section of a typical reflection ray path from the transmitter to the receiver (Modified from Baker et al., 2007), where Φ_1 is the critical angle and ϵ_1 and ϵ_2 are different permittivity values for the material.

The GPR data are presented with a color scheme that relates to the GPR signal amplitude. The numbers range from + or – 50,000 microvolts, but are divided by 1.56 and rectified to save them in a range of 0 to 32767 (Greg Johnston, pers. comm.) as the dynamic range of the instrument is based on a 16-bit system. The scale bar shown on each data set therefore range from 0 to 32767 with corresponding colors, such that the hot colors are closer to the high value and the cool colors are closer to the low value. GPR scale bars are consistent in these values throughout this manuscript.

For this study, a Sensors & Software Pulse EKKO Pro Smart Cart GPR system was used for all data collection (Figure 2.2). The Pulse EKKO Pro is a versatile unit that can be used with several antenna sizes for a variety of applications. The system uses an odometer

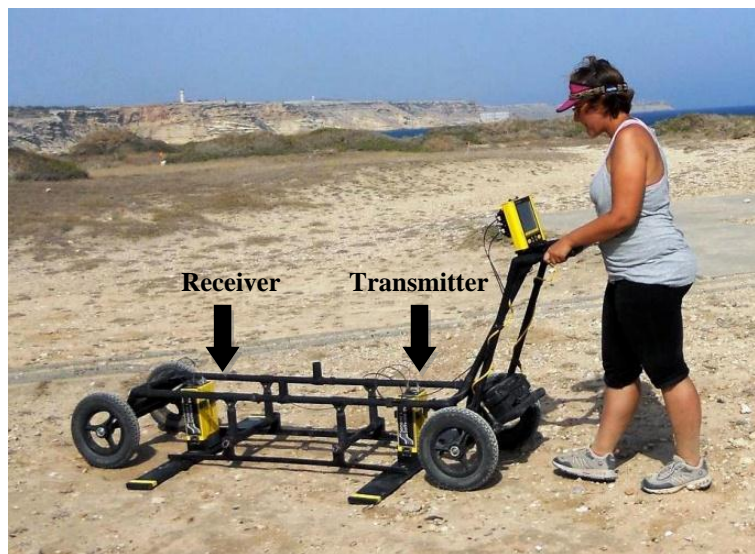


Figure 2.2. A photo of the Pulse EKKO Pro Smart Cart System being used in the field.

wheel which triggers the GPR system to take a data sample at regular intervals along the profiles. By using the odometer wheel, data samples are collected properly, even if the cart speed isn't constant, and when the cart stops, data acquisition stops. This particular system was chosen because it is available from the University of Tennessee Near-Surface Geophysics Lab (Dr. Gregory S. Baker, director), and all field personnel were familiar with its operation procedures.

2.2 Magnetic Gradiometry

The goal of magnetic surveys is to investigate subsurface geology using small anomalies in the total Earth's magnetic field resulting from magnetic properties of rock and soil. These investigations can range from small-scale near-surface geophysical surveys to large-scale regional mapping.

A magnetic flux is developed around a bar magnet and flows from one end of the magnet to the other. Points where the flux converges are known as the poles (Kearey, 2002). Earth's magnetic field resembles that of a large bar magnet near its center (Figure 2.3ab) and is generated by electric currents passing through the liquid outer core and the motions of the liquid metal. The direction of the field is vertical at the magnetic north and south poles, and horizontal at the magnetic equator. Magnetic surveying generally relies on the concept of induced magnetism, which is the idea that all materials generate a secondary magnetic field when

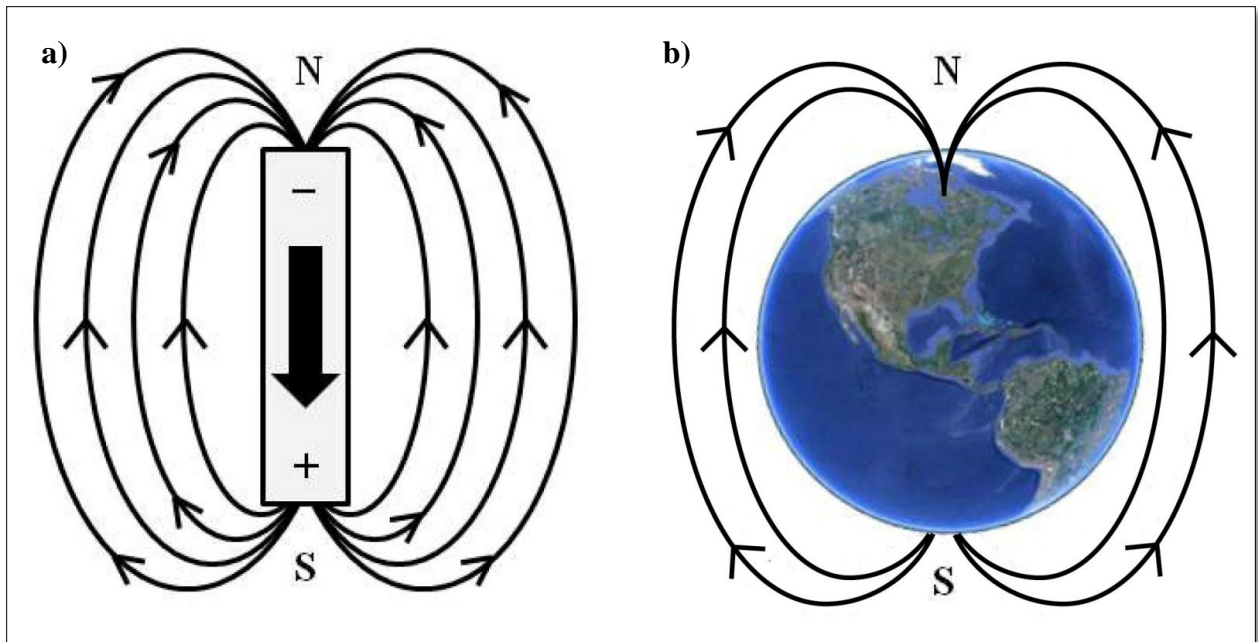


Figure 2.3. a) Shows the magnetic field created by a bar magnet. By replacing the image of the magnet with a globe (b), a diagram is created which demonstrates the magnetic field of the earth.

exposed to a strong primary magnetic field (e.g. Earth's magnetic field). Portable magnetometers identify and describe spatial changes in the Earth's total field. Specifically, magnetometers measure the sum of Earth's magnetic field (considered the primary field) plus the induced field (secondary field) of the surrounding materials (Ambrose, 2005).

Magnetic measurements are useful for geophysical surveys in that they are relatively simple, rapid, and totally noninvasive (Hansen, 2005), which is why they are often used in geoarchaeological studies. Many different types of magnetometers can be used in surveys (e.g. fluxgate gradiometer, proton precession magnetometers, cesium vapor magnetometers), and for the purposes of this study a fluxgate magnetic gradiometer was used.

Fluxgate magnetometers were developed during the Second World War to detect submarines (Reynolds, 1997). They use a core sensor made of a highly permeable ferromagnetic material held in the vertical direction to measure vertical intensity with an effective sensitivity on the order of several gammas, which is the unit of measure for the magnetic field (Breiner, 1999).

Gradiometers measure the gradient of the total field as it changes between two identical magnetometer sensors separated by a small fixed distance. More precisely, a gradiometer is defined as a differential magnetometer where the spacing between sensors is fixed and small with respect to the distance to sources whose gradients are to be measured (Breiner, 1999).

A main advantage of gradiometers is that because they take differential measurements, typically no correction for diurnal variation or solar activity is necessary, as any changes will affect both sensors in the same way. As the gradiometer is used with sensors oriented in the vertical direction, noise effects from large-scale features are suppressed and discrete anomalies show up more prominently. Separation distance between sensors is dependent on target depth, magnetometer strength and the size of the instrument. However, the best survey results are

obtained with the sensors approximately 20 cm from the ground. On average, this height will produce the highest sensitivity to buried features while simultaneously minimizing surface noise (Bartington, 2009).

During archaeological investigations, man-made anomalies are generally the expected targets in a survey. These anomalies fall into three different categories: ferrous materials, current-carrying conductors, and disturbances of the natural environment. Ferrous materials are any sort of man-made object that is created from iron, such as tools or weapons. Artifacts made from iron have the ability to maintain a magnetic field that has been imposed on the object. Current-carrying conductors are any sort of metallic object not made of iron. These non-ferrous items are still affected by an induced magnetic field, but cannot maintain the field like an iron object. Disturbances constitute the weakest, but most interesting of the man-made effects when seen in the data (Breiner, 1999). Disturbances in the natural environment encompass features like fire hearths or post-holes where the earth has been disturbed by digging or burning.

Each feature has its own magnetic characteristics, and these cause disturbances in the Earth's magnetic field around the object (Bartington, 2009). For example, digging a pit will destroy the bulk remnant magnetization in soil (typically uniform in direction) by randomizing the orientation of the grains. Remains of buildings will also show up, as the building material will have a remnant magnetization different than that of the surrounding material (Hansen, 2005).

For the purpose of this study, a Bartington Grad 601-2 Magnetic Gradiometer was used for data collection (Figure 2.4). The instrument is made up of two cylindrical fluxgate gradiometers, a data logger, and a battery cassette. A specialized carrying harness is used to aid the operation in holding the instrument during surveying. As the instrument has four

magnetometers (and can thus collect two gradients simultaneously) it can record two lines of data during each traverse. This set-up reduces survey time and distance walked. Since one is not owned by the University of Tennessee Near-Surface Geophysics Lab, a gradiometer was rented directly from Bartington, Inc. This particular gradiometer was chosen due to its portability, ease of use in the field, and because field personnel were familiar with its operation.

2.3 Differential Global Positioning System (dGPS)

For accurate GPS coordinates, a real-time differential GPS unit was used. A Trimble Ranger was the specific model used since one is owned by the University of Tennessee Near-Surface Geophysics Lab. The Trimble Ranger has a reputation for being a very rugged piece of equipment which can be used in a variety of terrains and climates. The Trimble Ranger has an accuracy of two to four meters, before the differential correction is applied, once corrected the accuracy is ± 5 cm horizontal and ± 15 cm vertical. Typically, GPS coordinates are collected after a survey has been completed, but before the survey area markers are removed.

2.4 Data Processing

Data from each instrument are processed using specific, proprietary software. The GPR data are processed using two different software packages, GFP Edit and EKKO Mapper 3, both

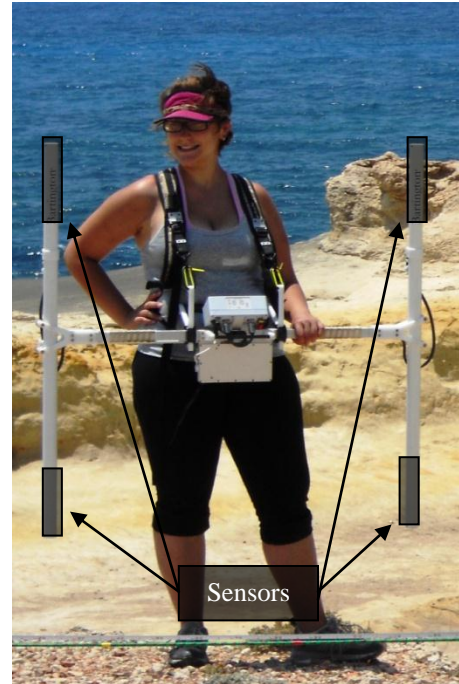


Figure 2.4. A photo of the Bartington Grad 601-2 being used in the field. Sensors located at the top and bottom of each arm of the instrument measure the magnetic field and the gradient is calculated as the difference between the two measurements.

created by Sensors and Software Inc., for their GPR units. GFP Edit enables graphical viewing of survey lines and allows for them to be edited to the survey parameter. This software is mainly used to calibrate transect length and spacing as well as switch transect direction to express the bi-directional nature of an alternating survey pattern. EKKO Mapper 3 uses the data created in GFP Edit to create a pseudo 3D map of the subsurface and generates depth slice images of features.

ArcheoSurveyor is a program created by DW Consulting specifically designed to assemble, process and visualize 2D archaeological data gathered with a variety of geophysical instruments, including the Bartington 601-2 Dual Magnetic Gradiometer. The program downloads data as individual grids and then allows the user to configure them into a composite that is representative of the survey area. It also is capable of a wide range of processes that allow the data to be manipulated to remove any errors in data collection and to enhance specific features in the data.

2.5 Error

There are a variety of errors that must be taken into account during a geophysical survey, and for the purposes of this research we will divide them into two categories: positioning error and instrument error.

2.5.1 Positioning Error

Errors in positioning represent data spatial positioning errors due to inaccuracies in GPS and field surveying. Because of governmental restrictions on GPS satellites, positioning errors range from one to two meters for professional systems to as much as five or more meters for the

personal handheld variety. On the Trimble Ranger, the accuracy ranges from two to four meters. However, at the University of Tennessee Near-Surface Geophysics Lab, we have a subscription to OmniStar Inc., which applies a real-time differential correction to the data that reduces the error to ± 5 cm horizontal and ± 15 cm vertical (Trimble Navigation Limited, 2011).

Field survey errors are also a concern, and encompass inaccuracies with each individual data point collected. This type of positioning error can also be broken down into two categories: in-line error and cross-line error (Figure 2.5). In-line errors occur within each transect (Y-direction). For example, the operator changing walking speed or an error in the odometer wheel can affect the spatial positioning of the data point by as much as ± 0.5 m within each 10 m of transect. Cross-line error encompasses variations within each transect in the X-direction and is caused by lateral “operator wobble” or the inability of the operator to walk in a perfectly straight line. This type of error can be caused by an uncoordinated operator or the necessity to maneuver around obstacles (e.g. rocks, bushes, wildlife), and typically affects each data point by ± 0.5 m per 100 m, of profile length.

There is also error inherent in the creation of a GIS database for any given project (Lo and Yeung, 2006). Of primary concern is the systemic error in all GPS coordinates. This error then translates to the georeferencing of the data images to those GPS coordinates (For information about georeferencing, see Chang et al., 2009 and Sheppard and Cizek, 2009). If the images are georeferenced incorrectly, that increases the error obtained from these data sets. As for the software, Google Earth purposefully adds error to the satellite images used to create the virtual globe. This error is added in military sites in order to maintain security and is manifested by the appearance of strange offset in the data (e.g. data points in densely vegetated areas or in a body of water). Because details of the Google Earth georeferencing process are not available

publicly, it is not possible to give any concrete values for the direction and magnitude of the error vectors at these locations (Potere, 2008).

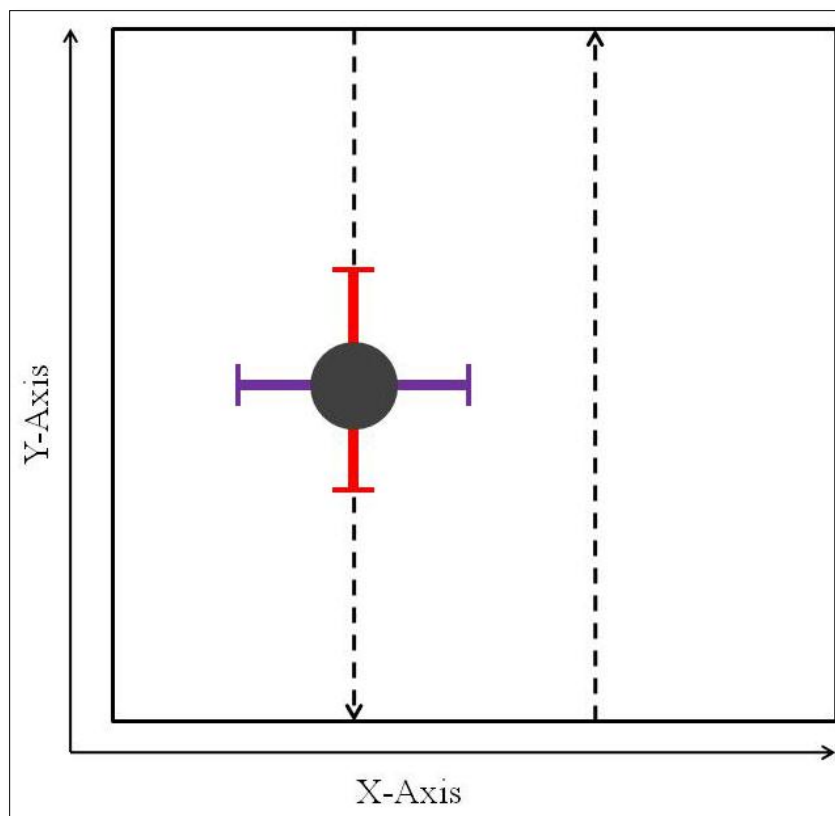


Figure 2.5. Schematic representation of in-line and cross-line error relative to the instrument survey direction, shown with dashed lines. The red line indicates the in-line error in the Y-direction, while the purple line indicates the cross-line error in the X-direction. Note that figure is not to scale.

2.5.2 Instrument Related Error

The GPR positioning error is typically manifested through either the odometer wheel (described above) or by variations in the area illuminated by changes in the shape of the electromagnetic wavefront generated by the transmitting antenna (as described in section 2.1). The horizontal area that the wave affects is dependent on the depth the transmitted wave can travel. Typically, the horizontal resolution worsens as the wave travels deeper into the subsurface. Some of this effect can be counteracted by choosing a lower frequency antenna. However, the tradeoff is poorer resolution in the data. Another cause for error in the GPR is the changes in the signal amplitude. GPR amplitude signal is a function of the maximum amplitude in each pulse, because the dynamic range of the recorded signal is normalized to that amplitude. Total dynamic range is 16-bit, therefore the amplitude error is variable depending on site conditions. Table 2.1 outlines the GPR error.

For the magnetometer, there is an inherent error in the amplitude of the signal. For the Bartington the error is ± 0.1 nT. This indicates that the magnitude of the anomaly recorded by the instrument will be ± 0.1 nT from the real value. Magnetic hygiene of the operator is another potential cause of error in the instrument's readings. Magnetic hygiene is defined as the lack of magnetic objects located on the person of the operator. It is imperative that before using the instrument, the operator must make sure that they have no magnetic objects on his/her person. For the purpose of our research, the geophysicist who operated the Bartington removed all her jewelry and her cell phone from their person before using the instrument, and all field assistants did the same. Table 2.2 outlines the error in using the magnetometer.

Table 2.1. Table describing the different types of error applicable when using the GPR.

| GPR Error | | |
|-------------|---|-------------|
| Type | Description | Amount |
| Positioning | Odometer Wheel | ± 0.5 m |
| | Operator Wobble | ± 0.5 m |
| Signal | Change in signal amplitude | Variable |
| | Change in electromagnetic wavefront shape | Variable |

Table 2.2. Table describing the different types of error applicable when using the magnetic gradiometer.

| Magnetometer Error | | |
|--------------------|--------------------------|--------------|
| Type | Description | Amount |
| Positioning | Change in walking speed | ± 0.5 m |
| | Obstacles in survey area | ± 0.5 m |
| Signal | Amplitude | ± 0.1 nT |
| | Magnetic hygiene | Variable |

3. A Multi-tool Geophysical Investigation of the Dreamer's Bay Ancient Roman Port, Akrotiri Peninsula, Cyprus

This chapter is based on a paper submitted for publication to *Geoarchaeology: An International Journal* by Caitlyn M. Williams, Gregory S. Baker, Bradley A. Ault. It has been edited to reduce redundancy within the thesis. My contributions to this paper include (i) creation of an acquisition plan for and collection of data, (ii) processing and interpreting the GPR and magnetic data, (iii) preparing the manuscript.

Abstract

The objective of this research is to perform the first geophysical survey at an active archaeological region on the Akrotiri Peninsula in Cyprus to identify evidence of a Roman naval base thought to have been used between the 4th and 7th centuries AD. Two study sites were identified by an on-site archaeologist: Dreamer's Bay and St. Mark's. A total of fifty-two, 10m by 10m grids were surveyed using ground penetrating radar and magnetic gradiometry. Data from each site were processed using to create maps of the subsurface to aid in the development of future excavation plans. Results from the survey revealed the remains of numerous buried and previously undocumented structures. Features detected at Dreamer's Bay have similar dimensions to the documented warehouses at the surface. Those identified at St. Mark's likely had some ecclesiastical function as surface remains indicate the site likely had some religious purpose.

3.1 Introduction

Using geophysics to aid in archaeological investigations has become more common as archaeological investigations can be very time consuming and invasive to the site area (e.g. Rogers et al., 2010; Baker and Ambrose, 2007; Abdallatif et al., 2010). There is a plethora of near-surface geophysical methods that can be used to locate man-made objects in the subsurface. Two of the most popular are ground penetrating radar (GPR) and magnetic methods. While these methods are successful on their own, when used in tandem they can create more useful maps of the subsurface for locating a variety of buried features (e.g. hearths, building foundations, remnant walls, etc.). Also, using multiple methods is the best way to gather the most data from a site. What one tool may miss, another may detect. Combining data sets creates more detailed and accurate results.

3.1.1 Motivation

The site in question is located on the British Royal Air Force Base on the Akrotiri Peninsula in Cyprus; thus, obtaining excavation permits was challenging due to security issues. To date, no excavation has taken place at this particular site, and the only indications that there may be buried features present are building remains on the surface. Surface remains already discovered include a quarry, rutted tracks, tombs, warehouses, and a submerged stone breakwater off the coast. A report written by Ault and Leonard (2009) states that remains are extensive and that there are at least a dozen sites worth investigation. Given the sensitive military nature of the site location, there is a need to prove the existence of these features in order to obtain excavation permits.

3.1.2 Objective I

To reiterate, Objective I of this investigation was to collect geophysical data at an active archaeological region on the Akrotiri Peninsula in Cyprus. This objective has been accomplished by (1) completing a multi-tool geophysical survey of the site using GPR and magnetic gradiometry and (2) processing, interpreting, and comparing these multiple data sets to locate any features present in the subsurface.

The site in question was purported to be a naval garrison that was in use between the 4th and 7th centuries CE. Among industrial building remains, there are also Byzantine-age churches present at the site that merit further investigation. Results from this investigation will aid archaeologists in developing precise excavation plans for the future.

3.1.3 Hypothesis I

Hypothesis I is that near-surface geophysical methods can be used successfully to locate previously unmapped subsurface features at archaeological sites in Cyprus.

3.2 Geophysical Techniques

3.2.1 GPR

Ground penetrating radar has been used successfully in many archaeological investigations (e.g. Bonomo et al., 2009; Grasmueck et al., 2004) and in many cases it has become a preferred method as - despite the complexity of operating the instrument - massive amounts of data are quickly collected and are capable of yielding high-quality three-dimensional maps of the subsurface (Conyers, 2004). This instrument is capable of collecting data in a

variety of terrains in a variety of climates and has a reputation for being used successfully in investigations in arid environments (Baker and Ambrose, 2007).

For the purpose of this study, a Sensors & Software Pulse EKKO Pro Smart Cart GPR system was used for all data collection with both the 100 and 200 MHz antenna (reference Figure 2.2). This particular GPR system was selected because it is available from the University of Tennessee Near-Surface Geophysics Lab and all field personnel were already familiar with its operation procedures. The Smart Cart is able to survey large, open areas quickly and efficiently and can be pushed over most minor obstacles with little effort.

3.2.2 Magnetic Gradiometry

Magnetic measurements are useful for archaeological surveys in that they are simple, rapid and totally noninvasive (Hansen et al., 2005). Many different types of magnetometers can be used in surveys (e.g. fluxgate gradiometer, proton precession magnetometers, cesium vapor magnetometers), and for the purposes of this study a fluxgate magnetic gradiometer was used. A main advantage of gradiometers is that because they take differential measurements, typically no correction for diurnal variation or solar activity is necessary, as any changes will affect both sensors in the same way. As the gradiometer is used with sensors oriented in the vertical direction, noise effects from large-scale deep features are suppressed and discrete anomalies show up more prominently (Breiner, 1999).

For this study, a Bartington Grad 601-2 Magnetic Gradiometer was used for data collection (reference Figure 2.4). Since one is not owned by the University of Tennessee Near-Surface Geophysics Lab, it was rented directly from Bartington, Inc. This particular gradiometer

was chosen due to its portability and ease of use in the field, and due to our familiarity with its operation procedures.

3.3 Case Study – Akrotiri Peninsula, Cyprus

3.3.1 Site Description

In the 1950s, the Cypriot Department of Antiquities carried out the first modern archaeological survey of the site, due to the pending construction of a British Royal Air Force Base. The main goal of the survey was to identify architectural remains at the surface which would limit the location of military buildings. Additional studies of the site were carried out during the early 1980s, with the continued mapping of surface artifacts (Heywood, 1982). In 2006, the Akrotiri-Dreamer's Bay Ancient Port Project (ADBAPP) began at the University at Buffalo, SUNY, to further map the artifacts in the area (Ault and Leonard, 2009). Additionally, an underwater field school associated with the University of Cyprus was conducted in 2007. The objective was to gather further information about a breakwater located off the southern coast of the peninsula. While underwater, students also located several stone anchors and two pottery concentrations on the sea bed. Conclusions of ADBAPP from the first two field seasons indicate that the archaeological remains are extensive, both chronologically and spatially (Ault and Leonard, 2009). These first studies delineated at least a dozen sites that archaeologists believe are worth further investigation. For the purpose of this geophysical study the two main sites, Dreamer's Bay, and St. Mark's, are discussed.

3.3.1.1 Geographic Setting

Cyprus is the third-largest island in the Mediterranean Sea and lies about 386 km north of Egypt and 64 km south of Turkey. While most of the island is relatively flat, the main topographic features are the Troodos Mountains which lie in the central part of the island. The Mediterranean climate is best described as hot and dry from June to September. For the remainder of the year, the island has rainy winters (Solsten, 1993).

The sites are located along the southern coast of the Akrotiri Peninsula in Cyprus, near the modern city of Akrotiri, which lies off-base (Figure 3.1). The peninsula is approximately 12 km north to south and 9 km wide, and is flanked on the sides by the Akrotiri Bay to the east and the Episkopi Bay to the west. The peninsula itself is a relatively recent formation, geologically speaking, with the first sediments being deposited during the Pliocene (Heywood, 1982). The site lies within the confines of the Akrotiri RAF Air Force Base, which is considered British Sovereign Territory.

The coast of the southern-most portion of the peninsula is made up of Miocene sandstone and marl cliffs that rise approximately 64 m above the Mediterranean Sea. Moving inland, the remains of the Akrotiri Forest cover the terrain, dominated by low, shrubby plants. The Akrotiri Salt Lake lies in the low-lying flat interior of the peninsula. Approximately 4 km in diameter, it was likely once a protected bay open to the sea on the east (Figure 3.2) (Heywood, 1982).



Figure 3.1. a) Google Earth image of the island of Cyprus with the area of interest located in the white rectangle. b) The location of the modern cities of Akrotiri and Kourion in relation to the sites at St. Mark's and Dreamer's Bay. The city of Kourion has been made famous by the spectacular archaeological remains discovered there.



Figure 3.2. Artist's rendition of what the Akrotiri Peninsula might have looked like during the Roman period (4th to 7th century CE).

3.3.1.2 Archaeological History

Since the site under investigation lies within the confines of the British Royal Air Force Base, it presents a unique opportunity to study an undisturbed archaeological landscape: the combination of restricted access to the site and a specific construction plan that was conscientious of the location of surface remains led to the protection of the archaeological landscape. The site at Akrotiri appears to have served as a port and maritime trans-shipment point likely associated with the modern city of Kourion (not to be confused with Kourias, which is an ancient city with its current location unknown), which lies 13 km to the northwest. A port was likely established due to its locale, being both militarily and economically strategic as it served as a way point between Greece, Egypt, and Turkey. The majority of the remains visible at Dreamer's Bay date to the late Roman/Early Byzantine period, approximately during the 4th to 7th centuries AD (Ault and Leonard, 2009).

Past studies of the area have been purely archaeological in nature dealing with surficial features and have yielded artifacts both offshore and on land. Most significant of these recent finds is a quarry, located on a cliff approximately 30 m above the bay. Associated with the quarry are rutted tracks of an ancient roadway utilized to cart stone to the nearby settlement (current location unknown) of Kourias (Ault and Leonard, 2009). Archaeologists believe the remains of this settlement lie within the boundaries of the modern Akrotiri RAF Air Force Base. At Dreamer's Bay, two structures with partial surficial expression had previously been identified as warehouses given their location and geometry (Figure 3.3). Sections of eroded walls are also visible at the surface here, though no statement has been made as to their purpose.

St. Mark's had previously been identified as an area of archaeological significance as a potential site of an ancient church known locally as S. Mercourios. Features visible on the



Figure 3.3. Photo of previously mapped warehouse structures at Dreamer's Bay.



Figure 3.4. Photo inside the alleged catacombs located at the St. Mark's site.

surface include loose building debris as well as areas of mortared rubble ‘floor’ construction. Many wall alignments and possible paved surfaces are scattered across the areas of high terrain, but no complete structures have yet been found. Also located at this site is a nine meter length of tunnel cut into the rock and finished with plaster (Figure 3.4). The tunnel is open to the surface at either end, but is filled with debris, leaving only the uppermost 1-1.5 m visible. Archaeologists speculate that this tunnel is the remains of a crypt (Ault and Leonard, 2009).

3.3.2 Data Acquisition

Geophysical data acquisition took place at both sites from June 6, 2010 to June 13, 2010. The research team consisted of a lead geophysicist and two graduate students from the University of Tennessee, and lead archaeologist from the ADBAPP at SUNY Buffalo.

3.3.2.1 Dreamer’s Bay Site

Special consideration was made when delineating the survey boundaries, since two different geophysical data acquisition techniques were to be used. Thirty-eight, 10 m by 10 m grids (hereafter referred to as minor grids) were set up in an area of interest as suggested by the lead archaeologist, based on previous work (Figure 3.5). Individual grid size was chosen by taking into consideration the capabilities of the Bartington gradiometer, the GPR unit, and the necessity to work around obstacles such as excessive brush, rock outcroppings, and coastal cliffs.

For later ease with data processing, the X-axis was laid out in a roughly east-west direction, with the Y-axis running roughly north-south. Nails with yellow flagging tape were pounded into the ground to mark the corners of each minor grid, as the ground was too hard to allow the usage of conventional PVC flags. Tape measures were laid down along the X-axis for precision when setting up the grids and to maintain transects’ separation during the survey.

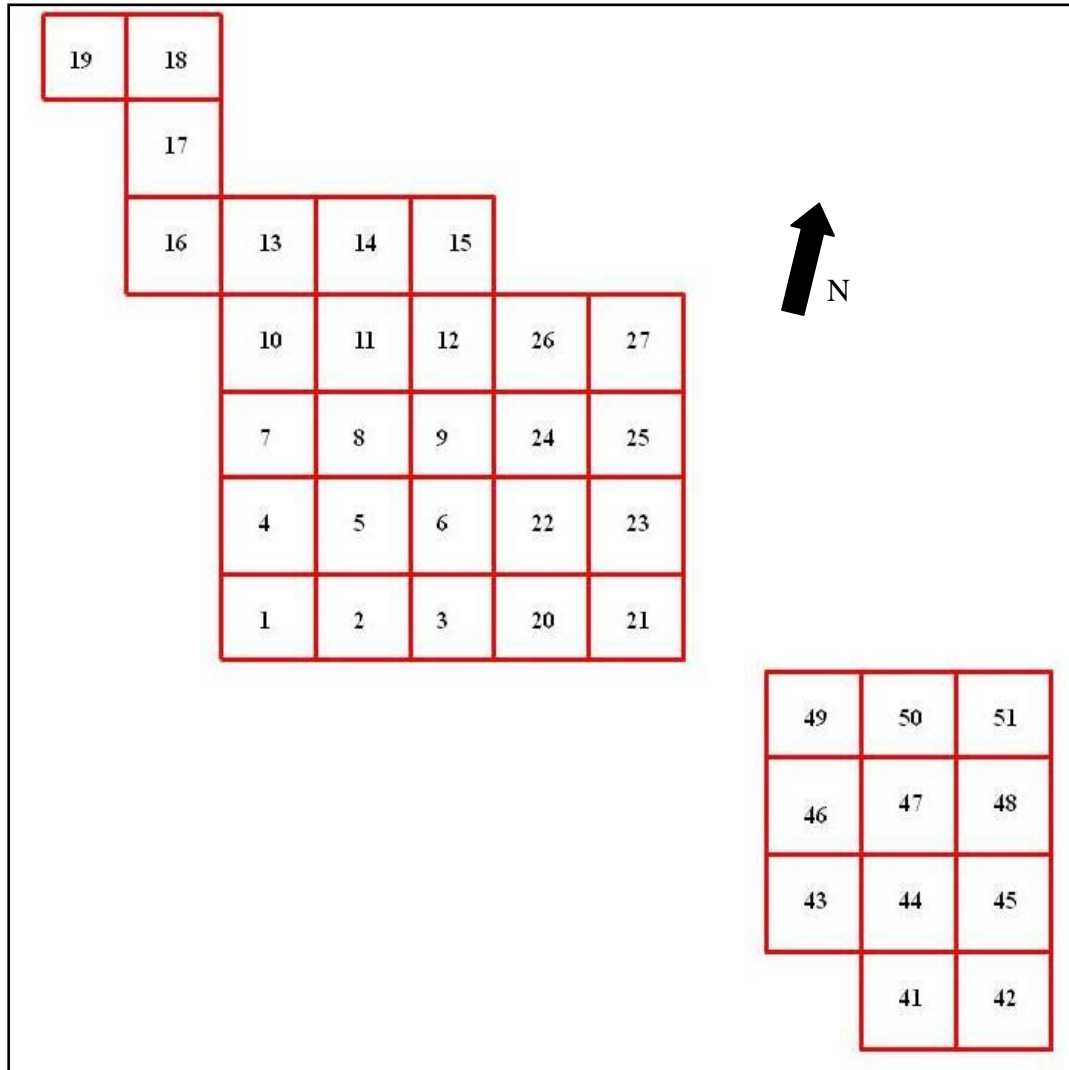


Figure 3.5. Schematic of the survey area showing the survey area geometry and the number of each grid as assigned by the Bartington Grad 601-2.

3.3.2.1.1 Magnetic Gradiometer

The start point for all surveys was the southwest corner of each of the minor grids and the surveyor began the first transect by walking northward. All data were collected in an alternating pattern, and spacing between transects alternated from 1.25 m to 2.0 m depending on the direction of that transect (Figure 3.6). Guide ropes were used in order to maintain lateral spatial accuracy as well as monitor the pace of the operator: green ropes were used on the north and south sides of the area which had alternating red and yellow markings at half meter increments in order to maintain the correct transect spacing throughout the execution of the survey. One yellow rope, with meter increments marked with red tape, was used solely to aid the operator in maintaining pace. Maintaining proper pace is an integral part of operating the gradiometer as the machine takes readings at regular time increments as opposed to taking readings when prompted

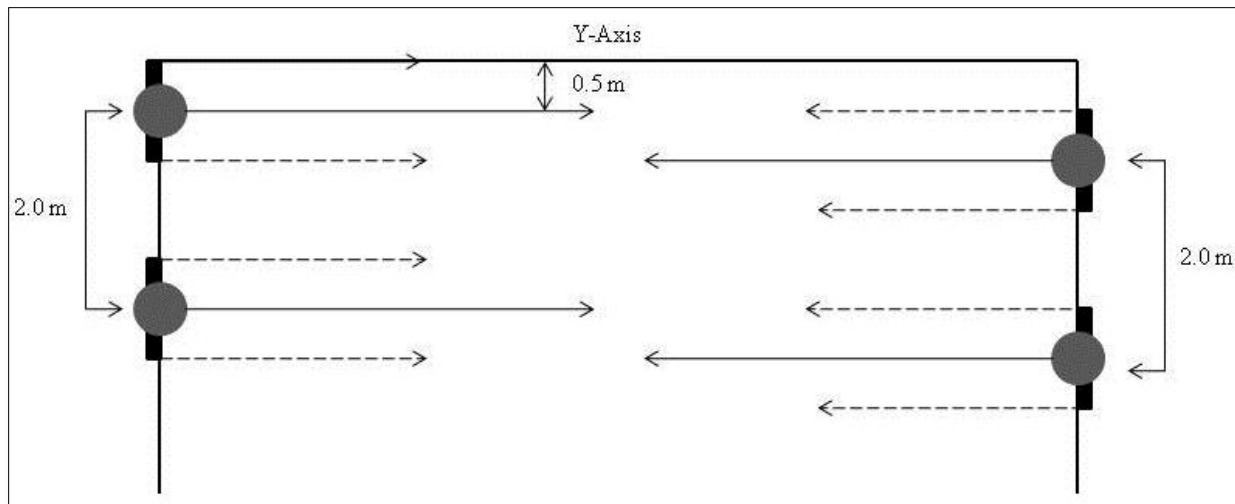


Figure 3.6. Survey design for the Bartington Grad 601-2 with the solid bars representing the width of the instrument and the gray circles representing the operator. The dashed lines show the path of each sensor on either side of the instrument while the solid lines show the path walked by the operator. The first transect is walked 0.5 m from the origin in the X-direction. The subsequent transect is walked with 0.5 m spacing from the first. All remaining transects have 2.0 m spacing.

by an operator or with an odometer wheel. With the completion of one grid, the operator would move to the southwest corner of the next grid to be surveyed. The gradiometer data logger records and numbers each grid in a sequential manner automatically for later ease in data processing.

Topography across any given grid had minimal impact on the operator's ability to correctly collect data, as did in-situ rock and archaeological features at the surface. The principal obstacle with regard to this method of data collection was the thick shrubbery that covered portions of the survey area. Some brush could be navigated around, while others were large enough to prohibit data collection in the area.

3.3.2.1.2 GPR

The same grid setup used for the gradiometer survey was also used for the GPR survey. However, the GPR did not have to work within the same strict area confines. Surveying with the 200 MHz antenna began in the southwest corner of the grid to keep consistency with data "origin" orientation. Transects ran in a north-to-south, zig-zag pattern with 0.5 m spacing. The survey area was L-shaped for the 200 MHz antenna, with the survey area being divided up into a 20 m by 20 m section in the west and a 30 m by 10 m section in the east. The first pass with the GPR used 10 m long transects and ran north-south from 0 to 50 m. The second pass started back at the west end and only extended 20 m east.

The area was later re-surveyed with the 100 MHz antenna due to poor resolution of the 200 MHz antenna data. Eight transects were run in an east-west direction in a zig-zag pattern with 0.5 m spacing. Transects were 50 m long and the start direction was to the west. Added to these data were a number of 'wildcat' transects taken north of the first block of data. These 40 lines were run north-south in an area of interest slightly more inland (north) of the first set of

data in an area where the brush thinned out. The length of transects ranged from 20 m to 40 m and spacing between transects was 0.5 m. Length was determined by the amount of free space in which the instrument could be operated.

An area southeast of the original site was surveyed later with the 100 MHz antenna due to the presence of some visible artifacts at the surface. This area, deemed ‘the peninsula’, extends from visible warehouse remains at the northern boundary to the Mediterranean Sea at the southern boundary. GPR was run using the 100 MHz antenna to allow for better penetration. Transects ran north-south in a zig-zag pattern with 0.5 m spacing. Due to constraints imposed by cliffs to the south and fenced-in archaeological features to the north, transects range in length from 20 m to 40 m.

3.3.2.1.3 GPS

Spatial positioning data points at Dreamer’s Bay were acquired via dGPS at the corners of each minor grid when both the GPR and gradiometer surveys had been completed. Points were also taken where archaeological remains were visible at the surface.

3.3.2.2 St. Mark’s

Survey delineation was slightly more difficult at St. Mark’s due to its more remote location and the presence of vegetation, large rocks, and significant rock outcrops. Gardening shears and shovels were used to remove smaller bushes, while larger patches of vegetation were omitted from the survey area. A total of 13 minor grids were set up to maximize the potential to cross buried features whilst surveying (Figure 3.7). PVC flags were placed at each corner of the individual grids to streamline the process of data collection. Coincident grids were used both for the gradiometer survey and the GPR survey.

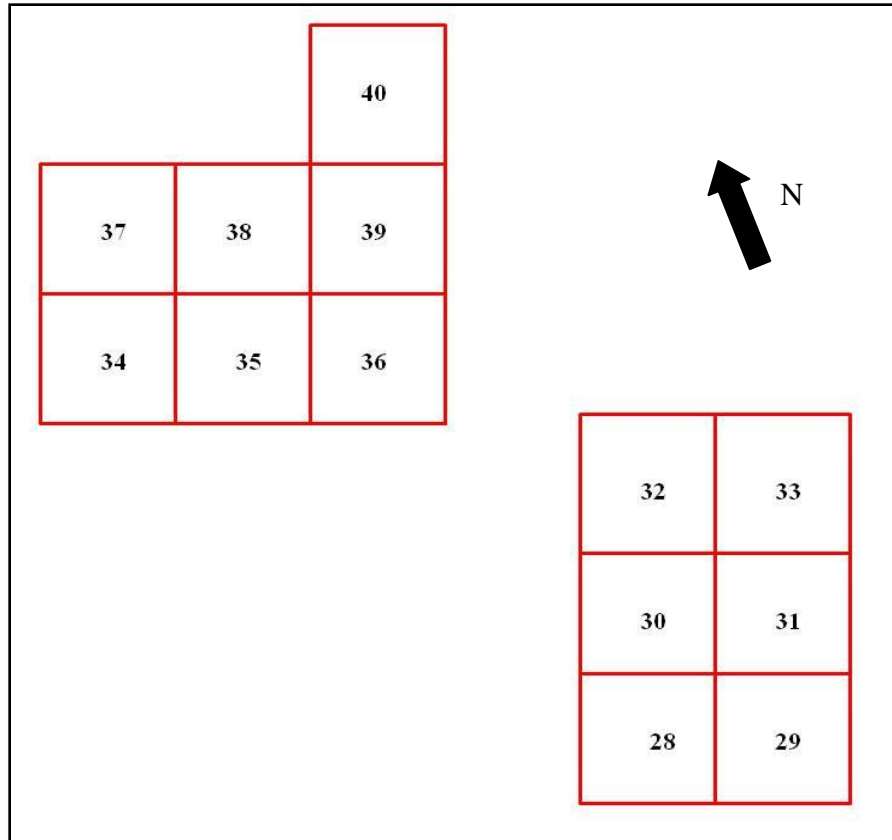


Figure 3.7. Schematic of the survey area at St. Mark's. Grid numbers were assigned automatically with the Bartington Grad 601-2.

3.3.2.2.1 Magnetic Gradiometer

Surveying via dGPS was conducted by dividing the entire survey area into two sections to allow for ease in instrument operation. Guide ropes, parameters for the gradiometer, and survey design were the same as those used at Dreamer's Bay.

3.3.2.2.2 GPR

Data collection with the GPR was accomplished using the 100 MHz and the 200 MHz antennae. Transects were collected in a zig-zag pattern with 0.5 m spacing. Using the 200 MHz antenna first, both the northern and southern portions of the site were surveyed. After taking a

preliminary look at these data, the geophysics team decided to re-survey the area using the 100 MHz antenna in order to improve the imaging. Surveying with the second set of antennae began in the northern half of St. Mark's, and approximately one-third of the area was surveyed on the first pass. The surveyor then had to move to the southern part of the survey area due to the potential for interference with the gradiometer (which was being used at the same time by a different operator). Only half of the southern survey was completed when the data logger overheated and surveying was stopped for the remainder of the day. Surveying was completed the following day, after the data logger had time to cool. First the southern portion was finished and then the northern portion of the site was finished. Due to the flexibility offered by using the GPR, some additional transects were run outside of the survey boundary as surface remains were visible north of the survey area.

3.3.2.2.3 GPS

Spatial positioning data points were collected at each corner of the minor grids that make up the site after the geophysical surveys had been completed.

3.3.3 Data Processing

All GPR data were processed the same day they were collected using Sensors & Software proprietary software. The gradiometer data were processed upon return to Knoxville, Tennessee as special software had to be acquired. GPS data were also processed upon return to the lab as the proper software was not correctly installed on the field laptop.

3.3.3.1 Dreamer's Bay

3.3.3.1.1 GPR Data

Data profiles were imported from the data logger on the GPR unit to a laptop running a processing program called GFP Edit (Sensors & Software). The purpose of this program is to set up line data such that they can be imported into a mapping program in order to make a 2D image of the subsurface. Data obtained from the 200 MHz antenna were imported as Y-lines, and length was set to 10 m to account for any human error in running the GPR unit. The start direction for every other line was switched to allow the data to represent the zig-zag pattern in which it was collected, and lines were lagged in the start direction approximately 0.25 m.

This process was repeated for the 100 MHz data, with a few significant differences. Primarily, the first data set for the northern portion, which contained only eight east-west lines, was imported as X-lines into GFP Edit (Sensors & Software) with 0.5 m spacing and length was fixed at 50 m. The start direction of every other line was switched to compensate for the zig-zag pattern in which it was collected. For the second set of data collected to the north, lines were again imported as Y-lines and the direction of every other line was switched to take into account the zig-zag pattern in which data were collected. Length varied from 12 to 24 m due to obstacles encountered on the surface and spacing between transects was set to 0.5 m.

For the peninsula area, 40 lines of data were imported into GFP Edit as Y-lines with length ranging from 20 m to 40 m. Directions of every other line were then switched to accommodate the zig-zag pattern in which data were collected, and spacing was set to 0.5 m.

Once the raw GPR data were set up using GFP Edit (Sensors & Software), the files were saved and imported into EKKO Mapper 3 (Sensors & Software) that uses GFP files to create pseudo 3D maps of the subsurface. Once GFP files were imported, the velocity and the depth

slice interval were picked in order to better display the data and highlight the subtleties in the data (see Table 3.1). The best data slices were then chosen based on the number of possible features which could be interpreted in the data set, and the clarity of the data for interpretation and display.

3.3.3.1.2 Gradiometer Data

Magnetic data were processed using proprietary ArcheoSurveyor software (DW Consulting), which is a program specifically designed to download, assemble, enhance, publish and save data from a range of geophysical instruments (Wilbourn, 2011). One of the benefits to this program is that it already contains pre-loaded information for importing data from a variety of common near-surface geophysical surveying instruments, including the Bartington Grad 601-2 Magnetic Gradiometer.

Each minor grid was imported one at a time and positioned such that the geometry of the whole survey polygon was reconstructed. When the data were first imported into ArcheoSurveyor they had a distorted appearance due to the inability of the operator to exactly mark the end lines consistently in each direction. As a result, the outgoing traverse was out of

Table 3.1. Velocities and depth slice picks for data are shown for each survey location at Dreamer's Bay.

| Survey Location | Antenna Size | Picked Velocity (m/ns) | Depth Slice (m) |
|-----------------------|--------------|---------------------------|--------------------|
| Dreamer's Bay North | 200 MHz | 0.060 | 0.1515 |
| Dreamer's Bay North 1 | 100 MHz | 0.060 | 0.2155 |
| Dreamer's Bay North 2 | 100 MHz | 0.070 | 0.2000 |
| Dreamer's Bay South | 100 MHz | 0.084 | 0.2000 |

sync with the incoming traverse. To compensate for the error, the data were destaggered by five sample intervals. Destaggering compensates for data collection errors caused by the operator starting recording of each traverse too soon or too late: it shifts each traverse forward or backward by a specific number of intervals (DW Consulting, 2010). Next, a low-pass 2D spatial Gaussian filter was applied to all data in order to enhance large, low-amplitude features (i.e. subsurface man-made features as opposed to metallic objects at the surface). Low-pass spatial filters calculate the mean of all the values within a specified window (in this case a three pixel by three pixel window was used) and replace the center value with the mean. Gaussian refers to the higher weight given to values closer to the center point of the given window. All data were also clipped at plus or minus three standard deviations. Clipping replaces all values outside a specified minimum and maximum with those values. This process was done to remove extreme data points created by metallic debris at the surface. Data were also despiked in order to smooth out the very high amplitude anomalies created by surface metallic objects (e.g. nails, wires, etc.). The despiking routine scans the composite grid using a uniform weighted window that looks for data points exceeding the median value. If a high value is found, it is replaced with the median value. The main difference between clipping and despiking is that clipping is applied to all the data, while despiking is applied to anomalous data points.

Some individual grids required special attention and additional processing. Grids 6, 9, 13, 24, 25, and 27 (see Figure 3.7) had to be destriped in order to equalize differences between those grids and the rest of the composite. Destriping calculates the median of each traverse of a grid and then subtracts that value from all data points; thereby excluding extreme data points in this calculation. This process will equalize underlying differences between grids that can be

caused by directional effects in the instrument, instrument drift or orientation, or delays in surveying adjacent grids.

To make the data more aesthetically pleasing and for features to be more obvious, a graduated shade function was applied to the data. This function continuously calculates interpolated values for every pixel in the image in order to blend them together and make the image look less pixilated. The color palette was also flipped, so that high values were darker shades of grey and black and low values were light grey to white. This step simply increases the aesthetic of the data and makes the features of interest ‘pop’ against the dark background.

3.3.3.1.3 GPS Data

Spatial positioning data from the dGPS were imported onto the lap top using a program created by Trimble called TerraSync. From this program a map of the dGPS points was created and the points were imported into a Microsoft Excel spreadsheet for later manipulation.

3.3.3.2 St. Mark’s

3.3.3.2.1 GPR Data

Data were imported into GFP Edit (Sensors & Software) in the same fashion as they were for the Dreamer’s Bay site. As described in the Data Acquisition section, data were collected in both the north and south portions of St. Mark’s with both the 100 MHz and 200 MHz antenna. All lines were imported as Y-lines with 0.5 m spacing and start direction for every other line was switched. For the northern portion of the St. Mark’s survey area, transects collected with the 200 MHz antenna varied in length from 10 to 21 m. Length for transects collected with the 100 MHz antenna range from 14 to 40 m. For the southern portion of St. Mark’s, transects collected with both the 200 MHz and 100 MHz antennae, length was set at 30 m.

| Table 3.2. Picked velocity and depth slice values for data collected at St. Mark's. | | | |
|--|--------------|------------------------|-----------------|
| Survey Location | Antenna Size | Picked Velocity (m/ns) | Depth Slice (m) |
| St. Mark's North | 200 MHz | 0.150 | 0.1000 |
| St. Mark's North | 100 MHz | 0.132 | 0.2000 |
| St. Mark's South | 200 MHz | 0.300 | 0.1449 |
| St. Mark's South | 100 MHz | 0.150 | 0.2041 |

Once data were processed using GFP Edit (Sensors & Software), the files were saved and then imported into EKKO Mapper 3 (Sensors & Software) in order to create a map of the subsurface. Velocities and depth slices were picked to best represent the data (see Table 3.2). The best data slices were then chosen based on the number of possible features which could be interpreted in the data set, and the clarity of the data for interpretation and display.

3.3.3.2.2 Gradiometer Data

Magnetic data collected at St. Mark's were processed in the same fashion as they were for Dreamer's Bay. All 13 minor grids were set up into one composite which represents the survey geometry. For ease in processing, St. Mark's was divided into north and south sections. The composite was destaggered by five intervals, which is approximately equal to 10 cm. Data were also despiked, clipped and a low-pass 2D spatial Gaussian filter applied in order to remove high amplitude anomalies while simultaneously allowing greater visibility of low magnitude features. Finally, before the data images were saved, a graduated shade function was applied to all the data and the color palette was flipped.

3.3.3.2.3 *GPS Data*

Spatial positioning data from the GPS were imported into TerraSync upon return to Knoxville, Tennessee. Using this program, a map of the GPS points was created and then the points were imported into an Excel spreadsheet (in decimal degrees) for later manipulation.

3.3.4 Results

The geophysical results from both sites are very promising. In general, the magnetic data show more interpretable structures than the GPR data. The soil at the two sites clearly attenuated the radar signal rapidly. Additional data can be found in Appendix A.

Various criteria were used when interpreting these data. These criteria had been established in personal communication with the lead archaeologist and by examining patterns in Roman architecture. As a general rule, we were mostly concerned with linear features that were continuous, and any rectilinear features that roughly matched the dimensions of features mapped on the surface (approximately 24.4 m by 8.8 m, with walls 0.5 m thick). Also, we were concerned with features that truncated each other at 90° angles as straight lines and right angles are diagnostic of the architecture of this period and are not commonly found in nature. Table 3.3 shows all of the criteria used to make interpretations. In order to be consistent with our interpretations, any picked features had to meet at least two of the criteria. As no excavations have occurred in this area, we were unable to ground truth any of the interpreted subsurface features. However, a more explicit report on the archaeological significance of the geophysical results from Dreamer's Bay and St. Mark's is anticipated.

Table 3.3. Criteria for geophysical interpretation. All interpretations made had to have at least two of these attributes.

| Criteria for Geophysical Interpretation |
|--|
| Structure is linear |
| Structure is continuous |
| Structure has similar dimensions to previously found artifacts |
| Structure “walls” appear to have a thickness of 0.5 m |
| Features truncate at 90° angles |

The interpretation lines drawn on each photo take into account all the errors described in Section 2.5 (reference Tables 2.1 and 2.2). The peak value of the magnetometer data is approximately 45 nT, and as the error of the instrument is ± 0.1 nT, amplitude error is not a concern for these particular data sets. When making interpretations in the GPR data, features are typically mapped between a high amplitude and low amplitude region in the data (this would denote a change in the electromagnetic properties of the subsurface, indicating either a ‘boundary’ had been crossed or the detection of an anomaly), thus signal error is not a factor.

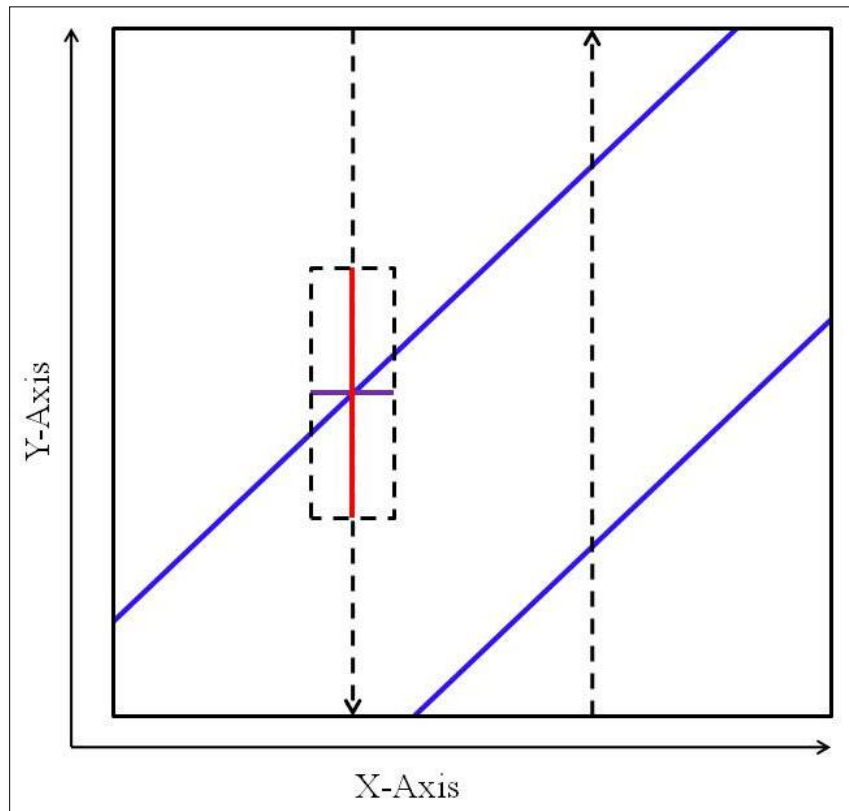


Figure 3.8. Figure illustrating the error inherent in the data collected in Cyprus in 2010. The red lines indicate in-line error and the purple line indicates the cross line error (values for these are within the body of the text), and the black, dashed rectangle represents the total error of any given point in the survey. Blue diagonal lines represent subsurface linear features. As transects were run at a 45° angle to the anticipated orientation of features, so to be certain of maximizing the possibility of detecting features in the subsurface.

Average in-line error associated with the magnetometer is approximately $0.075 \text{ m} \pm 1.36 \text{ m}$ at a 95% confidence level and average cross-line error is approximately $0.28 \text{ m} \pm 1.47 \text{ m}$ at a 95% confidence level, while those values for the GPR data are approximately equal to $0.0038 \text{ m} \pm 1.08 \text{ m}$ at a 95% confidence level and $-0.22 \text{ m} \pm 1.66 \text{ m}$ at a 95% confidence level, respectively (Figure 3.8). A full description of the calculation of these values is forthcoming in Chapter 4. Using these values, we would recommend to archaeologists that they would set up their 5 m by 5 m square so that any geophysical features of interest would be at least 1.0 m away from the boundaries of the excavation area.

To reiterate, there are distinct differences in what each instrument will detect. The magnetometer will detect differences in the magnetic susceptibility between a target and the background material, while the GPR detects changes in the electromagnetic properties of the subsurface. It is likely that the features detected by the magnetometer are physical objects (e.g. walls, cut stone, etc.) while the features detected by the GPR are categorized as disturbances in the subsurface (e.g. a dug-out foundation, storage pits, etc.). Currently, we cannot say what any subsurface features are without excavation (where permitting may take up to 10 years due to the sensitive nature of this site), and at this time cannot provide final tested results of this interpretation.

3.3.4.1 Dreamer's Bay

3.3.4.1.1 GPR Data

The depth of penetration for Dreamer's Bay was approximately 1.5 m. The best depth slices were from 0.250 to 0.500 m in the northern part of the survey area and from 0.475 to 0.575 m in the south (Figure 3.9). Few linear features were discernable in the data (Figure 3.10). As we were unable to acquire soil or rock samples while in Cyprus due to export and permit

restrictions, we can only assume that the type of soil present at both sites was highly conductive and thus decreased resolution of the data. Those features that were discernable are likely additional warehouse structural remains.

3.3.4.1.2 Gradiometry Data

The magnetic data (Figure 3.11) revealed numerous linear features which appear to be long, narrow buildings approximately 20 to 30 m in length and 5 to 10 m wide (Figure 3.12). Given the two warehouses already exposed at the surface, it is likely that the structures revealed in the magnetic data are also additional warehouses.

3.3.4.2 St. Mark's

3.3.4.2.1 GPR Data

The depth of penetration for this site was also approximately 1.5 m. Depth slices shown are 0.750 to 0.950 m in the north and 0.880 to 1.080 m in the south (Figure 3.13). As with the data collected at Dreamer's Bay, few linear features can be found in the data (Figure 3.14). Two circular features highlighted in these data were chosen due to the roughly circular shape of the anomaly as well as there being a distinct 'high' to the inside of the feature. While not linear like the majority of the features found on Cyprus, the distinct shape makes them areas of interest and worth further investigation.

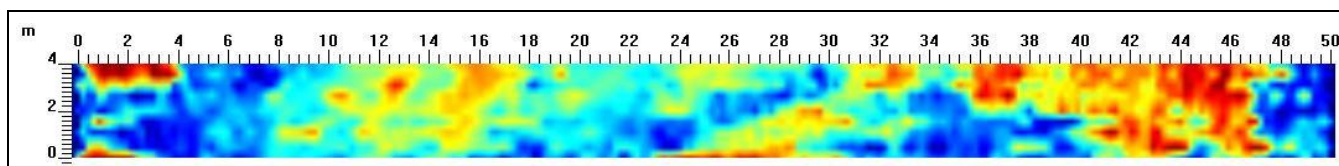
3.3.4.2.2 Gradiometry Data

Magnetic data (Figure 3.15) collected at St. Mark's show more promising results than the GPR data. The data for the northern portion of the survey area show what can be interpreted as

the southern corner of perhaps two northeast-southwest trending buildings (Figure 3.16).

Dipoles are recognized by a distinct high anomaly paired with a distinct low anomaly and are roughly circular. Dipoles are common in magnetic data and were easy to pick out among the other linear features. In the southern portion of the survey area, the magnetic data reveal a few more linear features that can be interpreted as buildings. Given the religious history of this area, we assume that the buildings found in the data had some ecclesiastical function.

a)



b)

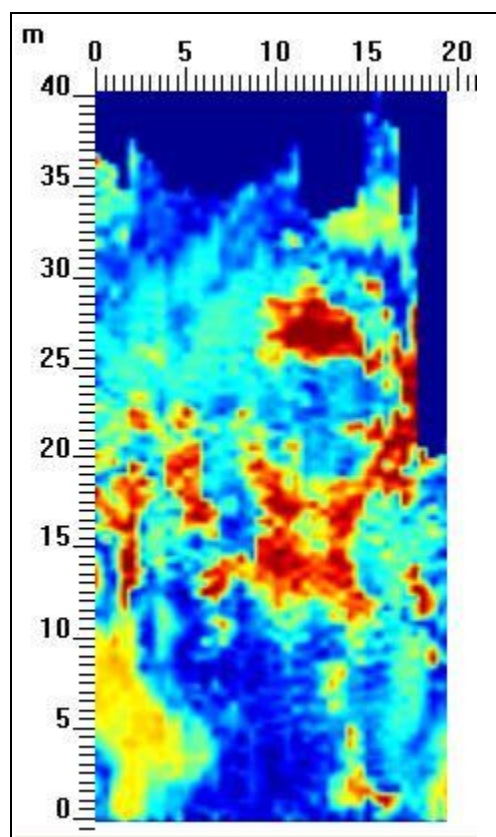
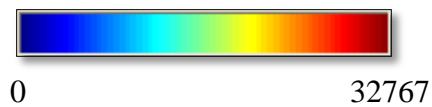
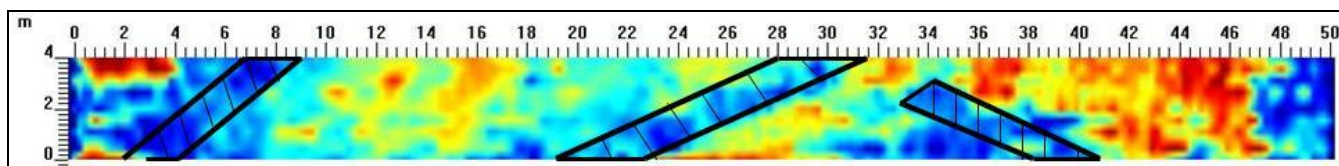


Figure 3.9. a) Uninterpreted GPR data for the northern portion of Dreamer's Bay. Data were collected with the 100 MHz antenna with eight transects running in an east-west direction. b) Uninterpreted GPR data collected with the 100 MHz antenna in the southern portion of the site at Dreamer's Bay. Transects were run in a north-south direction.



a)



b)

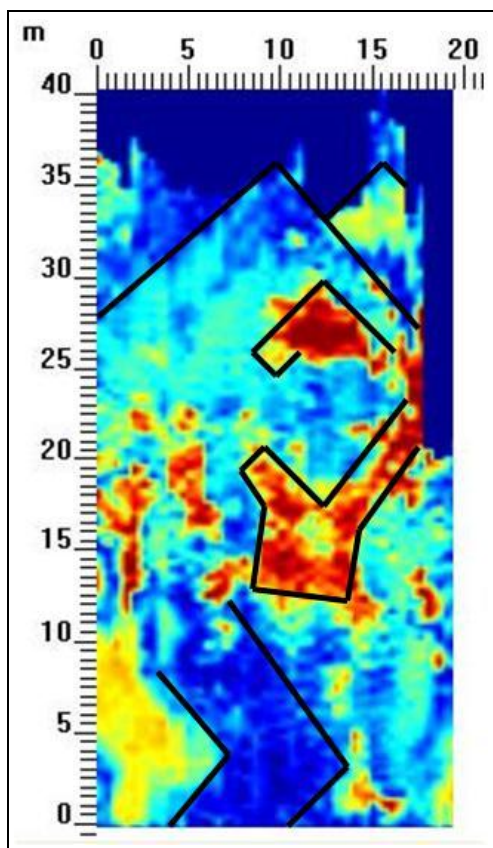
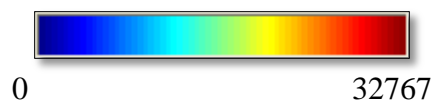


Figure 3.10. The solid black lines in these photos are interpreted linear features. The black polygons with the cross-hatching are wider features. a) GPR data for the northern portion of Dreamer's Bay. Data were collected with the 100 MHz antenna with eight transects running in an east-west direction. Linear features representing possible subsurface building remains are highlighted in black.

b) GPR data collected with the 100 MHz antenna in the southern portion of the site at Dreamer's Bay. Transects were run in a north-south direction. Linear features are highlighted in black.



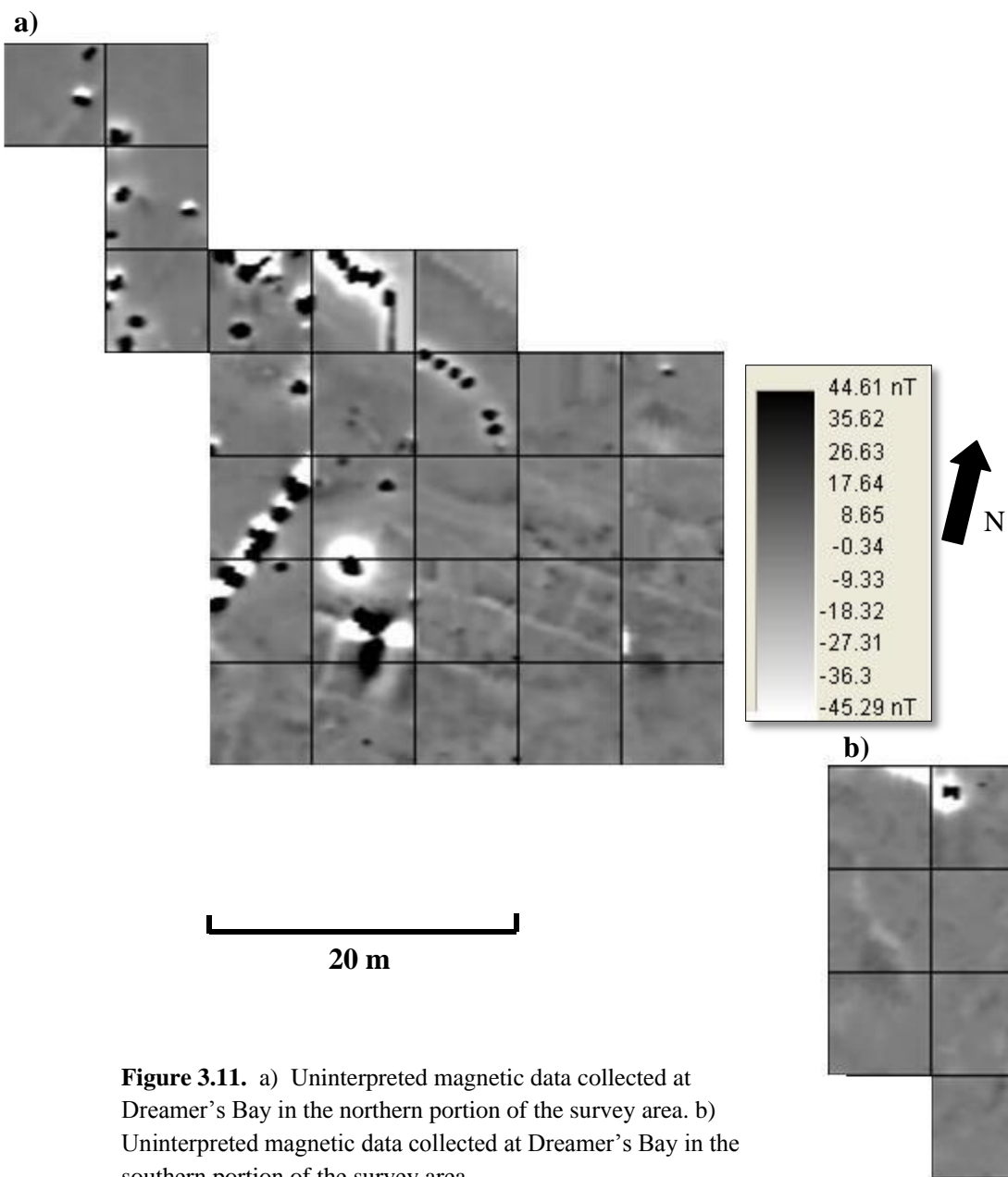


Figure 3.11. a) Uninterpreted magnetic data collected at Dreamer's Bay in the northern portion of the survey area. b) Uninterpreted magnetic data collected at Dreamer's Bay in the southern portion of the survey area.

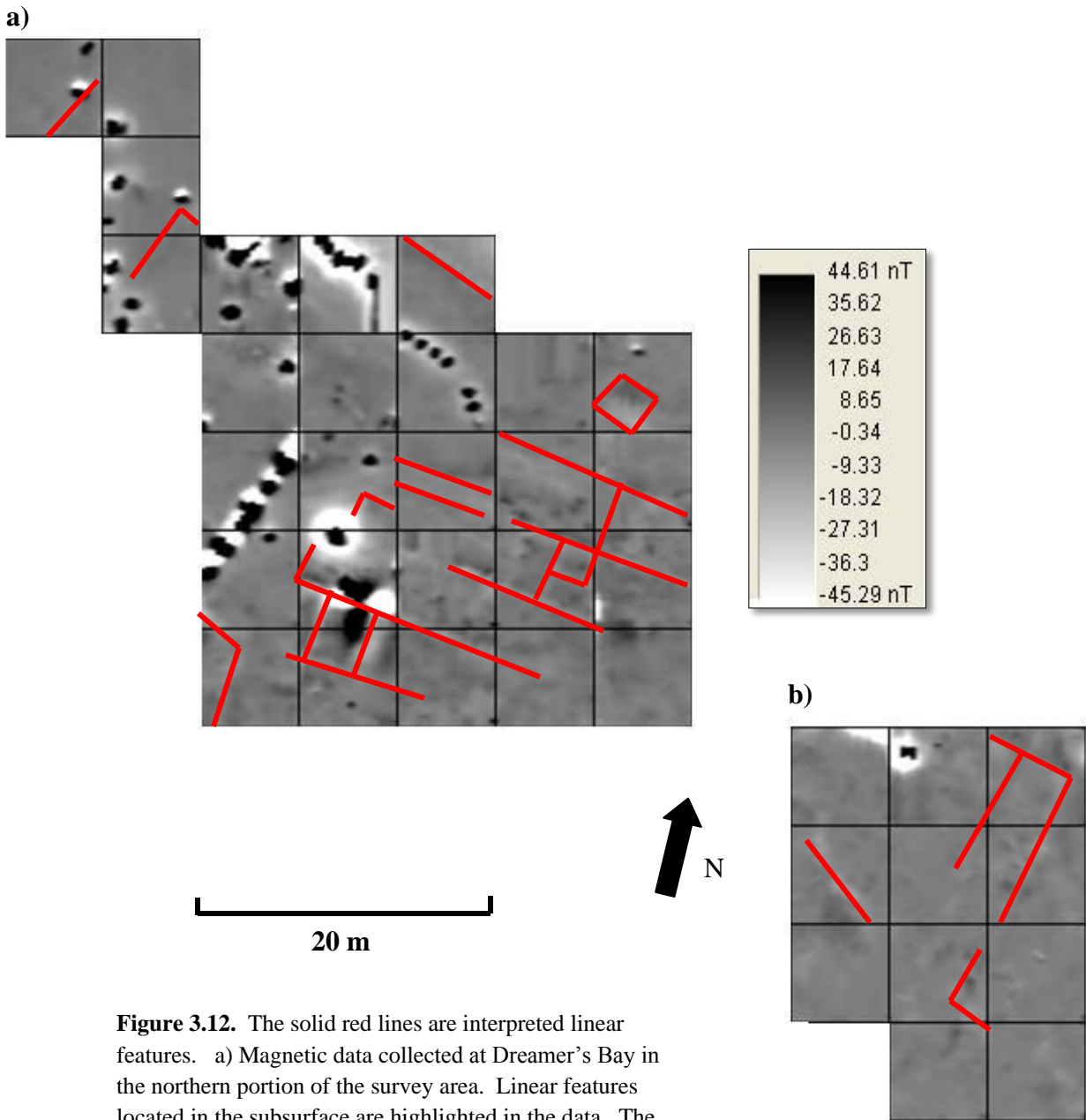


Figure 3.12. The solid red lines are interpreted linear features. a) Magnetic data collected at Dreamer's Bay in the northern portion of the survey area. Linear features located in the subsurface are highlighted in the data. The strong dipoles located on the northeastern portion of the data are the result of historic metal debris as this location was used for the British Air Force during World War II. b) Magnetic data collected at Dreamer's Bay in the southern portion of the survey area. A possible structure is highlighted in the data. This site lies directly south of a known warehouse at the surface.

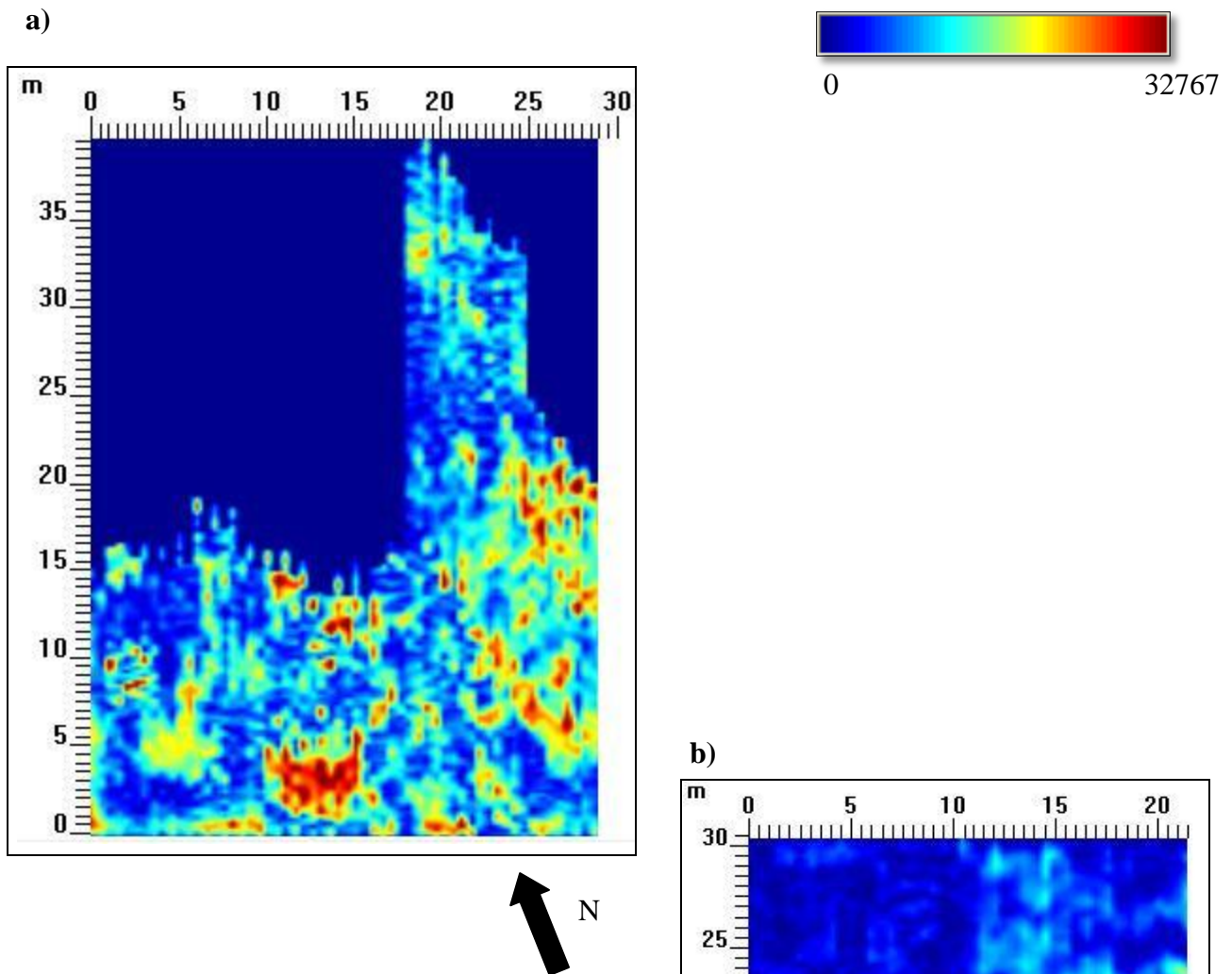
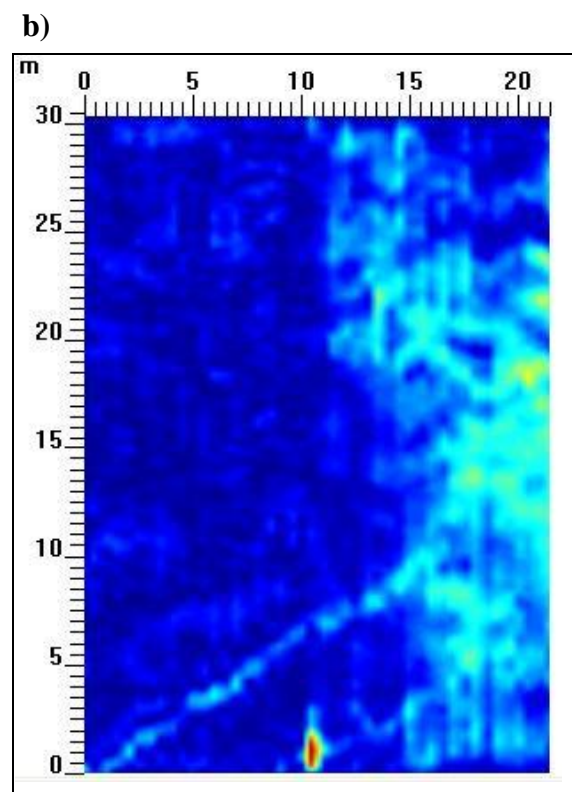
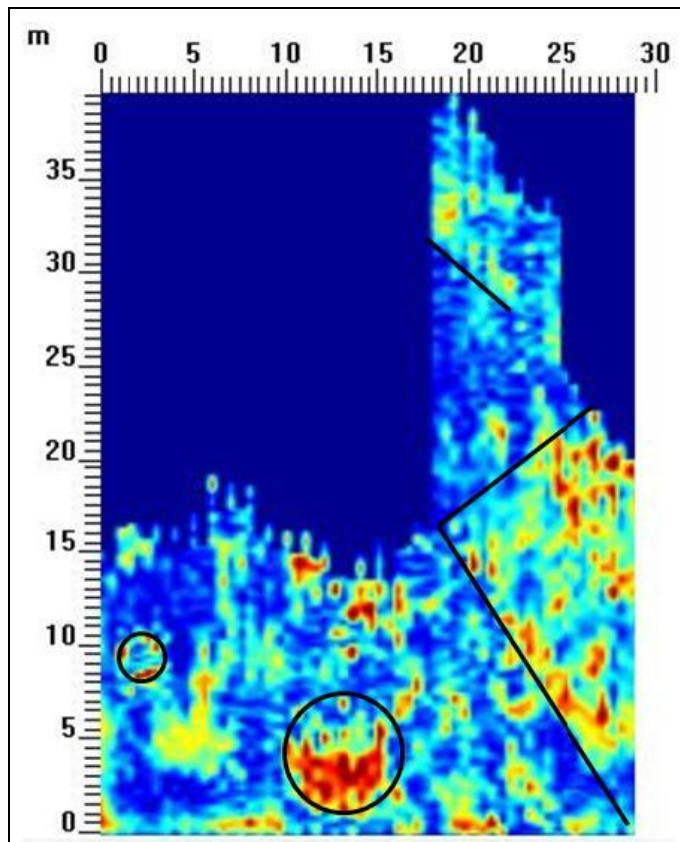


Figure 3.13. a) Uninterpreted GPR data collected with the 100 MHz antenna at St. Mark's in the northern portion of the survey area. b) Uninterpreted GPR data collected with the 100 MHz antenna in the southern portion of the survey area at St. Mark's.



a)



0

32767



b)

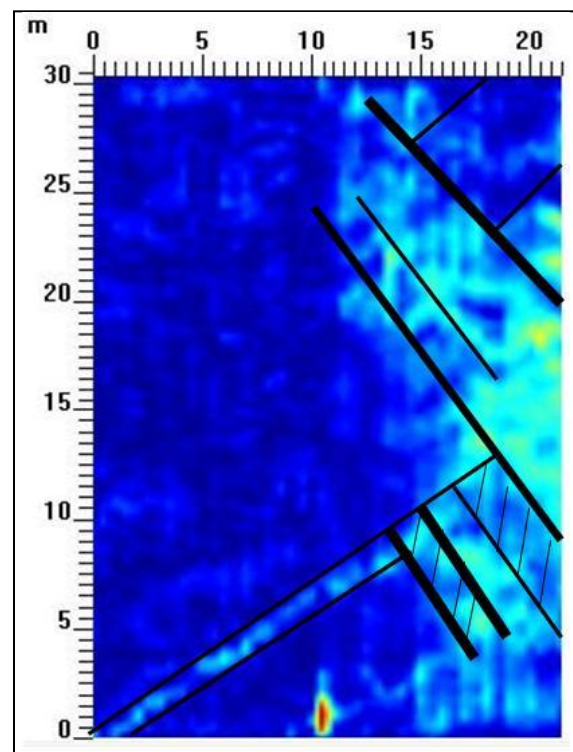
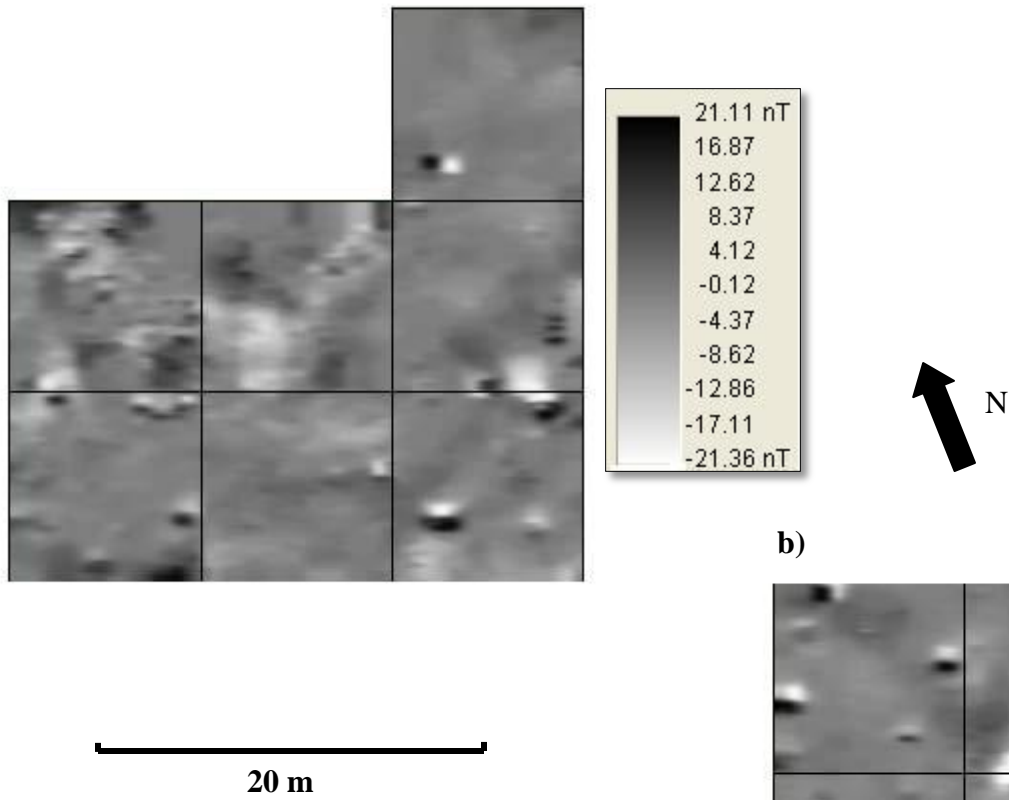


Figure 3.14. Black lines are interpreted linear features, while the circles indicate a distinct target. a) GPR data collected with the 100 MHz antenna at St. Mark's in the northern portion of the survey area. Linear features shown in the data are interpreted to be the remains of religious buildings. b) GPR data collected with the 100 MHz antenna in the southern portion of the survey area at St. Mark's. The fatter lines indicate where two linear features have interpreted to be very close together. This was done arbitrarily to enhance the aesthetics of the data. Linear features in the data are again interpreted to be more ecclesiastical structures.

a)



b)

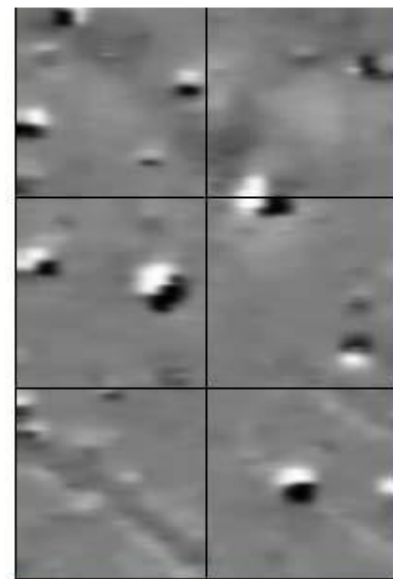


Figure 3.15. a) Uninterpreted magnetic gradiometry data collected at St. Mark's in the northern portion of the survey area. b) Uninterpreted gradiometer data collected in the southern portion of the St. Mark's survey area

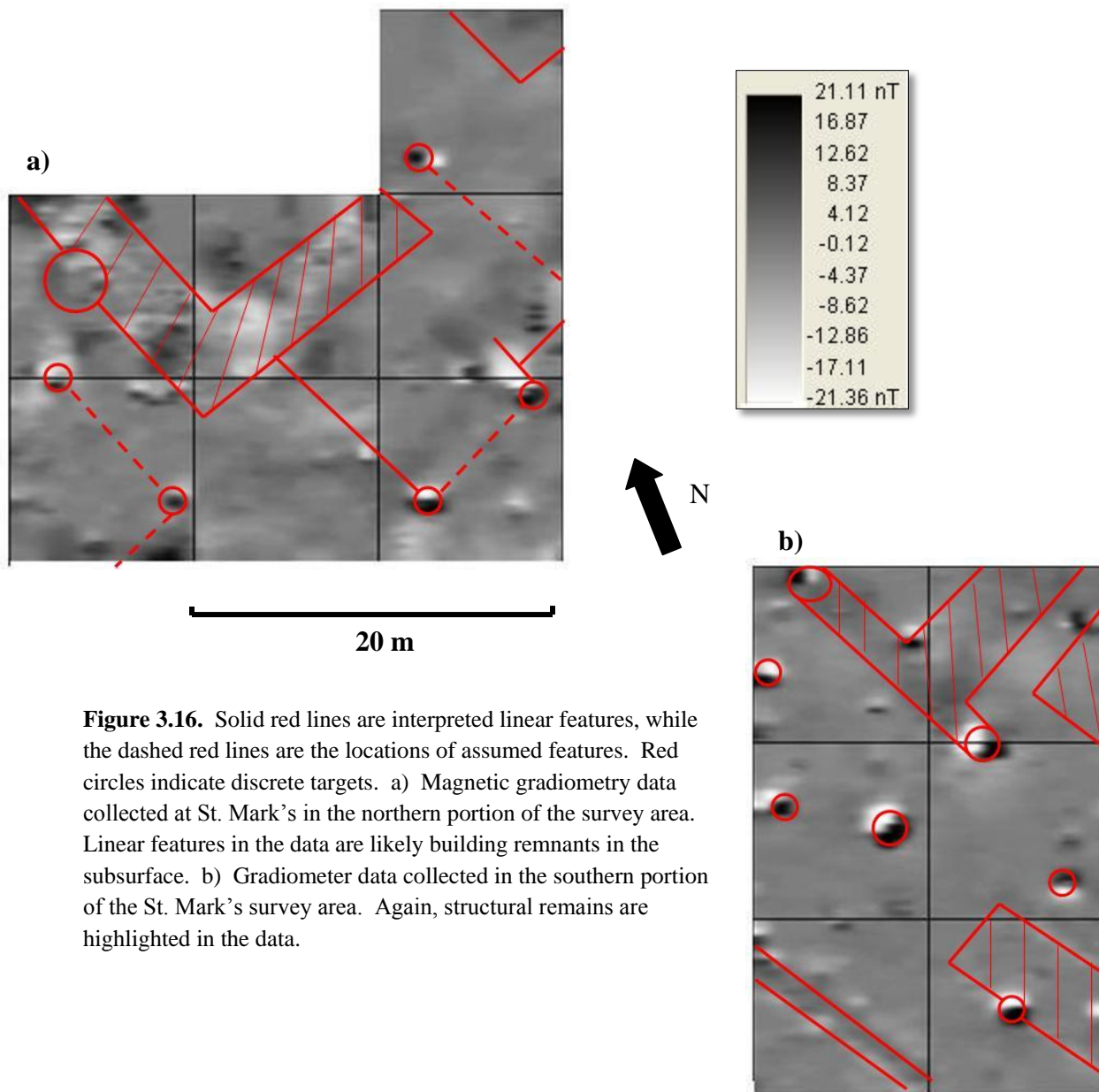


Figure 3.16. Solid red lines are interpreted linear features, while the dashed red lines are the locations of assumed features. Red circles indicate discrete targets. a) Magnetic gradiometry data collected at St. Mark's in the northern portion of the survey area. Linear features in the data are likely building remnants in the subsurface. b) Gradiometer data collected in the southern portion of the St. Mark's survey area. Again, structural remains are highlighted in the data.

3.4 Discussion

To reiterate, Objective I is to perform the first geophysical survey at an active archaeological site on the island of Cyprus in order to aid archaeologists in the development of future excavation plans. Hypothesis I is that near-surface geophysical methods can be used successfully to locate previously unmapped subsurface features at archaeological sites in Cyprus. To test Hypothesis I, it will be necessary to interpret subsurface features in the data that meet certain criteria developed with help from the on-site archaeologist.

Data were collected using two different geophysical surveying techniques: GPR and magnetic gradiometry. Both of these geophysical techniques have proven to be useful aids to excavation, providing a non-intrusive way to view features in the subsurface and supplement known feature data. As per the suggestion of an on-site archaeologist, two main sites were surveyed, locally known as Dreamer's Bay and St. Mark's. These sites were chosen based on the presence of extensive surface remains visible at the surface.

Data from both techniques yielded interesting linear features in the subsurface that had not been previously documented. The data produced by the gradiometer was much clearer and showed more potential features than the GPR data. Differences between data sets can be attributed to the fact that each instrument is recording a different property of the subsurface. The magnetometer records remnant magnetization of features and typically indicates features made out of brick or stone. Conversely, features that show up the most prominently in GPR data are typically soil disturbances. While both data sets are unique, we can say that the features visible in the data are real.

Although there has been no ground truth in this area, we can make some assumptions on what some of the features are by examining the dimensions and orientations of features found at the surface. Features located at Dreamer's Bay are likely warehouses: a few long, narrow buildings are visible at the surface at this site and the dimensions of the linear features in the data are very similar to those of the features at the surface. Building-like structures were also interpreted in the data collected at St. Mark's. While precise identification of these features is currently impossible without excavation, it is likely that features in these data relate to the religious nature of this site.

As a whole, this survey is determined to be a success in locating features in the subsurface and adding to the geophysical database of this site. We were able to successfully test two separate geophysical methods in order to describe the technique that is preferable at this type of site. Because all of the features interpreted to exist have not been excavated, it is impossible to test Hypothesis I with absolute certainty. However, through circumstantial evidence (i.e. comparison with geometry of known structures, etc.), Hypothesis I has been tested to the best of our abilities given existing constraints. The evidence suggests that Hypothesis I is likely correct. It is the opinion of the authors that, given the amount of features seen in these data; these sites merit further investigations both archaeological and geophysical in nature.

Acknowledgements

The authors would like to thank the Jones/Bibee Endowment for providing funding for field work in June 2010. Also thanks go to the Geological Society of America and Geometrics for funding to travel to conferences and present this research. The University of Tennessee Near-Surface and Environmental Geophysics Lab provided the equipment and lab space. Thanks also go to Greg Johnston from Sensors & Software for invaluable technical support, Rachel Storniolo for being a wonderful field assistant and to Frank Garrod and the WSBA Archaeological Society for allowing us to survey on their turf.

References

- Abdallatif, T., El Emam, A.E., Suh, M., El Hemaly, I.A., Ghazala, H.H., Ibrahim, E.H., Odah, H.H., and Deebes, H.A., 2010, Discovery of the causeway and the mortuary temple of the Pyramid of Amenemhat II using near-surface magnetic investigation, Dahshour, Giza, Egypt: *Geophysical Prospecting*, **58**, 307-320.
- Ault, B.A., and Leonard, J.R., 2009, The Akrotiri-Dreamer's Bay Ancient Port Project: Ancient Kourias Found?: In Press.
- Baker, G.S., and Ambrose, H.M., 2007, Ground penetrating radar imaging of a 4th Century Roman Fort, Humayma, Jordan, 4th International Workshop on Advanced GroundPenetrating Radar, 54-59.
- Bartington, Inc., 2009, Bartington Instruments: Magnetic Gradiometers, <http://www.bartington.com>, accessed October 24, 2010.
- Bonomo, N., Cedrina, L., Osella, A., and Ratto, N., 2009, GPR prospecting in a prehispanic village, NW Argentina: *Journal of Applied Geophysics*, **67**, 80-87.
- Breiner, S., 1999, Applications Manual for Portable Magnetometers: San Jose, Geometrics.
- Conyers, Lawrence B., 2004, Ground-Penetrating Radar for Archaeology: AltaMira Press.
- DW Consulting, 2010, ArcheoSurveyor User Manual: DW Consulting.
- Grasmueck, M., Weger, R., and Horstmeyer, H., 2004, Three-dimensional ground-penetrating radar imaging of sedimentary structures, fractures and archaeological features at submeter resolution: *Geology*, **32**, 933-936.
- Hansen, R.O., L. Racic, and V.J.S. Grauch, 2005, Magnetic Methods in Near-Surface Geophysics, in Butler, D.K., ed., *Near-Surface Geophysics*: Tulsa, Society of Exploration Geophysics.
- Heywood, H.C., 1982, The Archaeological Remains of the Akrotiri Peninsula, in Swiny, H.W., ed., *An Archaeological Guide to the Ancient Kourion Area and the Akrotiri Peninsula*: Nicosia, Department of Antiquities, Cyprus.
- Rogers, M.B., K. Faehndrich, B. Roth, and G. Shear, 2010, Cesium magnetometer surveys at a Pithouse Site near Silver City, New Mexico: *Journal of Archaeological Science*, **37**, 1102-1109.
- Solsten, E., 1993, Cyprus: a country study: Washington D.C., Department of the Army.

Wilbourn, D., 2011, DW Consulting: Geophysical Data Services: DW Consulting.

4. Enhancing Usability of Near-Surface Geophysical Data in Archaeological Surveys via Google Earth

This chapter represents a portion of a paper submitted for publication in a GSA Special Paper by Caitlyn M. Williams, Gregory S. Baker, Bradley A. Ault. My contributions to this paper include (i) creation of data management workflow, (ii) creation of an acquisition plan for collection of data, (iii) processing and interpreting the GPR and magnetic data, (iv) integration of data with Google Earth, (v) writing and preparation of the manuscript.

Abstract

Conventional archaeological excavation methods are, by design, extremely invasive and result in culturally sensitive areas being irrevocably altered. For this reason, near-surface geophysical techniques have been incorporated into archaeological investigations to aid in locating buried features and developing specific excavation plans with minimal damage to the sites. The objective of our research was to conduct a geophysical surveying campaign at a test site in Knoxville, Tennessee to develop a workflow for an improved data management methodology which would be applied to data acquired at an active archaeological site in Cyprus.

A multi-tool geophysical survey was completed at the B4 Plot on the University of Tennessee Agricultural Campus using both ground penetrating radar (GPR) and magnetic gradiometry. Using real-time differential corrected GPS data, we systematically imported the images into Google Earth as accurately georeferenced overlays on existing topographic maps and air photos. We added placemarks where we interpreted subsurface anomalies, and exported waypoints for the features into spreadsheet software. We tested this methodology with data from an active archaeological site in Cyprus. Data were displayed in Google Earth and accurate GPS coordinates for features were exported into a spreadsheet file. We were able to share an easily-

accessible final product that was immediately useful and accessible to the archaeologists on the team and the broader archaeological community.

4.1 Introduction

Our research is focused on improving the standard methodologies for actively integrating geophysical data into active archaeological investigations. While numerous multi-tool geophysical surveys have been executed successfully in the past (e.g. Chianese et al., 2010; Kamei et al., 2002), problems have arisen with the data acquisition, processing, and interpretation workflow. Typically, a significant amount of time (months to years) can elapse between the completion of the survey and the actual usage of the data in the field. By developing new techniques for rapid geophysical data integration, archaeologists will have near-real-time access to accurately positioned geospatial data and may be able to revise excavation plans within their current field season accordingly.

4.1.1 Motivation

Archaeology has integrated geophysical surveys as a means to maintain site integrity (e.g. Baker et al., 2007 and Abdallatif et al., 2010). Traditional archaeological surveying methods are extremely invasive to the site area (Wynn, 1986); conventional methods utilize trowels, shovels and occasionally heavy machinery to excavate and these methods essentially destroy the site area for the sake of research. Thus archaeologists have begun using near-surface geophysics as a non-invasive means to detect features or artifacts in the subsurface.

Within the past decade, there has been little change in archaeogeophysics, with the exception of improving instrumentation. Current limitations to geophysics are due to the time and money needed to complete a survey and process the data. Generally, there is only a finite amount of time to complete a survey within the given field season and it costs money to hire field personnel, rent equipment, and ship it to the site to be surveyed.

Another problem with the process is that there is often a large gap in time between data acquisition and their physical use in the field; data that can be easily used and shared enhance the flow of information. There is a distinct disconnect between archaeologists and geophysicists in the field. Geophysicists are more concerned with the survey design, data acquisition tools, and processes, whereas an archaeologist is more interested in the presence (or absence) of discrete targets in the subsurface (i.e. artifacts).

Figure 4.1 represents a traditional workflow for a geoarchaeological survey. The initial step is that survey boundaries are delineated with help from an archaeologist, typically based on the presence of surface remains, and GPS coordinates are taken for the survey area. Then, a geophysical survey is planned and executed with one or more techniques, and data are uploaded onto a field computer. Software specific to each instrument is then used to process the data, often involving multiple, expensive programs. Data must then be interpreted in order to identify any subsurface anomalies, and interpretations are made at the discretion of the geophysicist in a

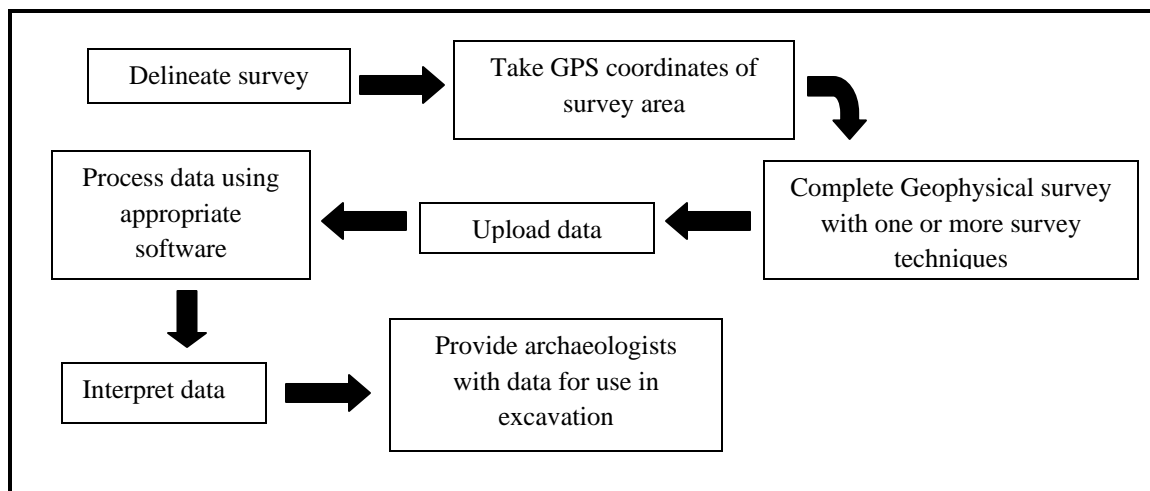


Figure 4.1. Diagram showing the conventional workflow for geophysical data acquisition at an archaeological site. The disconnect in geoarchaeological surveying often occurs with the last three steps of the workflow; commonly a long time lapse in completing the final two steps makes data less effective.

variety of software packages. Finally, the data are given to the archaeologist in some format and then he or she must decipher it with or without the help of the geophysicist. It is this disconnect between archaeologist and geophysicist which undermines the usefulness of the data presented.

4.1.2 Objective II

To reiterate, Objective II of this research is to identify inefficiencies in the geophysical surveying process. Specifically, we are attempting to streamline the data acquisition, processing, and interpretation workflow that will allow for near real-time feedback between archaeologist and geophysicist. In order to accomplish this aim, we incorporate Google Earth with data from a control site in Knoxville, Tennessee, to create an improved geophysicist-archaeologist interface. By using Google Earth, archaeologists are provided with near-real-time feedback about the locations of possible features in the subsurface.

4.1.3 Hypothesis II

Hypothesis II is the effectiveness and efficiency of multi-tool, near-surface geophysical surveys for archaeological applications can be improved by displaying data with accurate GPS coordinates using a virtual globe.

4.2 Test Study I – B4 Plot, Knoxville, Tennessee

The purpose of this primary study was to test the viability of Google Earth as an effective platform for displaying near-surface geophysical data and to test its accuracy in providing precise GPS coordinates to locate targets. A geophysical survey was completed during the

spring of 2011 at a control site on the University of Tennessee campus in order to test a new data management workflow.

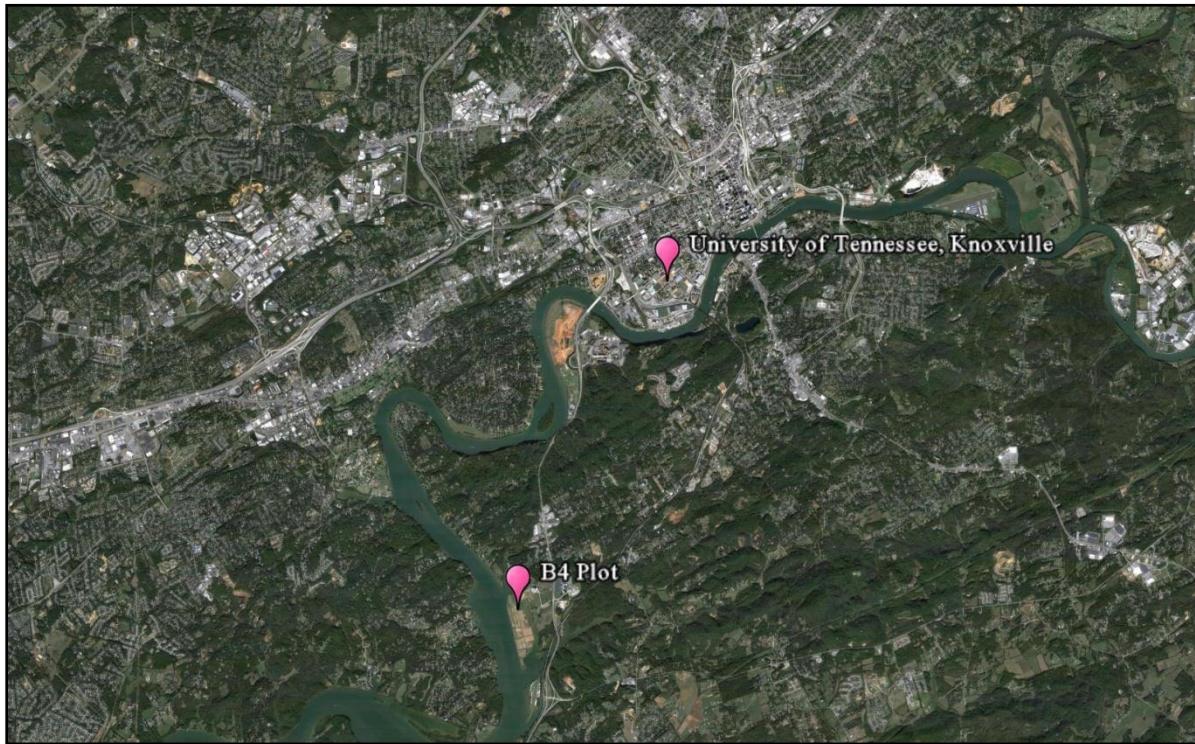
4.2.1 Site Background

The B4 Plot is located between Alcoa Highway 129 and the Tennessee River. It lies approximately two miles south of the University of Tennessee main campus in Knoxville, Tennessee, on the Experimental Agricultural Research Station (Figure 4.2ab). This site is also referred to as the Environmental Hydrology and Geophysics Teaching and Research Site and is used for upper-level undergraduate and graduate hydrogeology field courses as well as the TINGS (Tennessee Intensive Near-surface Geophysics Seminar) course and a few engineering courses (William E. Doll, pers. comm.).

Soil conditions across the site vary from residual soils developed directly on Ordovician sedimentary bedrock (near the highway) to loamy soils developed on alluvial terraces at different elevations above the river. These soil types are common to east Tennessee and are important for forestry and agriculture. Relative permittivity of loamy, dry soil lies anywhere in a range from four to six (relative permittivity is unit-less) and for loamy, wet soil it ranges from 15 to 30 (Baker et al., 2007).

Silt or sandy silt dominates the top 6.1 m of strata, which overlie approximately 0.9 to 1.5 m of fine to medium sand and cemented sand. Sediments are underlain by fractured shale and limestone bedrock. Bedrock is Ottossee Shale, which is a Middle Ordovician member of the Chicamauga Group. As a whole, it is generally characterized by fine-grained calcareous shale with some interbedded limestone. As depth of penetration did not surpass six meters, bedrock was not considered to be a key factor in this investigation (William E. Doll, pers. comm.).

a)



b)



Figure 4.2. a) Google Earth image showing the location of the B4 Plot in relation to the University of Tennessee main campus in Knoxville, Tennessee. b) Photo taken of the B4 Plot, looking to the south. The fenced-in hydrogeology station can be seen on the right-hand side of this photograph.

Plot B4 contains 24 known targets buried in the spring of 1999. The locations of the objects are accurately known as dGPS coordinates for each target were documented upon burial and data have been recorded on the size, shape, and orientation of each object. Depths to buried objects range from 0.30 to 1.11 m. It is assumed that there has been sufficient time for the ground to settle, and any major disturbance to the subsurface and resulting signal in the data is minimized.

4.2.2 Methodology

4.2.2.1 Geophysical Techniques

GPR and magnetic gradiometry were used together as a part of a comprehensive multi-tool survey. These techniques have been successfully used in previous geoarchaeological surveys (e.g. Chianese et al., 2010; Kamei et al., 2002) and the equipment was readily available for use in this investigation. A Pulse EKKO Pro Smart Cart (manufactured by Sensors and Software) was used to complete the GPR survey. This particular model was chosen since a unit is owned by the University of Tennessee Near-Surface and Environmental Geophysics Lab, and the Smart Cart is a versatile piece of equipment which can be used to survey in a variety of terrains. The entire area was surveyed with the 100 MHz antenna in order to obtain the best possible depth of penetration and to maintain consistency with the data. For the magnetic survey, a Bartington Grad 601-2 Dual Gradiometer was used. In addition to the field crew's familiarity with its operation, the Bartington gradiometer has a reputation for being extremely portable and easy to use in the field. The B4 Plot has an area of 40 m by 50 m and the entire area was surveyed with the exception of a small fenced-in area in the southwest corner of the survey area.

4.2.2.2 Data Collection

For the magnetic survey, the site area was divided up into three 20 m by 20 m grids to ease with data processing. The Bartington has strict, pre-set survey parameters and the whole area could not be surveyed at one time. Data were collected for each grid in an alternating pattern. We collected GPR data in a similar alternating pattern, but kept spacing between transects constant at 0.5 m. Data over the entire 40 m by 50 m were collected as one cohesive grid and the fenced-in area was simply omitted from the survey area by making lines 15 through 37 shorter than the others (Figure 4.3).

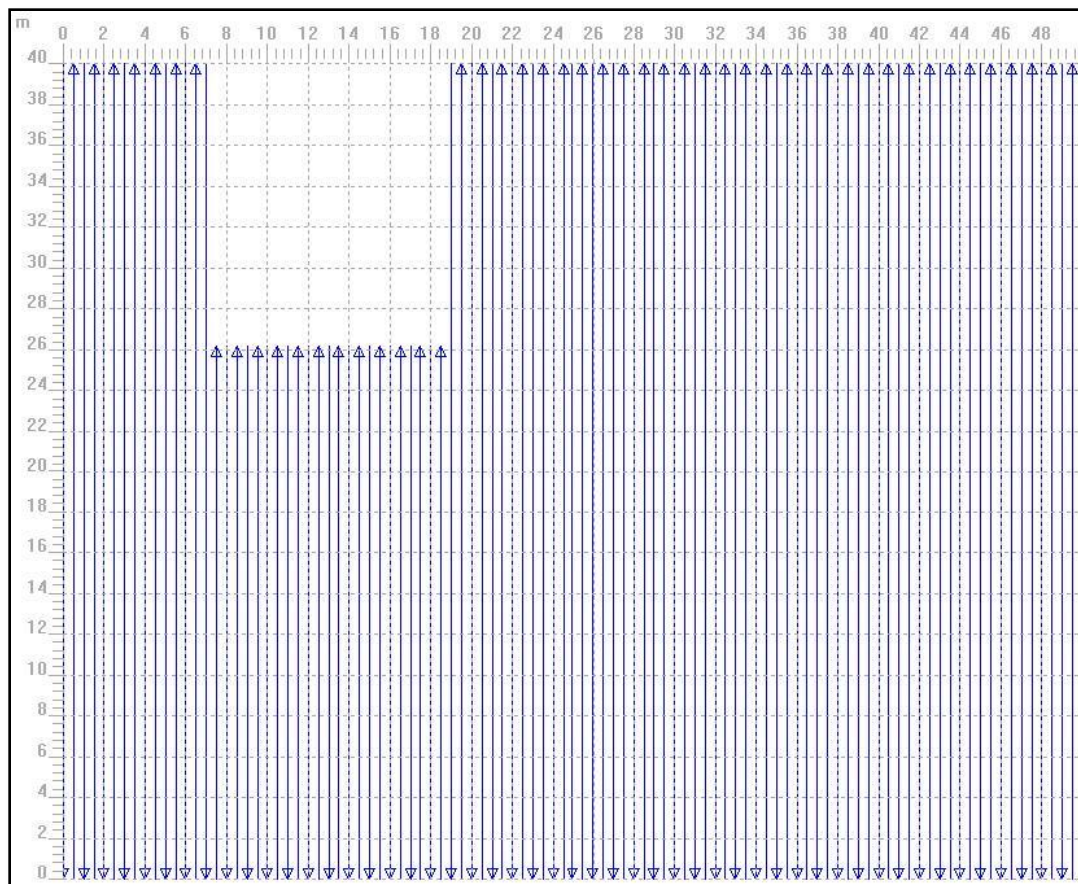


Figure 4.3. Image of the survey geometry for GPR data collection at the B4 Plot. Note the zig-zag pattern in which the data were collected and the shorter transects run around the fenced-in area.

4.2.2.3 Data Processing

GPR data were first imported into a program called GFP Edit (Sensors & Software) as Y-Lines with spacing between transects set to 0.5 m. The length of profiles 1-14 and 38-99 was set to 40 m and the length of lines 15-37 was set to 26.15 m to allow for the omission of the fenced area which was not surveyed. The start direction of every other line was flipped to account for the zig-zag pattern of data collection. Once we created the GFP file, we opened it using EKKO Mapper 3 (Sensors & Software). Slice resolution was set to 0.50 m and the velocity was set to 0.086 m/ns.

Magnetic gradiometer data were processed using proprietary ArcheoSurveyor software (DW Consulting). Functions of destagger and clip were applied to get the clearest data possible. Destaggering compensates for data collection errors caused by the operator starting recording of each traverse too soon or too late. It shifts each traverse forward or backward by a specific number of intervals (DW Consulting, 2010). Clipping replaces all values outside a specified minimum and maximum with those values. This process removed extreme data points (created by metallic objects at the surface, like well heads) and highlighted the fine details in the data.

4.2.3 Geophysical Results

In looking at these data, we were primarily concerned with high-amplitude anomalies that presented themselves as hot colors in the data sets. In the GPR data there were a few discrete anomalies that were not chosen as targets. Primarily, at the B4 Plot, there are metallic well-heads at the surface, which show up very prominently in the data. As we have the GPS coordinates for the locations of these objects, and they were visible on the surface, it was not difficult to rule them out as possible subsurface features. There were also two linear features in

the GPR data that were not chosen as targets. These features were a result of the transmitting antenna ‘mis-firing,’ and the locations of these transects were accurately recorded in a field notebook for later use.

In the magnetic data, we were mainly concerned with the dipole anomalies present. These anomalies are characterized by having both a positive (red) and a negative (blue) anomaly. Any anomaly that did not have this pairing was not interpreted to be a feature.

Differences between the two data sets can easily be explained by the presence of both metallic and non-metallic buried objects. The GPR is capable of detecting all targets at the B4 Plot, while the magnetometer is only able to detect metallic targets. Because of this fact, and because we know for certain that there are both metallic and non-metallic targets buried there, we can say that all anomalies are real.

4.2.3.1 GPR

The depth slice was selected from 1.250-1.500 m that shows the most features buried in the subsurface (Figure 4.4ab). Out of the 24 buried targets at the site, a total of 15 targets were identified in the data. The image was saved as a JPEG for ease in later data manipulation.

4.2.3.2 Gradiometry

The three 20 m by 20 m grids were stitched together as one composite grid and a total of 13 targets were identified out of 24 (Figure 4.5ab). The composite grid was then saved as a JPEG file for later ease with data manipulation.

4.3 Incorporating Google Earth with Near-Surface Geophysical Data

Ground overlays are most appropriate when dealing with geoarchaeological data as they are images draped onto the terrain of Google Earth satellite images and follow the natural

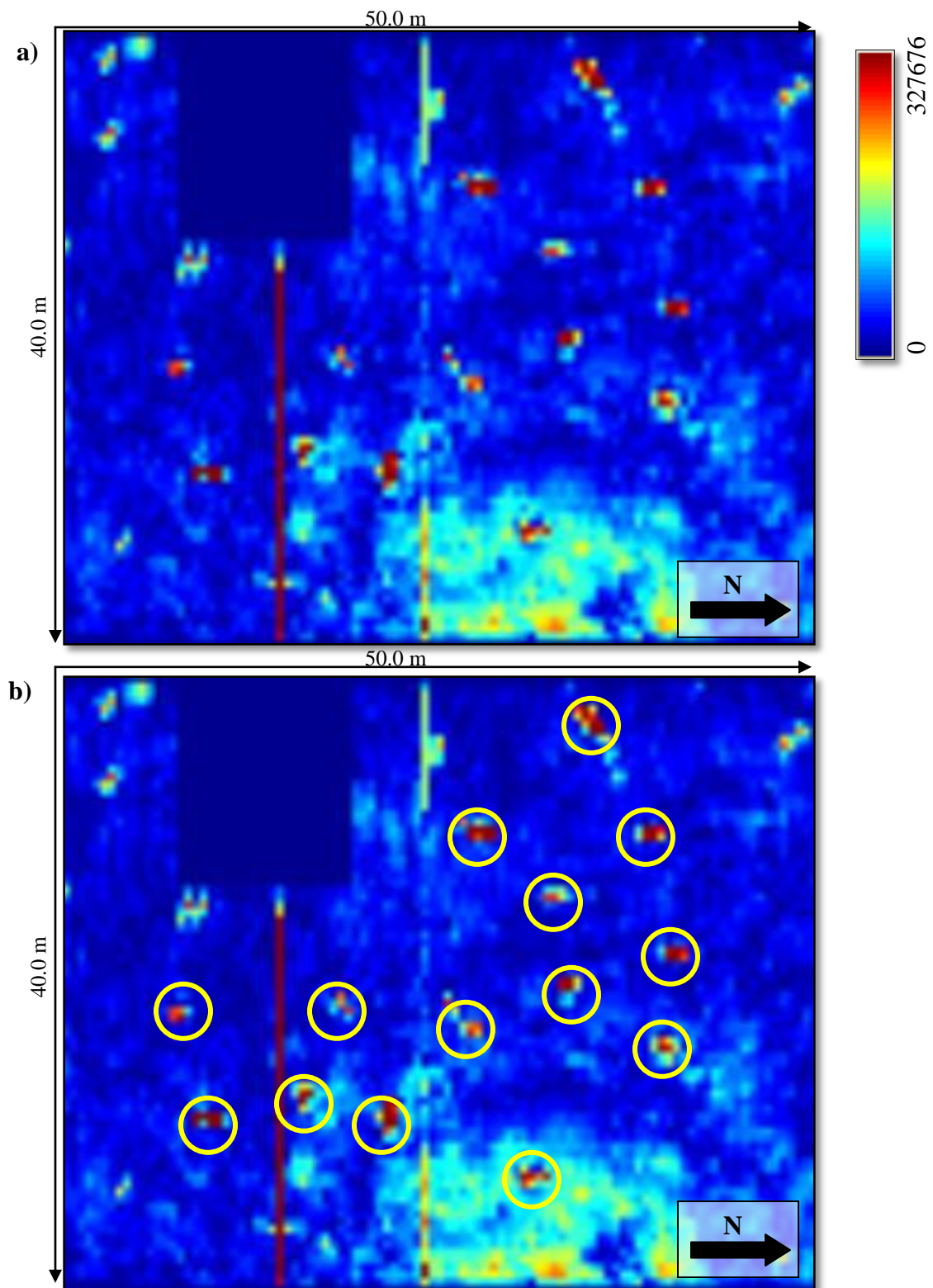


Figure 4.4. Images of the GPR data collected at the B4 Plot. a) Uninterpreted GPR data. The two horizontal lines in the center of the data image are attributed to problems with the transmitting antenna. The dark blue rectangle is representative of the fenced-in area where no data were collected. b) Targets are circled in yellow on the interpreted data.

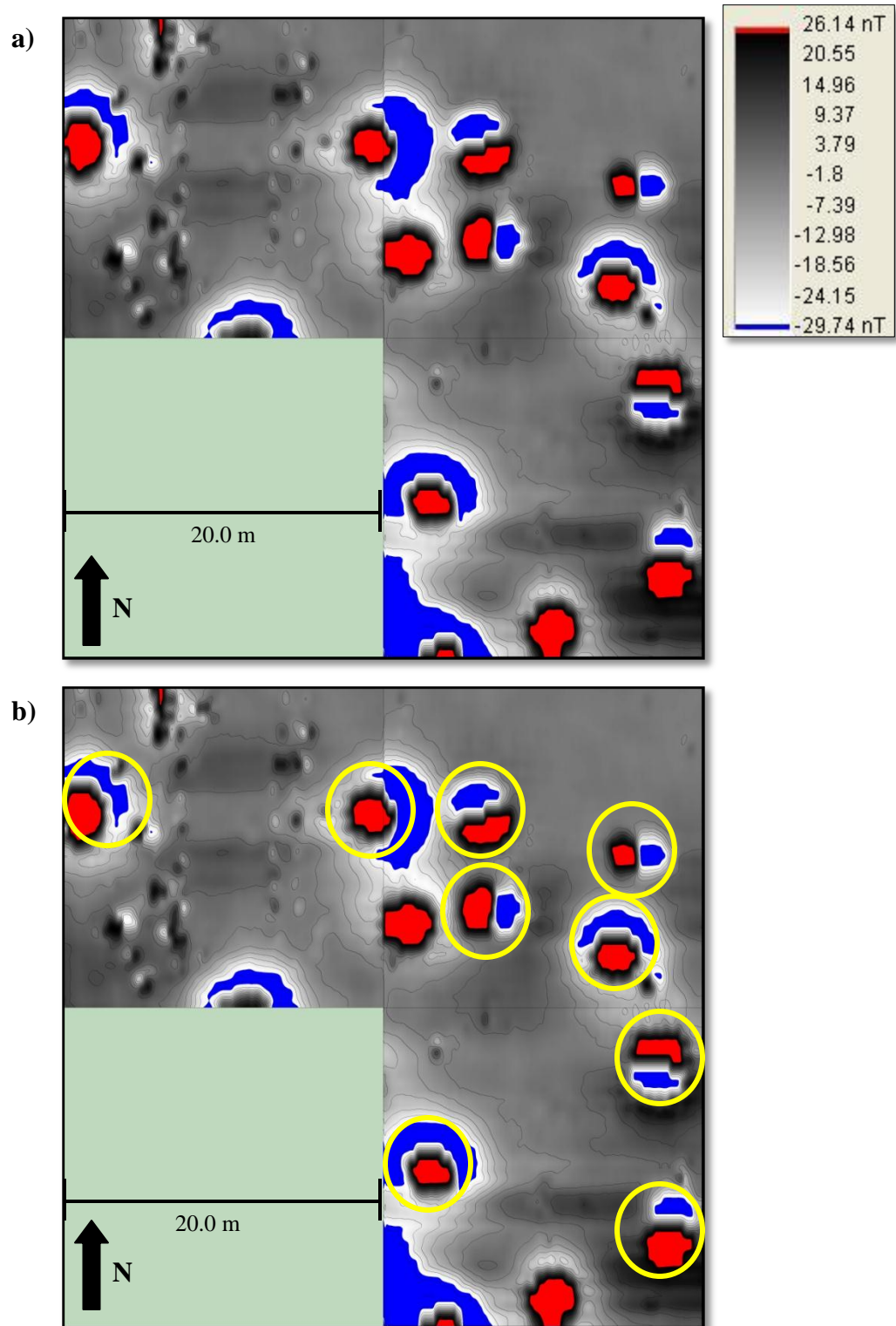


Figure 4.5. Image of the magnetic data collected at the B4 Plot. a) The uninterpreted magnetic data. b) Possible Targets are circled in yellow in the interpreted data. The green rectangle in the lower left of the photo is the location of the fenced-in area where no data were collected.



Figure 4.6. Placemarks added to the Google Earth satellite image delineating the survey boundary at the B4 Plot.

curvature of the earth. Images can be in a variety of formats (e.g. JPG, TIFF, BMP etc.), which is one reason Google Earth is such a useful and versatile tool for data display (Werneck 2009).

Displaying data in Google Earth is a relatively simple process. To begin, the latest version of Google Earth was installed on the field laptop (at the time of this research, Google Earth 6 was the latest version of the software). As a default, Google Earth will display latitude and longitude coordinates as degrees, minutes, and seconds, but for our purposes the coordinate system was changed to display in decimal degrees for manipulation ease. Placemarks were

created for the corner points of each grid using the GPS data uploaded from the TerraSync software (Figure 4.6). Icon style and size was changed to the user's preference in order to make the icons easily visible on the map. Once all placemarks were created, they were saved in a folder under the Places menu.

Creating overlays is the next step in displaying data. For ease in setting up an overlay, all images of data should be saved as the same file type and in the same folder at a specified location on the computer. To create a map of the data, click the overlay button and browse for the location of the appropriate photo in the 'Link' space. While the overlay menu is still open, green corners appear on the image and are used to re-size and rotate the images so that it is georeferenced to the GPS coordinates. The opacity is not changed and no extra description was necessary. All files were again saved in their own folder in the Places menu.

Interpretations are made on these overlays using either the path or placemark option depending on the geometry of the features. In this example, placemarks were used as the features were not linear. All interpretation placemarks were saved in their own folder in Google Earth. Locations were saved as a KMZ archive on the desktop. A KMZ archive is a collection of files used to create a single KML presentation which includes all local files referenced in each KML file. The KMZ archive is a self-contained package that does not need to be hosted on a network server and can be emailed and shared easily as files are compressed. Final interpretations from Google Earth are saved as Keyhole Markup Language (KML) files for export. KML is an extremely versatile programming language that can be read by a variety of applications (e.g., Microsoft Virtual Earth, ESRI ArcGIS Explorer) and these files can easily be emailed between users and opened in Google Earth (Werneck, 2009).

As the focus of this study is to make geoarchaeological data more user friendly, Microsoft Excel was used to display the coordinates of features exported from Google Earth. To import a KMZ file into Excel, data are imported as XML data (XML stands for Extensible Markup Language and it is a coding language that encodes documents in a machine-readable form). After selecting the appropriate file, data are displayed in an easy-to-read table. Some cleanup is required to condense data to the pertinent information, but that task is easily accomplished by deleting the rows and columns that are not needed.

Once data are organized into latitude and longitude columns, coordinates can be imported as waypoints into many GPS software programs. The GPS used in this investigation was a Trimble Ranger and coordinates were uploaded to the Pathfinder Office software using the ASCII import function. The GPS can then be used to physically map out the locations of features while in the field and their locations marked with PVC flags or spray paint. By mapping features on the surface archaeologists can alter excavation plans as needed in order to have the most efficient field season.

4.3.1 GPR Data

The GPR data shown in Figure 4.5 were displayed in Google Earth using the method described above. Placemarks were added where targets were seen in the data (Figure 4.7) with the placemark being located on the brightest pixel of the anomaly. Additional placemarks were added for the actual location of the objects based on the information recorded in 1999, when the targets were buried. Having both sets of data on the same map allowed for the distance between buried and measured locations to be calculated by using the ruler function in Google Earth.

Using the distances obtained from Google Earth, error was calculated in a spreadsheet in order to specify the in-line and cross-line error and how accurate Google Earth is as a platform for displaying near-surface geophysical data and exporting waypoints. From each data set, both in-line and cross-line error were calculated. Using the manner in which the data was collected, we set east as the positive Y-direction and south as the positive X-direction (north and west were the negative X and Y directions, respectively). Error values were calculated by measuring the distance from the interpreted target to the real target, first in only the X-direction and then in the Y-direction, and then the average of those values was calculated as well as two standard deviations in order to have a 95% confidence level (calculations were done using Microsoft Excel). The average in-line error was calculated to be $0.0038 \text{ m} \pm 1.08 \text{ m}$, and the average cross-line error was calculated to be $-0.22 \text{ m} \pm 1.66 \text{ m}$. Refer to table 2.1 for an explanation of the types of in-line and cross-line error that can occur with using the GPR.

4.3.2 Gradiometer Data

A total of 13 targets were identified in the magnetic data and each was assigned a yellow placemark (Figure 4.8). Using the same method as given in the above section, in-line and cross-line error were calculated for this data set. The in-line error was calculated to be $0.075 \text{ m} \pm 1.36 \text{ m}$ and the cross-line error was calculated to be $0.28 \text{ m} \pm 1.47 \text{ m}$. Refer to table 2.2 for an explanation of the types of in-line and cross-line error that can occur with using the magnetic gradiometer.

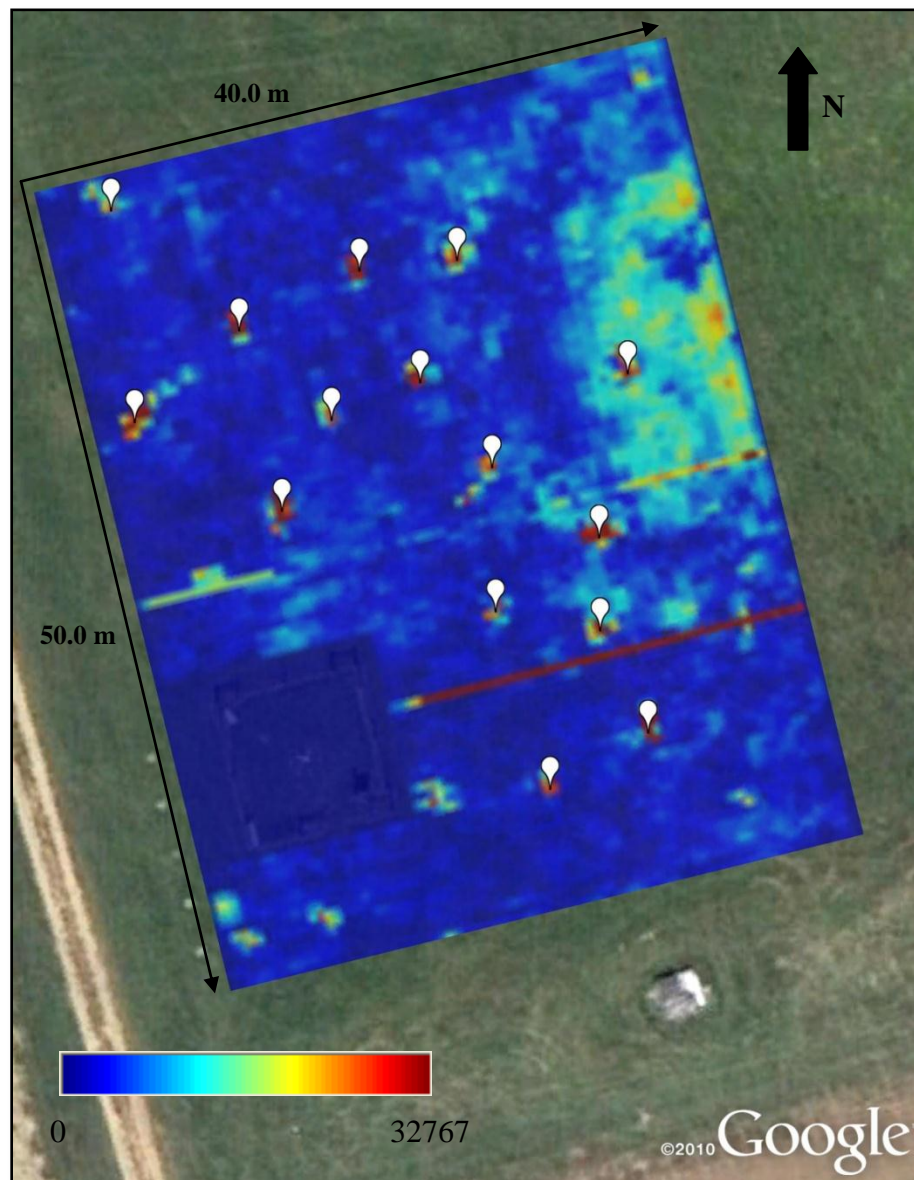


Figure 4.7. Georeferenced image of GPR data displayed in Google Earth. Targets are identified by white placemarks. Distance was measured between these and the actual location of targets and then error was calculated.

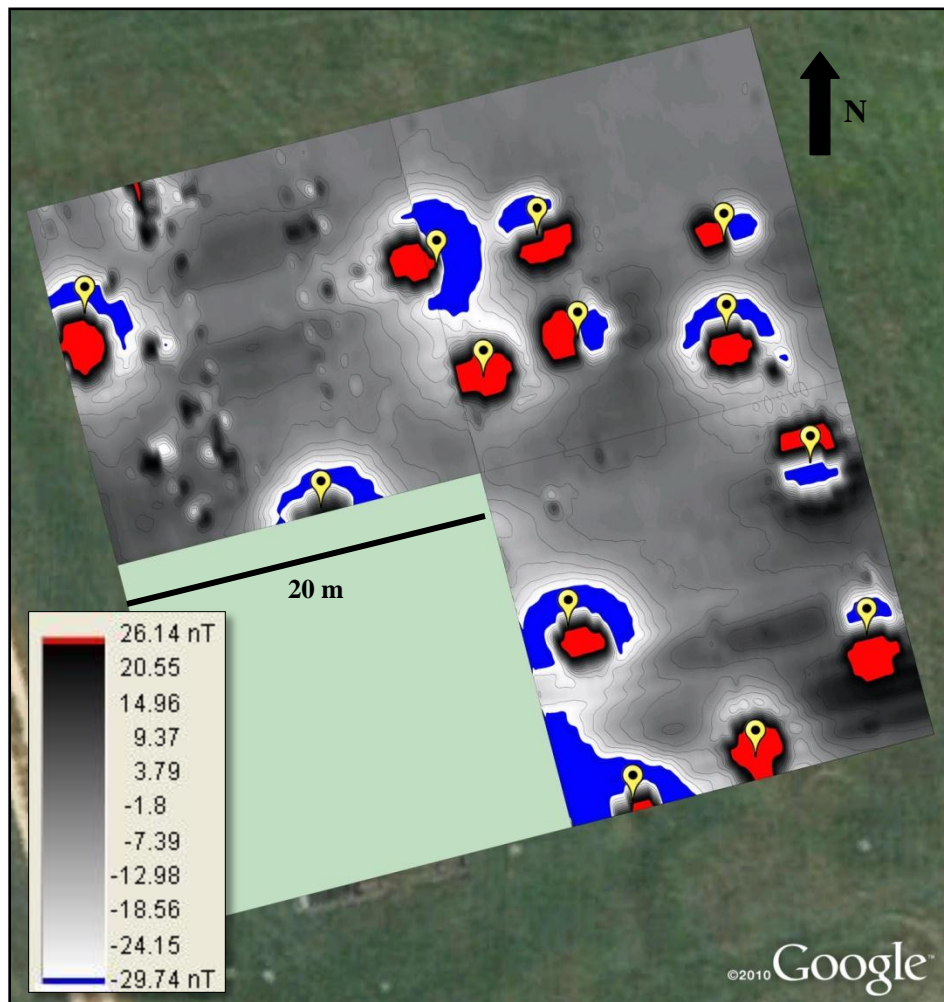


Figure 4.8. Georeferenced image of magnetic data collected at the B4 Plot and displayed in Google Earth. Yellow placemarks indicate the location of possible targets.

4.4 Test Study II – Akrotiri Peninsula, Cyprus

The purpose of this second study was to test the newly developed data management workflow on archaeological data collected in Cyprus in 2010. Surveying on the Akrotiri Peninsula took place from June 9, 2010 to June 13, 2010. For information on site description, data collection and data processing, refer to chapter three.

4.4.1 Importing Cyprus data to Google Earth

All data sets for Dreamer's Bay and St. Mark's were imported and georeferenced in Google Earth as described previously. GPS coordinates were displayed as pink placemarks and overlays were made slightly transparent in order to let some of the satellite image show through the data image. Interpretations were made on overlays using the path option as features found were linear (e.g. building walls/foundations) as opposed to single targets. Paths are created by pointing and clicking where features are in order to highlight them. The color of the paths was set to red and the width was set to 2.0 to make the interpretations easier to see. Once the interpretations were made, the paths were saved in their own folder on the Places menu. Placemarks were added at key locations along the paths (i.e. beginning and end of a path or where paths intersected) to roughly map out the locations of subsurface features. All placemarks were saved in their own folder and this folder was saved as a KMZ archive on the Desktop. This file was treated in the same fashion as the data points collected at the B4 Plot and coordinates for the locations of subsurface features were displayed in Excel.

Looking at the data images one might notice, especially at Dreamer's Bay, that some of the images appear to be skewed relative to the background image (e.g. some data appearing to be in the Mediterranean Sea). This offset is due to the error in the satellite images uploaded by

Google. As this particular location is on an Air Force Base, some intentionally introduced error was expected as security is a top priority. It is important to note that while the satellite photos may be skewed with respect to the data, the data images are accurately georeferenced to the correct dGPS coordinates. Maps were created for use by the consulting archaeologist where the image was correct, but the dGPS coordinates were wrong in order to prepare a report for the Cypriot Department of Antiquities illustrating the general location of features in the subsurface, however, those are not displayed here. The purpose of these maps presented is to extrapolate accurate data points for features located in the subsurface.

4.4.1.1 Dreamer's Bay

All gradiometry data sets were displayed in Google Earth while only two GPR data sets were used. The gradiometry data showed many more subsurface features than the GPR data did.

4.4.1.1.1 Magnetic Data

The magnetic gradiometry data for Dreamer's Bay showed many possible structures in the subsurface. Looking at the uninterpreted data (Figure 4.9), linear areas of lighter gray shading have been interpreted to be the remnants of warehouse-like buildings as they appear to have similar dimensions to the warehouses already exposed at the surface. These remains were highlighted using the path tool as described above in order to spatially describe their locations in the subsurface (Figure 4.10). Waypoints from the endpoints and corners of each feature were exported to Excel and displayed in columns of latitude and longitude. The data will potentially be useful to archaeologists in developing an excavation plan for this site.

4.4.1.1.2 GPR Results

Results from the GPR were not as spectacular as those of the gradiometer (Figure 4.11). Total depth of penetration was approximately 1.5 m for the entire area. Due to the presence of

salt and the calcareous nature of the soils the signal attenuated quickly and resolution for the most part was fairly poor. Despite these setbacks, a few linear features can be interpreted from the data (Figure 4.12). As with the magnetic data, waypoints for the endpoints and corners of each feature were exported to Excel and displayed in an easy-to-read table.

Figure 4.13 shows both data sets displayed together, with the GPR set to 40% transparency. It is important to remember that both instruments will detect different changes in the subsurface. The magnetometer is sensitive to changes in the magnetic susceptibility of the target versus the background material, while the GPR images contrasts in the physical properties that are likely created by disturbances in the sediment. While all features are considered real, we can hypothesize that those detected by the magnetometer are likely walls or remnants of buildings and that those detected by the GPR are trenches dug for foundations or storage.

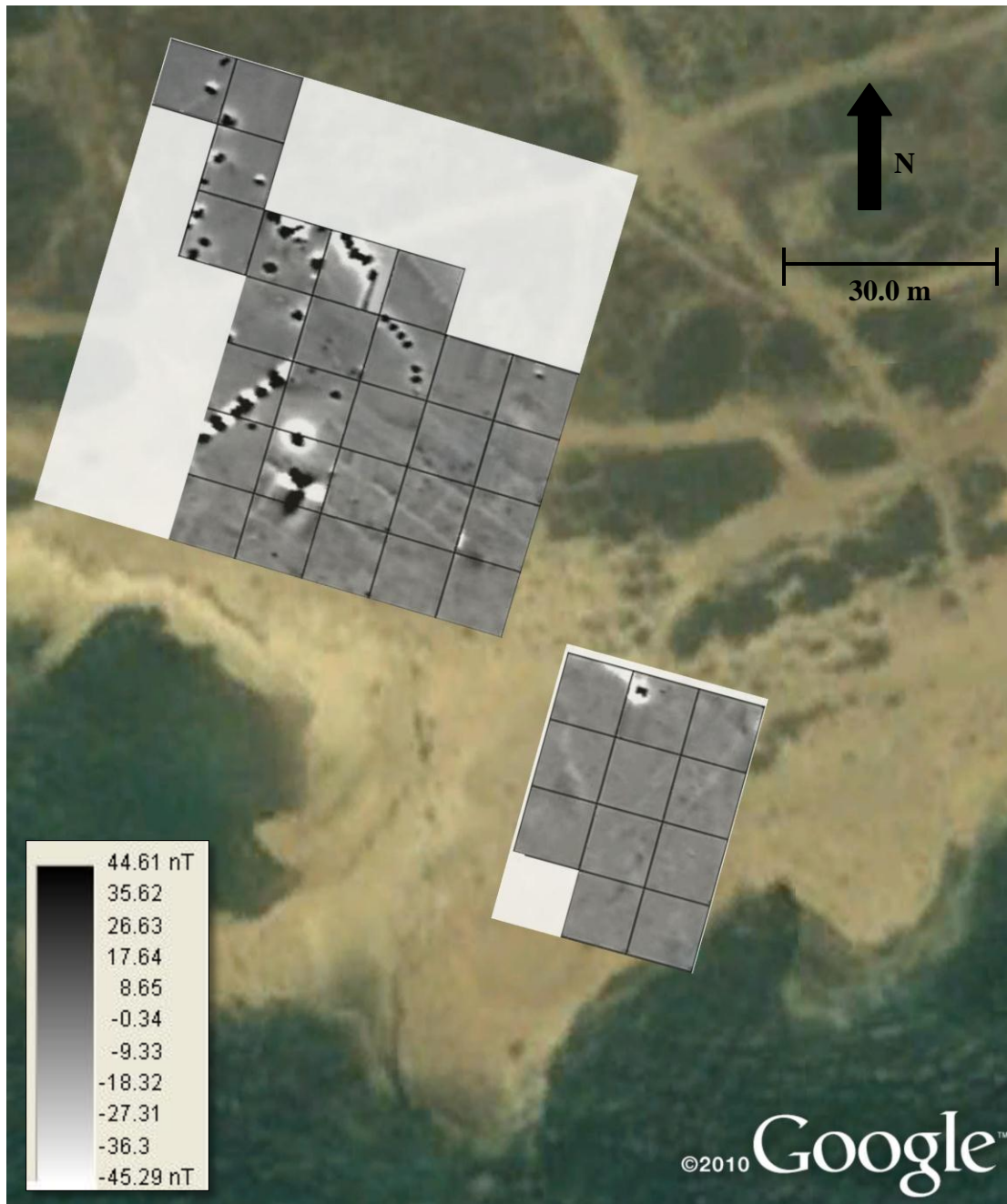


Figure 4.9. Magnetic gradiometry data for the site at Dreamer's Bay. Black and white dipoles that show up in the data were interpreted to be metallic debris left on the surface from historic military operations. The features of interest are the light gray linear features seen in the southeast portions of the data. Each small square represents a minor grid and is 10 m by 10 m.

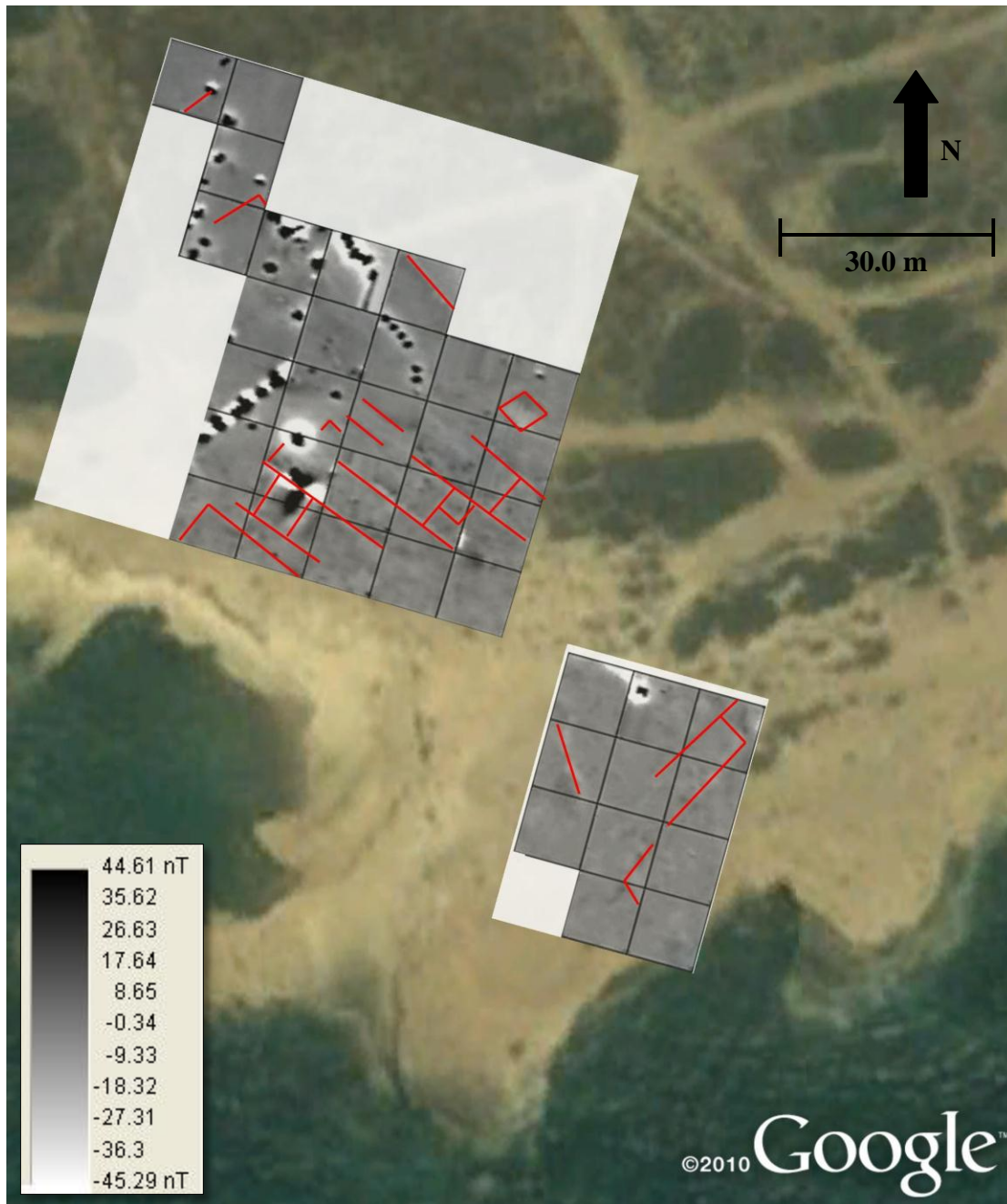


Figure 4.10. Magnetic data from Dreamer's Bay with features highlighted using the path tool in Google Earth. The solid red lines are interpreted linear features. Each small square represents a minor grid and is 10 m by 10 m.

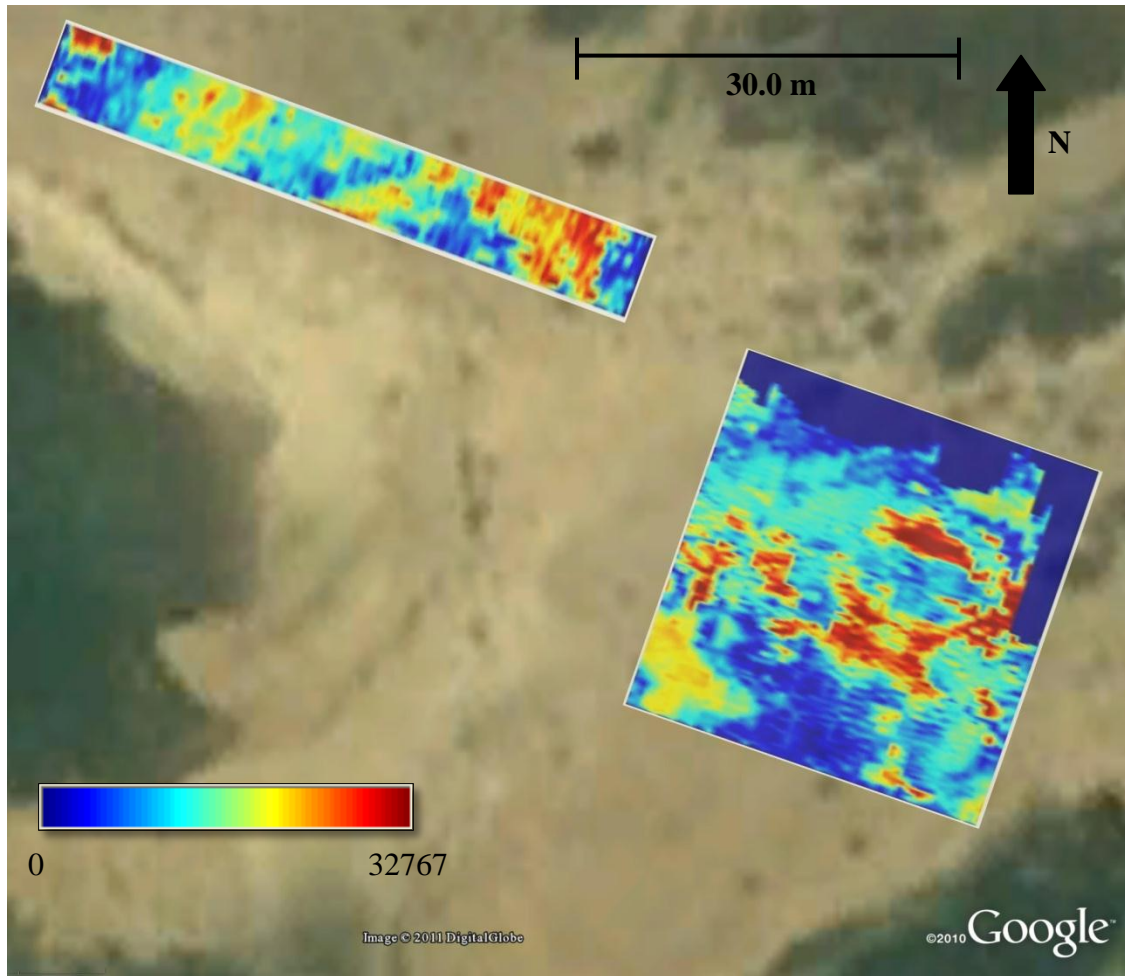


Figure 4.11. Uninterpreted GPR data collected at Dreamer's Bay with the 100 MHz antenna. Data were accurately georeferenced in Google Earth using GPS data collected at the site.

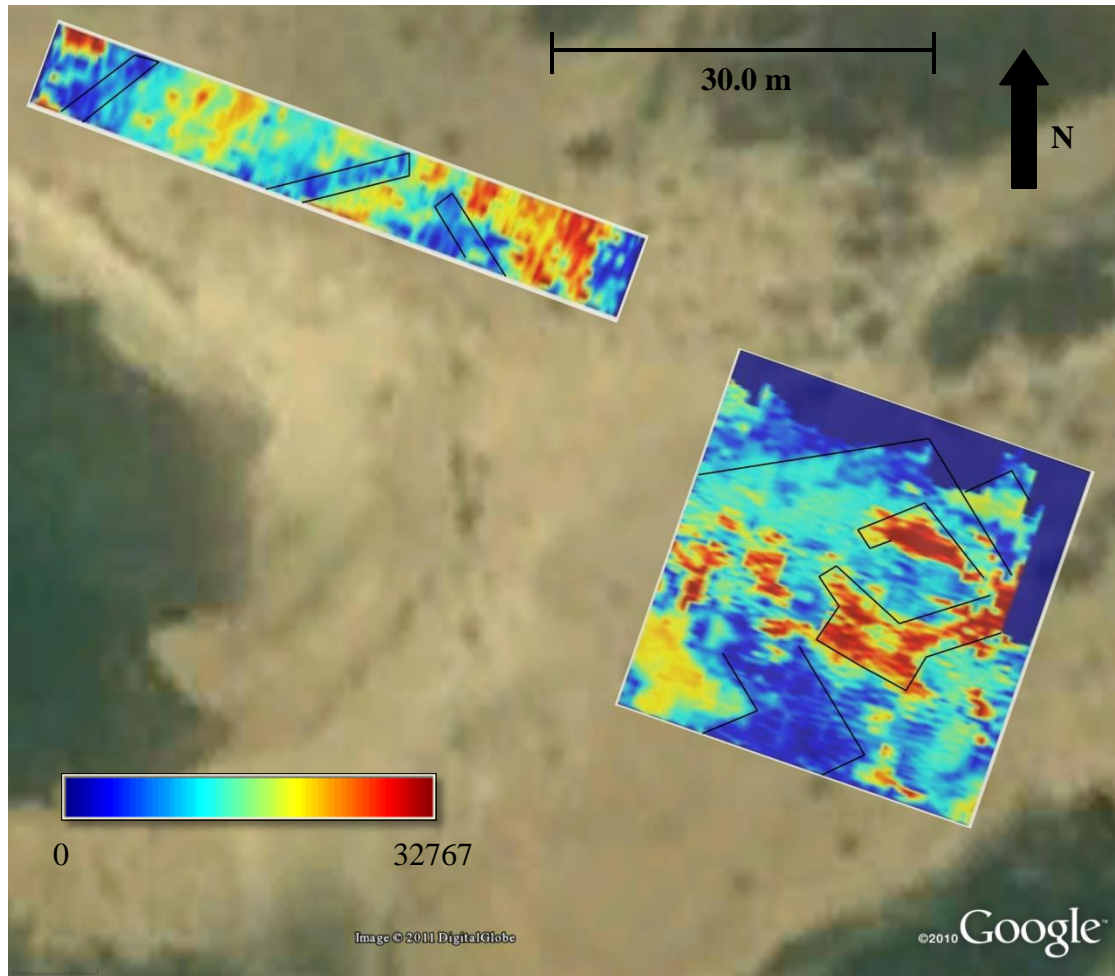


Figure 4.12. Interpreted GPR data collected with the 100 MHz antenna at Dreamer's Bay. Linear features are highlighted using the path tool in Google Earth. Black lines indicate interpreted linear features. GPR data show fewer features than the magnetic data as the survey area was smaller and depth of penetration was poor.

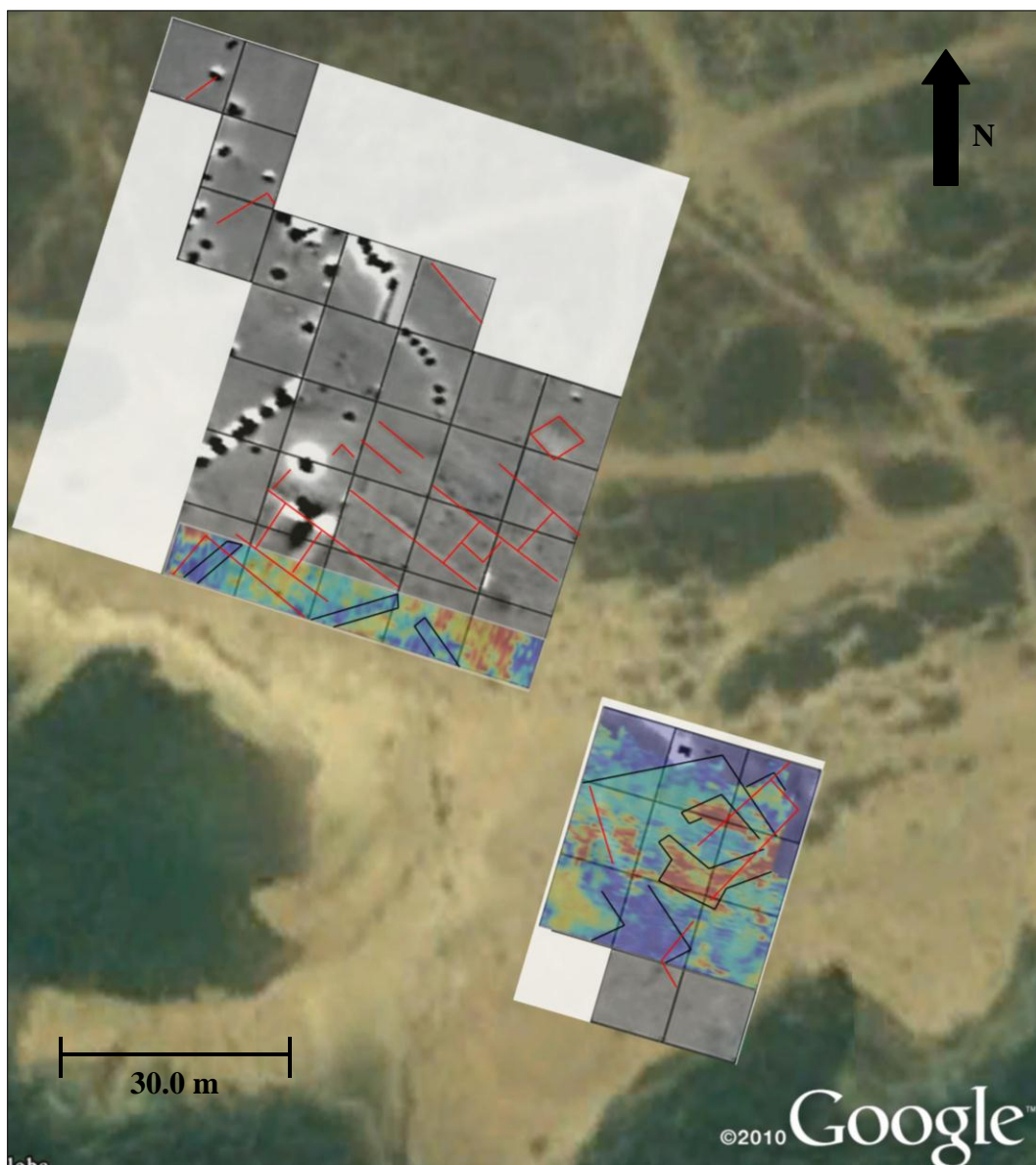


Figure 4.13. Google Earth image displaying the geometry of features found in both data sets. Transparency of the GPR data was set to 40% in order to be able to see both sets of data. All features seen in the data are interpreted to be real, however, we can hypothesize that features detected by the magnetometer are walls while those detected by the GPR are trenches.

4.4.2.2 St. Mark's

All gradiometry data for St. Mark's was displayed in Google Earth, while only the 100 MHz GPR data were displayed.

4.4.2.2.1 Magnetic Data

Uninterpreted magnetic data were accurately georeferenced in Google Earth using the dGPS coordinates recorded at the site (Figure 4.14). Data collected at St. Mark's show two large, L-shaped structures in the northern portion of the survey area (Figure 4.15). Also shown in the data are some dipoles which appear to be in a deliberate linear pattern. Coordinates for placemarks inserted at the ends and corners of each linear feature were exported as XML files into a spreadsheet program for later use in planning a future excavation.

4.4.2.2.2 GPR Data

Depth of penetration was approximately 1.5 m. The depth slice for the northern part of the survey area is approximately 0.750-0.950 m and the depth slice for the southern part of the survey area is from 0.840-1.040 m (Figure 4.16). GPR data for St. Mark's show different structures than the magnetic data (Figure 4.17). A Microsoft Excel file was created which displays the coordinates of features in the subsurface that were exported from Google Earth.

Figure 4.18 shows both data sets displayed together, with the GPR set to 40% transparency. While all features are considered real, we can hypothesize that those detected by the magnetometer are likely walls or remnants of buildings and that those detected by the GPR are trenches dug for foundations or storage.

4.4.3 Geoarchaeological Maps

While georeferenced images of near-surface geophysical data may be useful to geophysicists, maps that display the locations of subsurface features on the surface (think

earthquake focus versus epicenter) are more useful to archaeologists. Using these maps, archaeologists can create or alter excavation plans as needed to allow for a more productive field season. Feature maps were created of Dreamer's Bay (Figure 4.19) and St. Mark's (Figure 4.20) by simply turning off the data overlay layer.

Unfortunately, with the Cyprus data set, we had no ground truth information, due to permit restrictions, and thus we could not calculate the error in our interpretations as we had done with the data collected at the B4 Plot. The interpretations drawn on each satellite photo take into account all the errors described in Section 2.5 (reference Tables 2.1 and 2.2). The peak value of the magnetometer data is approximately 45 nT, and as the error of the instrument is ± 0.1 nT, amplitude error is not a concern for these particular data sets. When making interpretations in the GPR data, features are typically mapped between a high amplitude and low amplitude region in the data (this would denote a change in the electromagnetic properties of the subsurface, indicating either a 'boundary' had been crossed or the detection of an anomaly), thus signal error is not a factor.

Using the B4 study as a proxy, we select the in-line error associated with the magnetometer is approximately equal to $0.075 \text{ m} \pm 1.36 \text{ m}$ and cross-line error as approximately $0.28 \text{ m} \pm 1.47 \text{ m}$, while those values for the GPR data are approximately equal to $0.0038 \text{ m} \pm 1.08 \text{ m}$ and $-0.22 \text{ m} \pm 1.66 \text{ m}$, respectively. Using these values, we would recommend to archaeologists that they would set up their 5 m by 5 m square so that any features would be roughly 1.0 m away from the boundaries of the excavation area.

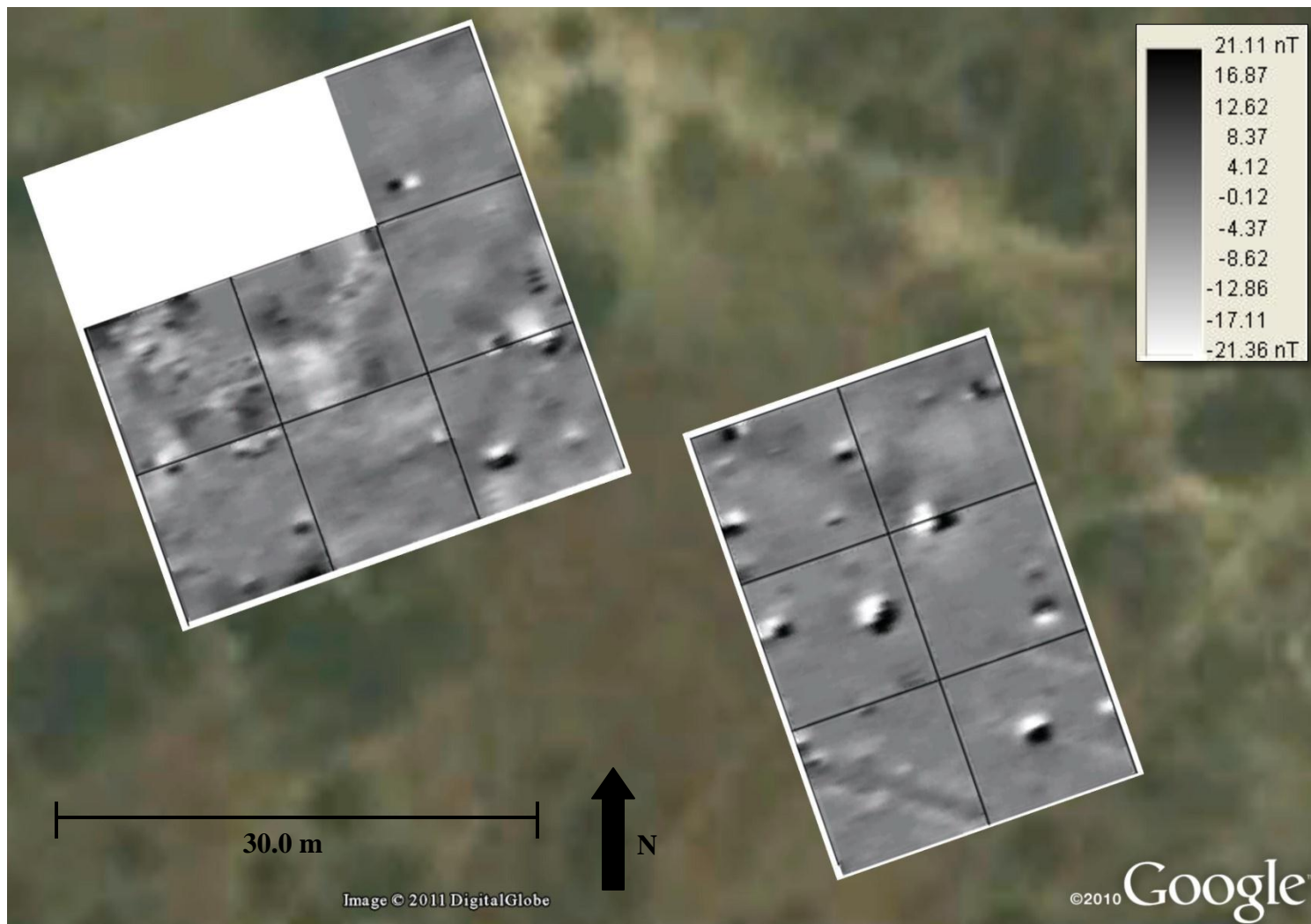


Figure 4.14. Uninterpreted magnetic gradiometry data collected at St. Mark's. Data were accurately georeferenced using GPR coordinates taken after surveying. Features are interpreted to be the light grey, linear areas which appear in the data. Each square represents a minor grid and is 10 m by 10 m.

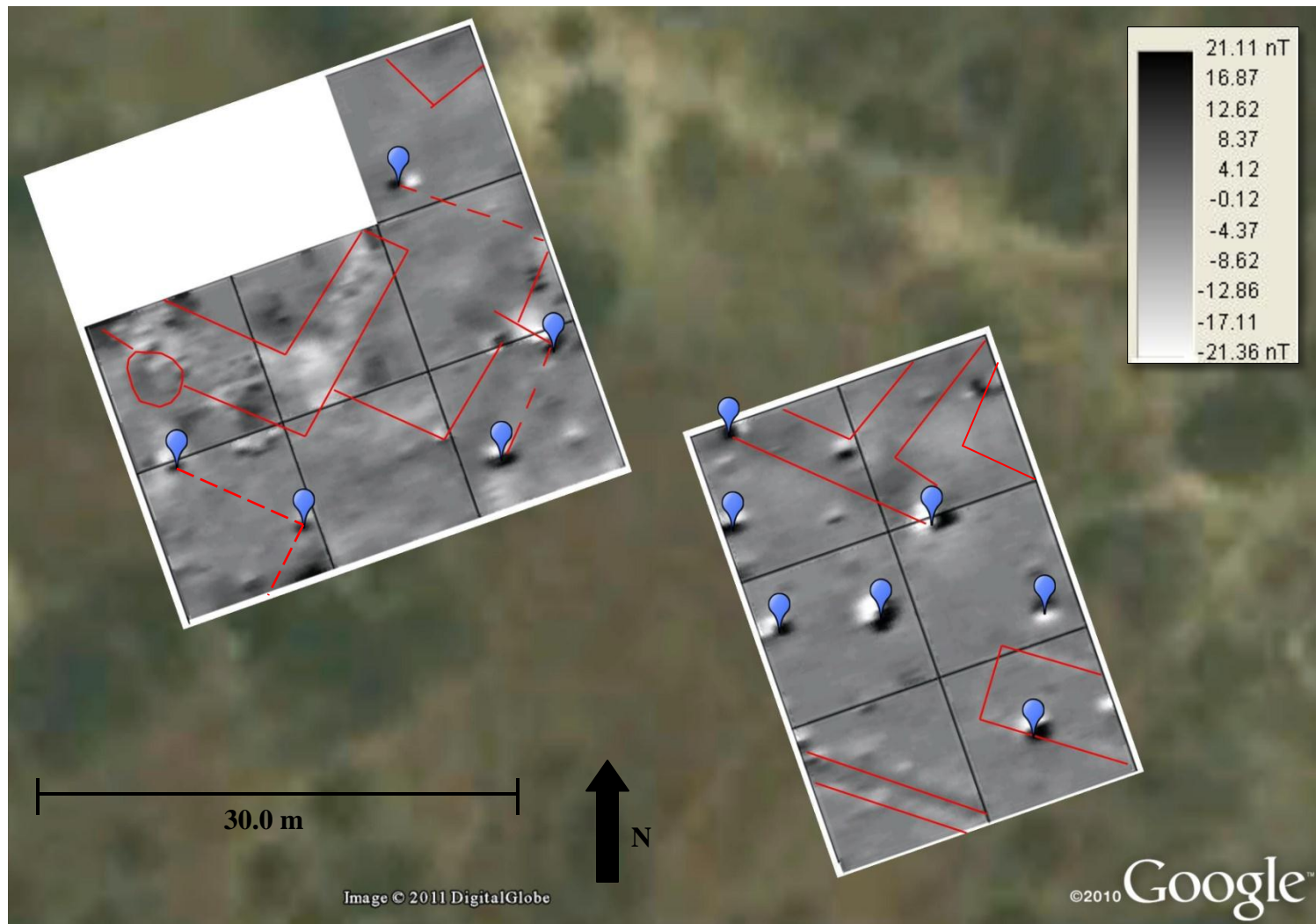


Figure 4.15. Interpreted magnetic data collected at St. Mark's. Interpretations were added with both the path and the placemark tool. The solid red lines indicate linear, subsurface features and the dashed red lines are more subtle features. Blue placemarks indicate discrete features that are not linear, but appear as dipole anomalies in the data. Each square represents a minor grid and is 10 m by 10 m.

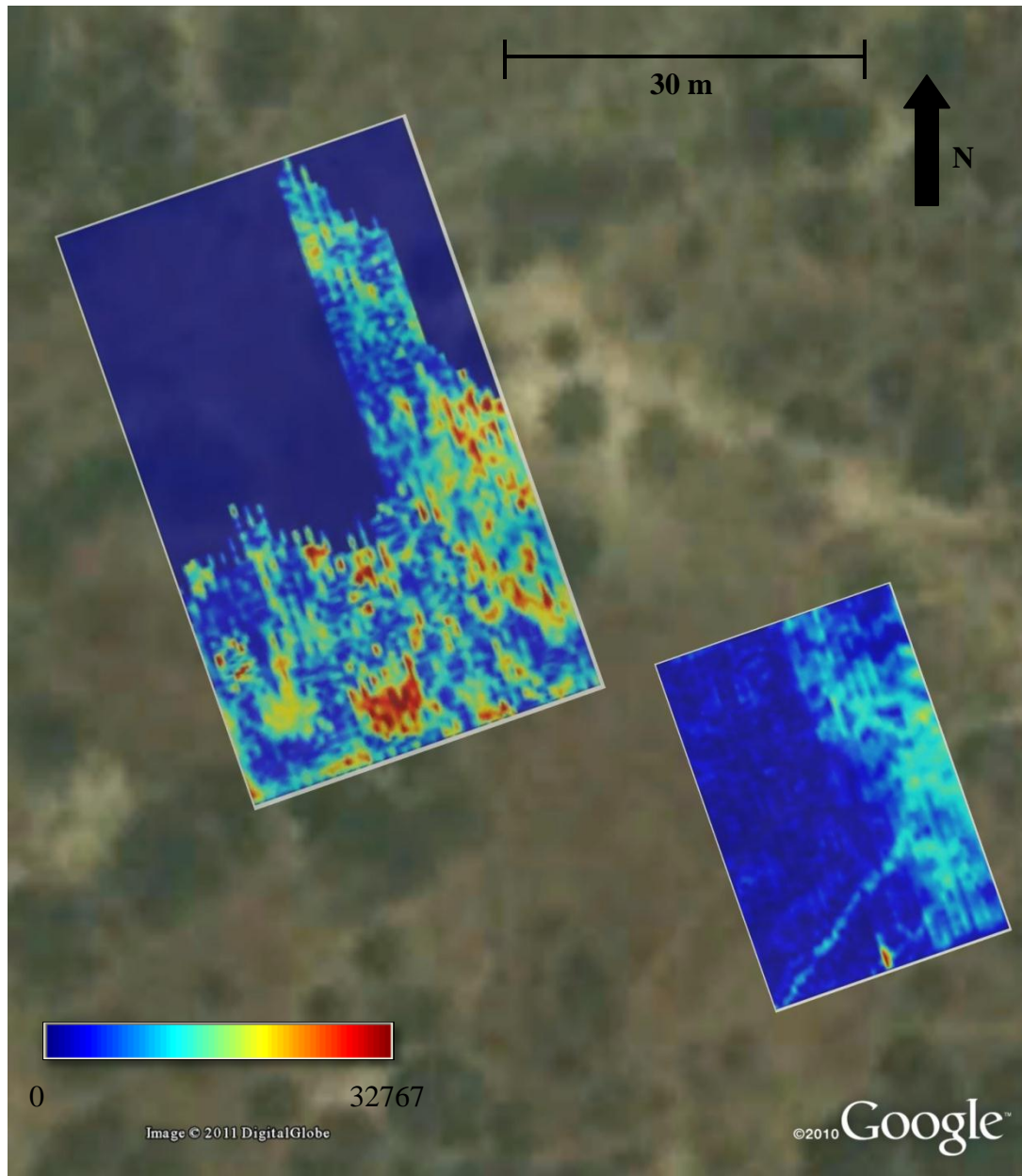


Figure 4.16. GPR data collected with the 100 MHz antenna at St. Mark's. Maximum depth of penetration was 1.5 m.

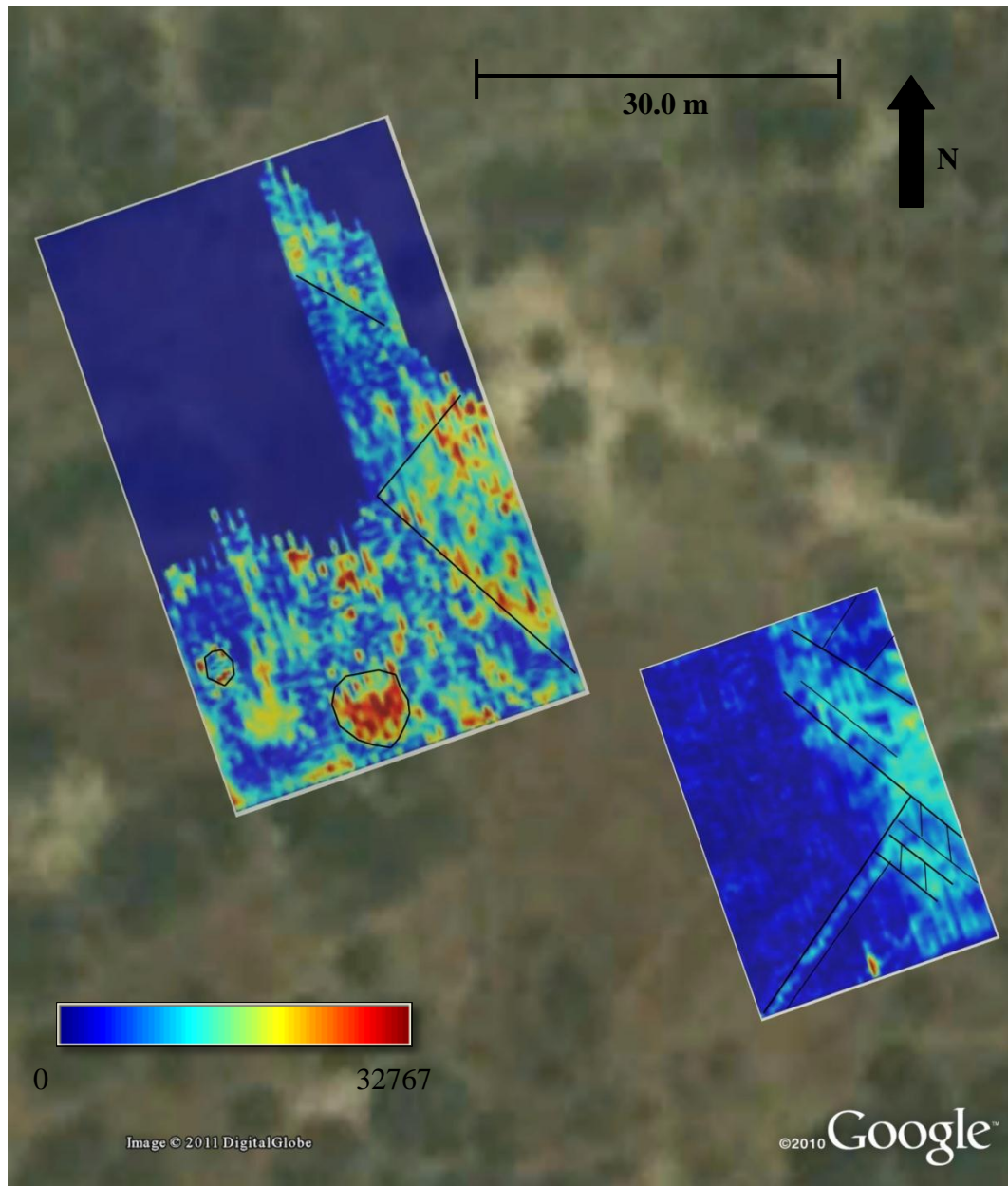


Figure 4.17. Interpreted GPR data for St. Mark's shows fewer subsurface features than the magnetic data. Black lines are interpreted linear features in the subsurface. Thicker lines indicate two linear features which were located very close together. Black circles encompass potential features which are not linear. Depth to features ranges from 0.75 m to 1.0 m.

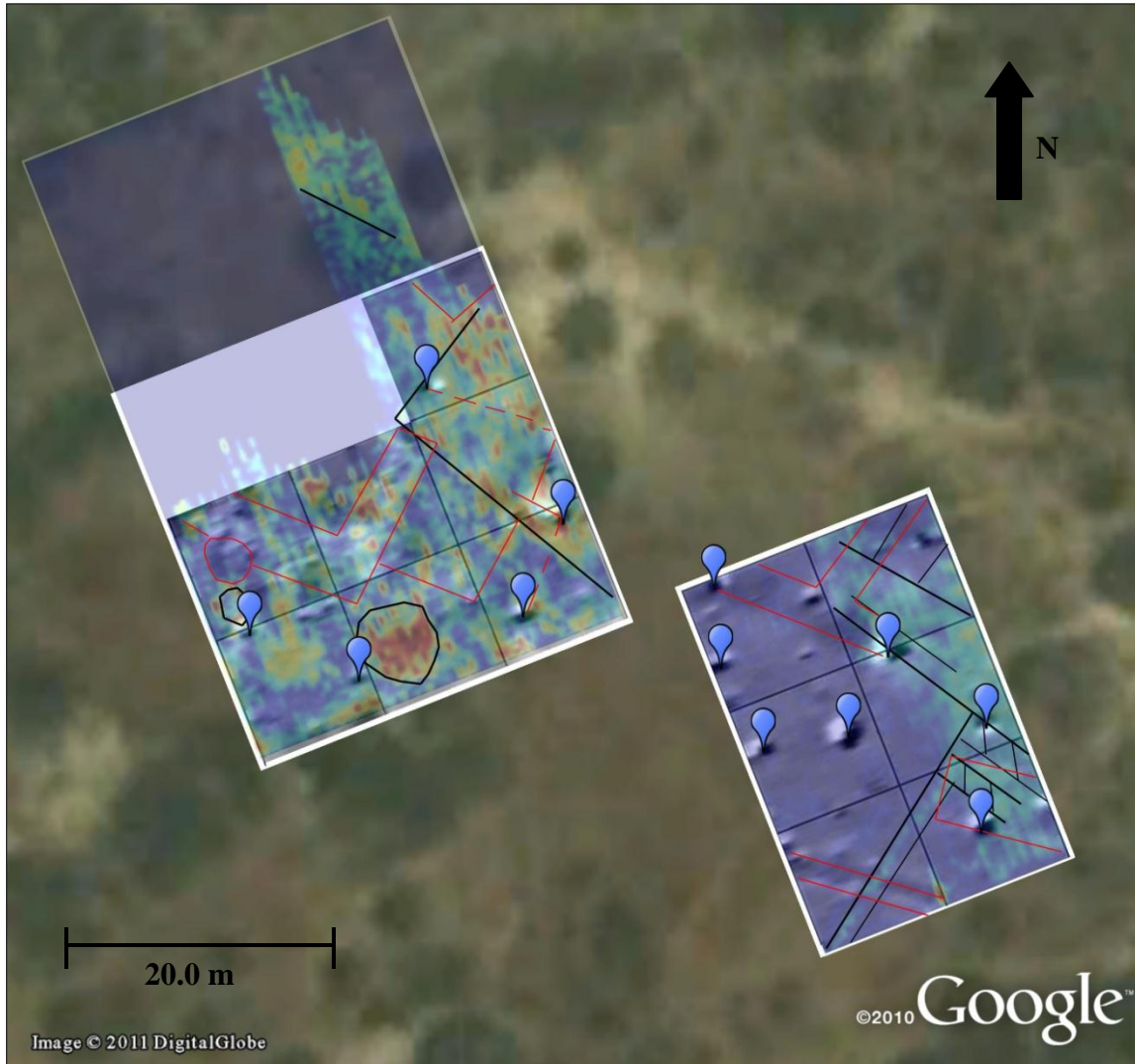


Figure 4.18. Google Earth image displaying the geometry of features found in both data sets. Transparency of the GPR data was set to 40% in order to be able to see both sets of data. All features seen in the data are interpreted to be real, however, we can hypothesize that features detected by the magnetometer are walls while those detected by the GPR are trenches.



Figure 4.19. Map of Dreamer's Bay with subsurface features appearing on the surface. This map is useful to archaeologists in order to develop excavation plans.



Figure 4.20. Map of subsurface features at St. Mark's. This map provides spatial data about features to archaeologists and aids in excavation plans.

4.5 Discussion

To reiterate, Objective II of this research was to identify and mitigate inefficiencies during the process of completing geophysical surveys at active archaeological sites. And Hypothesis II was the effectiveness and efficiency of multi-tool, near-surface geophysical surveys for archaeological applications can be improved by displaying data with accurate dGPS coordinates using a virtual globe. The success of this study was based on the error calculated at the test site, and comparing that with traditional excavation parameters.

Traditionally, geophysical surveys are time-consuming and taxing on both funds and personnel, which has a limiting effect on the lifespan of any geoarchaeological project. Normally, inefficiencies are encountered while in the field and the subsequent processing and interpretation of the data. Once the data are interpreted, they are often passed off to the archaeologist with little to no guidance from the geophysicist, and data manipulation generally requires computer programs which are expensive and difficult to learn. It is this final step of data manipulation that becomes the most draining on resources; thus, we incorporated Google Earth to display near-surface geophysical data and to create a user-friendly data manipulation interface.

An archaeogeophysical analog test study was done at a control site on the University of Tennessee Agricultural Campus in Knoxville, Tennessee where targets had been buried and their locations accurately recorded. This test study was performed in order to test a new data management workflow involving Google Earth. The survey was completed using two different geophysical techniques: ground penetrating radar and magnetic gradiometry.

To create a map, GPS coordinates of the survey area were imported into Google Earth as placemarks and data images were imported as overlays and accurately georeferenced using the

GPS coordinates. Targets were identified in the data, and waypoints for these data points were exported to an Excel file for ease with later manipulation. Error was calculated between the actual data points which were recorded when the targets were buried versus the data points calculated in Google Earth. For the GPR data, the error was calculated to be $0.0038 \text{ m} \pm 1.08 \text{ m}$ (in-line) and $-0.22 \text{ m} \pm 1.66 \text{ m}$ (cross-line) and error in the magnetic data was calculated to be $0.075 \text{ m} \pm 1.36 \text{ m}$ (in-line) and $0.28 \text{ m} \pm 1.47 \text{ m}$ (cross-line). These values fall well within the average size of an archaeologist's excavation square which is typically five meters by five meters.

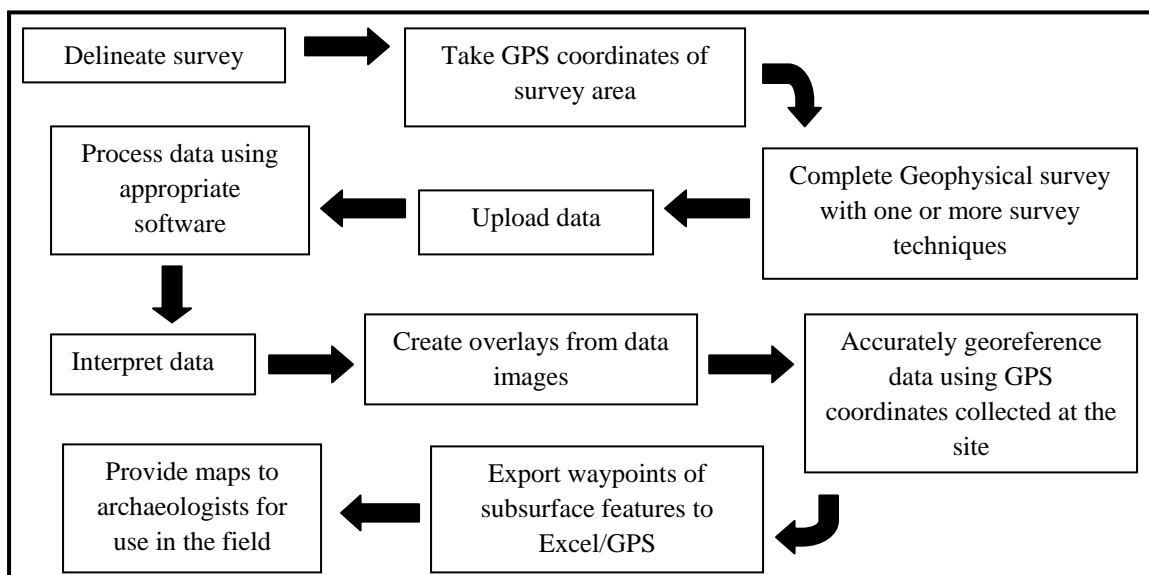


Figure 4.21. Diagram showing the new data management workflow developed at the B4 Plot in Tennessee. The first six steps of the workflow remain unchanged, as the focus of this research was expediting data processing and interpretation. Changes were made to the final steps of the workflow in order to provide archaeologists with a more useful final product.

Given the success of this test study, a new workflow has been developed (Figure 4.21). The main difference lies in the latter half of the workflow, and while there are more steps, they are more efficient at processing data. After data are interpreted, images are created of the subsurface data and are then accurately georeferenced in Google Earth. Waypoints can then be exported from Google Earth into a spreadsheet program (e.g. Microsoft Excel) and subsequently uploaded onto a GPS unit. This entire process can be done in a few hours, once data have been collected, and data are immediately accessible and useful to archaeologists during the time limits of their field season.

This new methodology was tested on data collected on the Akrotiri Peninsula in Cyprus in 2010. During this time, a multi-tool survey was completed using both GPR and magnetic gradiometry. Data were processed upon return to Knoxville, Tennessee and displayed in Google Earth for use in planning future excavations. Using the error calculated from the B4 Plot as a proxy, the geophysicists deemed this exercise a success as waypoints for features could be exported from Google Earth that were within the boundaries of the square size that an archaeologist would use for excavation.

Using Google Earth in this innovative way helps to expedite data processing, cut costs, and shorten the length of time needed for the execution of geoarchaeological surveys. Not only is the program free, but it is easy to use and can provide accurate data to archaeologists in the field. Giving accurate waypoints to archaeologists will enable them to develop a streamlined and potentially less-invasive excavation plan centered on known features in the subsurface.

Acknowledgements

The authors would like to thank the Jones/Bibee Endowment for providing funding for field work in June 2010. Also thanks go to the Geological Society of America and Geometrics for funding to travel to conferences and present this research. The University of Tennessee Near-Surface and Environmental Geophysics Lab provided the equipment and lab space. Thanks also go to Greg Johnston from Sensors & Software for invaluable technical support, Rachel Storniolo and Christian Hunkus for being wonderful field assistants and to Frank Garrod and the WSBA Archaeological Society for allowing us to survey on their turf.

References

- Abdallatif, T., El Emam, A.E., Suh, M., El Hemaly, I.A., Ghazala, H.H., Ibrahim, E.H., Odah, H.H., and Deebes, H.A., 2010, Discovery of the causeway and the mortuary temple of the Pyramid of Amenemhat II using near-surface magnetic investigation, Dahshour, Giza, Egypt: *Geophysical Prospecting*, **58**, 307-320.
- Ault, B.A., and Leonard, J.R., 2009, The Akrotiri-Dreamer's Bay Ancient Port Project: Ancient Kourias Found?: In Press.
- Baker, G.S., and Ambrose, H.M., 2007, Ground penetrating radar imaging of a 4th Century Roman Fort, Humayma, Jordan, 4th International Workshop on Advanced Ground Penetrating Radar, 54-59.
- Baker, G.S., Jordan, T.E., and Talley, J., 2007, An introduction to ground penetrating radar (GPR), in Baker, G.S., and Jol, H.M., ed., *Stratigraphic Analyses Using GPR: Geological Society of America Special Paper 432*, 1-18.
- Chianese, D., Lapenna, V., Di Salvia, S., Perrone, A., and Rizzo, E., 2010, Joint geophysical measurements to investigate the Rossano of Vaglio archaeological site (Basilicata Region, Southern Italy): *Journal of Archaeological Science*, **37**, 2237-2244.
- D.W. Consulting, 2010, *ArcheoSurveyor User Manual*: DW Consulting.
- Heywood, H.C., 1982, The Archaeological Remains of the Akrotiri Peninsula, in Swiny, H.W., ed., *An Archaeological Guide to the Ancient Kourion Area and the Akrotiri Peninsula*: Nicosia, Department of Antiquities, Cyprus.
- Kamei, H., Atya, M.A., Abdallatif, T.F., Mori, M., and Hemthavy, P., 2002, Ground-penetrating radar and magnetic survey to the west of Al-Zayyan Temple, Kharga Oasis, Al-Wadi Al-Jadeed (New Valley), Egypt: *Archaeological Prospection*, **9**, 93-104.
- Werneck, J., 2009, *The KML Handbook*: Addison-Wesley.
- Wilbourn, D., 2011, *DW Consulting: Geophysical Data Services*: DW Consulting.
- Wynn, J.C., 1986, A review of geophysical methods used in archaeology: *Geoarchaeology: An International Journal*, **1**, 245-257.

5. Conclusions

Objective I from the first part of this research is to perform the first geophysical survey at an active archaeological region in Cyprus and in doing so, determine which geophysical techniques are best suited for surveying in the area. Hypothesis I is near-surface geophysical methods can be used successfully to locate previously unmapped subsurface features at archaeological sites in Cyprus. Objective II of this research is to develop a workflow using a GIS to improve data processing and interpretation and to provide archaeologists with near real-time feedback about subsurface feature locations. Hypothesis II is the effectiveness and efficiency of multi-tool, near-surface geophysical surveys for archaeological applications can be improved by displaying data with accurate dGPS coordinates using a virtual globe. It is this last objective which is the more important to this research, because providing interpreted data to an archaeologist in a timely manner can lead to the creation of targeted excavation plans and consequently, preservation of more site area.

Data from Cyprus took approximately three months to process, interpret and input into a final report for the Cypriot Department of Antiquities as it was necessary to test many different software packages in order to find the best one to use for sharing and displaying the data. These months fell well outside of our given field season time, but during this time a new data management workflow was created in order to expedite the flow of data from geophysicist to archaeologist.

The test at the B4 Plot was meant to time the efficiency of Google Earth and to prove its effectiveness in archaeological investigations. Data collection at the site took approximately seven hours, and an additional four hours were needed to upload data, process them, and display them in Google Earth. GPS coordinates were then immediately downloaded from Google Earth and uploaded to a GPS for immediate usage. Using this timing as a proxy and assuming a

mathematical linear relationship, it would have taken approximately 5.3 days to collect, process, and interpret the data collected in Cyprus (assume a 12 hour field day, and usage of only two geophysical techniques). If data at the B4 Plot had been collected and processed in the same fashion as they were in Cyprus (i.e. the old workflow), it would have taken just under two months. The benefit of this ‘rapid-fire’ data processing is that relevant information can be sent off to an archaeologist a few hours after data were collected to use the next day in the field.

In Classical archaeology (Ancient Roman, Greek, and Egyptian) excavations typically take a long time to be approved, and archaeologists must be able to provide a concise excavation plan. And at the sites in Cyprus, this information is of particular importance as the site is located on British Sovereign Territory. The geophysics team was able to provide strong evidence of an abundance of subsurface features at the site, and this evidence will improve the likelihood of obtaining future excavation plans.

The broader implications of this research are that, by using Google Earth, scientists can save funds by using software that is free and save valuable time during their field season. This new workflow also allows for ‘rapid-fire’ collaboration between archaeologist and geophysicist so that data can be used in the more beneficial way possible. The accuracy of the real-time results will also help to preserve more of the site area by providing information for the development of targeted excavation plans. And most importantly, the new workflow will enable archaeologists to modify excavation plans during a field season which will allow them to focus on areas of interest where subsurface features have been found by geophysical techniques.

List of References

- Abdallatif, T., El Emam, A.E., Suh, M., El Hemaly, I.A., Ghazala, H.H., Ibrahim, E.H., Odah, H.H., and Deebes, H.A., 2010, Discovery of the causeway and the mortuary temple of the Pyramid of Amenemhat II using near-surface magnetic investigation, Dahshour, Giza, Egypt: *Geophysical Prospecting*, **58**, 307-320.
- Ambrose, H.M., 2005, Quantitative Integration And Three-dimensional Visualization of Multi-tool Archaeological Geophysics Surveys: M.S. Thesis, The State University of New York at Buffalo.
- Ault, B.A., and Leonard, J.R., 2009, The Akrotiri-Dreamer's Bay Ancient Port Project: Ancient Kourias Found?: In Press.
- Baker, G.S., and Ambrose, H.M., 2007, Ground penetrating radar imaging of a 4th Century Roman Fort, Humayma, Jordan, 4th International Workshop on Advanced GroundPenetrating Radar, 54-59.
- Baker, G.S., Jordan, T.E., and Talley, J., 2007, An introduction to ground penetrating radar (GPR), in Baker, G.S., and Jol, H.M., ed., *Stratigraphic Analyses Using GPR: Geological Society of America Special Paper 432*, 1-18.
- Bartington, Inc., 2009, Bartington Instruments: Magnetic Gradiometers, <http://www.bartington.com>, accessed October 24, 2010.
- Beck, A., 2006, Google Earth and World Wind; remote sensing for the masses?: *Antiquity*, **80**.
- Bonomo, N., Cedrina, L., Osella, A., and Ratto, N., 2009, GPR prospecting in a prehispanic village, NW Argentina: *Journal of Applied Geophysics*, **67**, 80-87.
- Breiner, S., 1999, *Applications Manual for Portable Magnetometers*: San Jose, Geometrics.
- Butler, D., 2006, Virtual globes: The web-wide world: *Nature*, **439**, 776-778.
- Chang, A.Y., M.E. Parrales, J. Jimenez, M.E. Sobieszczyk, S.M. Hammer, D.J. Copenhaver, and R.P. Kulkarni, 2009, Combining Google Earth and GIS mapping technologies in a dengue surveillance system for developing countries: *International Journal of Health Geographics*, **8**, 49-60.
- Chianese, D., Lapenna, V., Di Salvia, S., Perrone, A., and Rizzo, E., 2010, Joint geophysical measurements to investigate the Rossano of Vaglio archaeological site (Basilicata Region, Southern Italy): *Journal of Archaeological Science*, **37**, 2237-2244.
- Conyers, Lawrence B., 2004, *Ground-Penetrating Radar for Archaeology*: AltaMira Press.
- De Paor, D.G., and Whitmeyer, S.J., 2011, Geological and geophysical modeling on virtual globes using KML, COLLADA, and Javascript: *Computers & Geosciences*, **37**, 100-110.

- DW Consulting, 2010, ArcheoSurveyor User Manual: DW Consulting.
- Grasmueck, M., Weger, R., and Horstmeyer, H., 2004, Three-dimensional ground-penetrating radar imaging of sedimentary structures, fractures and archaeological features at submeter resolution: *Geology*, **32**, 933-936.
- Hansen, R.O., L. Racic, and V.J.S. Grauch, 2005, Magnetic Methods in Near-Surface Geophysics, *in* Butler, D.K., ed., *Near-Surface Geophysics*: Tulsa, Society of Exploration Geophysics.
- Hesse, A., 1999, Multi-parametric survey for archaeology: how and why, or how and why not?: *Journal of Applied Geophysics*, **41**, 157-168.
- Heywood, H.C., 1982, The Archaeological Remains of the Akrotiri Peninsula, *in* Swiny, H.W., ed., *An Archaeological Guide to the Ancient Kourion Area and the Akrotiri Peninsula*: Nicosia, Department of Antiquities, Cyprus.
- Kamei, H., Atya, M.A., Abdallatif, T.F., Mori, M., and Hemthavy, P., 2002, Ground-penetrating radar and magnetic survey to the west of Al-Zayyan Temple, Kharga Oasis, Al-Wadi Al-Jadeed (New Valley), Egypt: *Archaeological Prospection*, **9**, 93-104.
- Karastathis, V.K., Papamarinopoulos, S., and Jones, R.E., 2001, 2-D velocity structure of the buried ancient canal of Xerxes: an application of seismic methods in archaeology: *Journal of Applied Geophysics*, **47**, 29-43.
- Kearey, P., Michael Brooks and Ian Hill, 2002, *An Introduction to Geophysical Exploration*: Blackwell Publishing.
- Knight, R.J., and Endres, Anthony L., 2005, An Introduction to Rock Physics Principles for Near-Surface Geophysics, *in* Butler, D.K., ed., *Near-Surface Geophysics*: Society of Exploration Geophysicists.
- Lisle, R.J., 2006, Google Earth: a new geological resource: *Geology Today*, **22**, 29-32.
- Lo, C.P., and A.K.W. Yeung, 2006, *Concepts and Techniques of Geographic Information Systems*: Prentice Hall.
- Odah, H., Abdallatif, T.F., El-Hemaly, I.A., and El-All, E.A., 2005, Gradiometer survey to locate the ancient remains distributed to the northeast of the Zoser Pyramid, Saqqara, Giza, Egypt: *Archaeological Prospection*, **12**, 61-68.
- Piro, S., Mauriello, P., and Cammarano, F., 2000, Quantitative integration of geophysical methods for archaeological prospection: *Archaeological Prospection*, **7**, 203-213.

- Potere, D., 2008, Horizontal Positional Accuracy of Google Earth's High-Resolution Imagery Archive: *Sensors*, **8**, 7973-7981.
- Reynolds, J.M., 1997, *An Introduction to Applied and Environmental Geophysics*: John Wiley & Sons.
- Rogers, M.B., K. Faehndrich, B. Roth, and G. Shear, 2010, Cesium magnetometer surveys at a Pithouse Site near Silver City, New Mexico: *Journal of Archaeological Science*, **37**, 1102-1109.
- Sandweiss, D.H., Kelley, A.R., Belknap, D.F., Kelley, J.T., Rademaker, K., and Reid, D.A., 2010, GPR identification of an early monument at Los Morteros in the Peruvian coastal desert: *Quaternary Research*, **73**, 439-448.
- Sheppard, S.R.J., and Cizek, P., 2009, The ethics of Google Earth: Crossing thresholds from spatial data to landscape visualisation: *Journal of Environmental Management*, **90**, 2102-2117.
- Solsten, E., 1993, *Cyprus: a country study*: Washington D.C., Department of the Army.
- Sternberg, B.K., and McGill, J.W., 1995, Archaeology studies in southern Arizona using ground penetrating radar: *Journal of Applied Geophysics*, **33**, 209-225.
- Trimble navigation Limited., 2011, OmniStar, <http://www.omnistar.com>, accessed August 23, 2011.
- Wernecke, J., 2009, *The KML Handbook*: Addison-Wesley.
- Wilbourn, D., 2011, *DW Consulting: Geophysical Data Services*: DW Consulting.
- Wright, T.E., Burton, M., Pyle, D.M., and Caltabiano, T., 2009, Visualising volcanic gas plumes with virtual globes: *Computers & Geosciences*, **35**, 1837-1842.
- Wynn, J.C., 1986, A review of geophysical methods used in archaeology: *Geoarchaeology: An International Journal*, **1**, 245-257.
- Yalçiner, C.Ç., Bano, M., Kadioglu, M., Karabacak, V., Meghraoui, M., and Altunel, E., 2009, New temple discovery at the archaeological site of Nysa (western Turkey) using GPR method: *Journal of Archaeological Science*, **36**, 1680-1689.

Appendix A

Additional GPR data slices collected from the Dreamer's Bay and St. Mark's sites

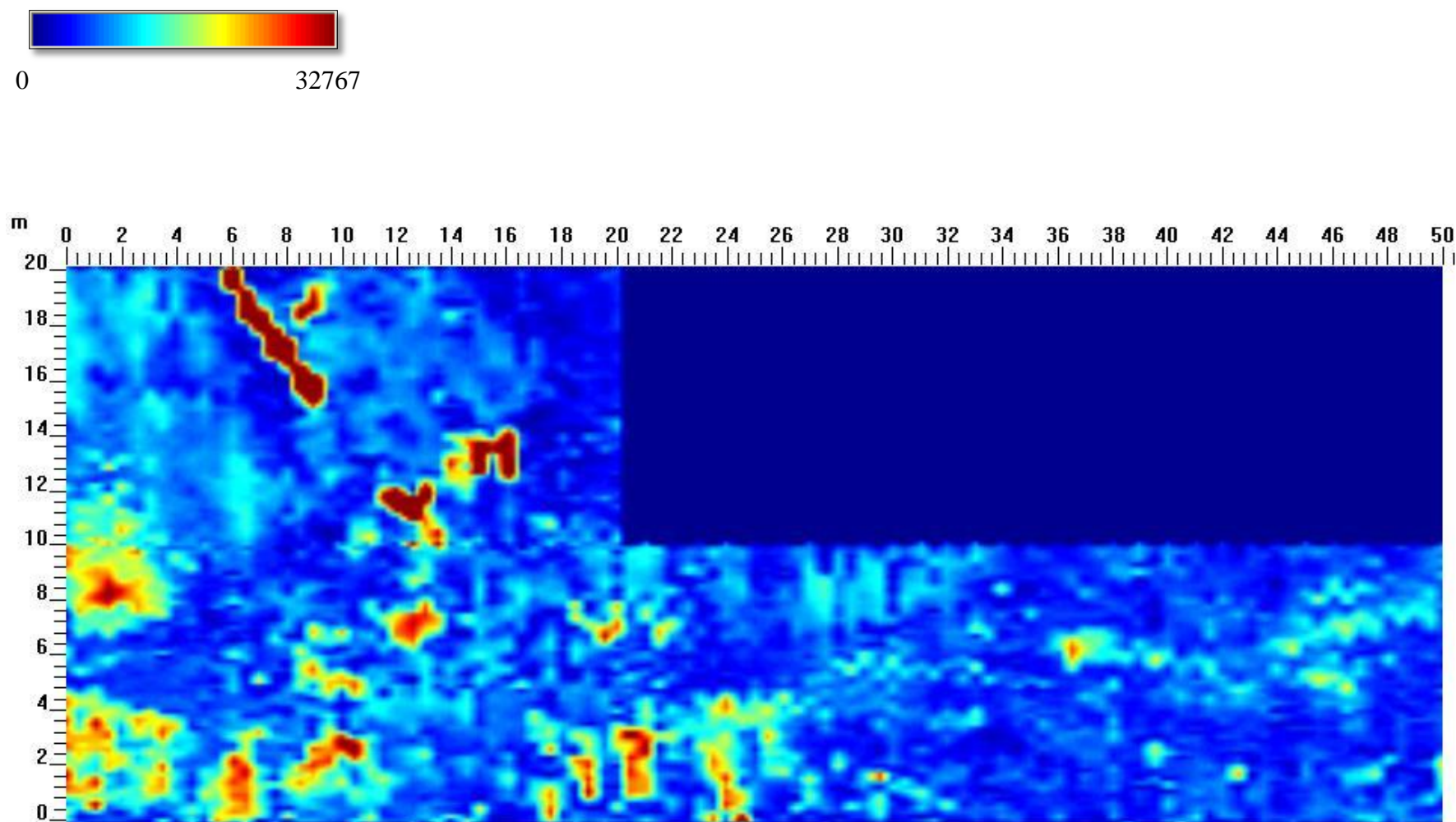
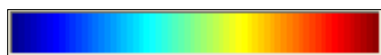


Figure A-1. Additional GPR data collected at Dreamer's Bay with the 200 MHz antenna. The depth of this slice is from 0.100 to 0.225 m and velocity was calculated to be 0.060 m/ns and the slicing interval was 0.1515 m. The dark red, linear feature in the northern part of the data is a man-made historic rail that was used to wheel artillery onto a cement pad during World War II.



0 32767

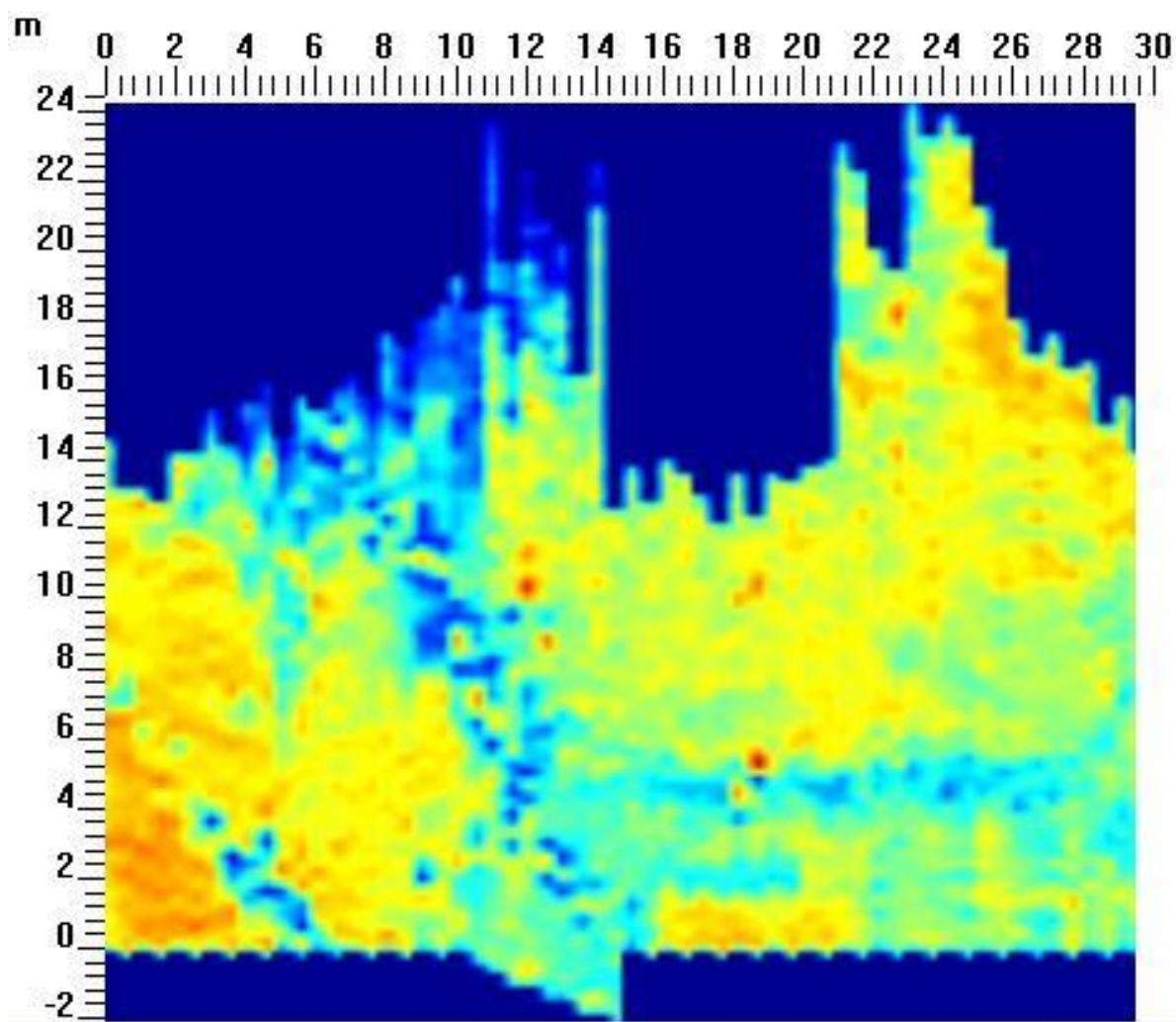


Figure A-2. GPR data collected at Dreamer's Bay with the 100 MHz antenna in the northern part of the survey area. This data slice represents a depth from 0.250 to 0.500 m. The picked velocity was 0.07 m/ns and the slice interval was 0.200 m. No discernable features were interpreted in this data set.

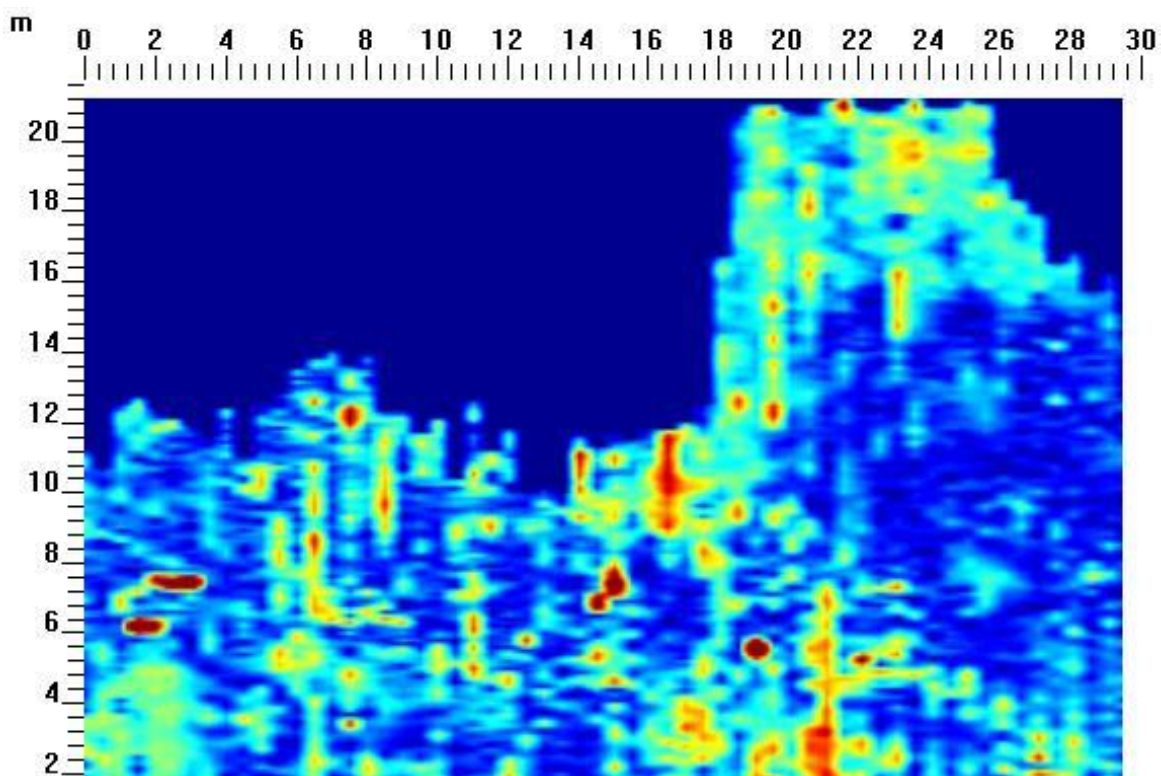
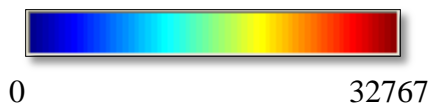


Figure A-3. GPR data collected with the 200 MHz antenna in the northern portion of St. Mark's. This slice represents a depth of 2.600 to 2.700 m and velocity was calculated to be 0.150 m/ns and the slice interval was set to 0.100 for the maximum resolution. No features were able to be interpreted in this data.

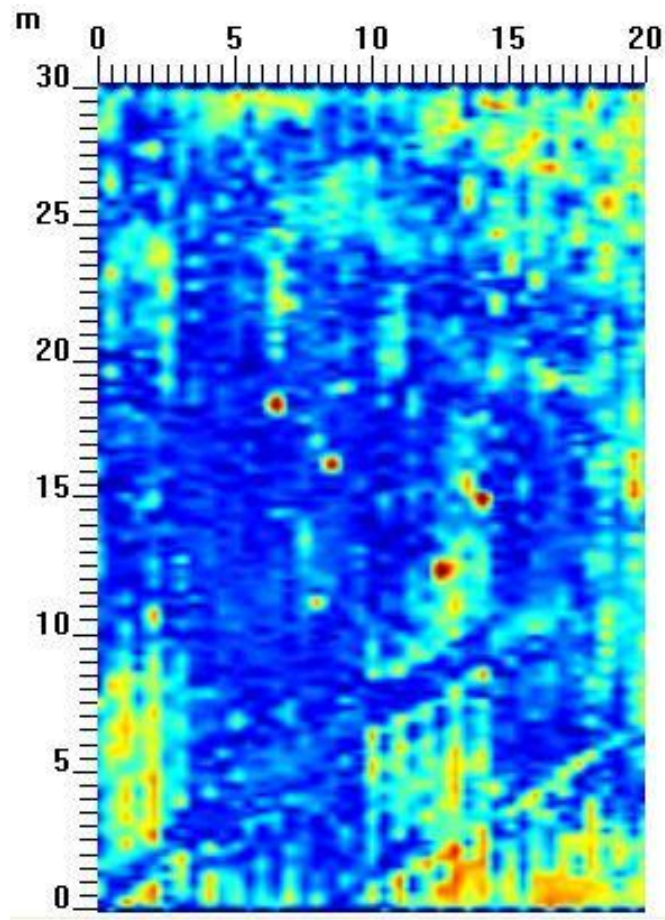


Figure A-4. GPR data collected with the 200 MHz antenna in the southern portion of the survey area in St. Mark's. The depth slice for these data is from 0.630 to 0.730 m. The picked velocity for the data was 0.300 m/ns and the depth slice interval was 0.1449 m.

Vita

Caitlyn Williams was born in Akron, OH, to the parents of Keith and Kelly Williams. She was exposed to science at an early age, and after high school attended the University of Wyoming in Laramie, Wyoming and majored in geology with a minor in Spanish. After graduating with her B.S. in 2008, she worked for UR-Energy USA for a year, before returning to school at the University of Tennessee to pursue a Master's degree in near-surface geophysics with Dr. Gregory S. Baker. She was lucky to have a project that appealed both to her geologic interests and her interest in archaeology. After graduation, she plans on continuing to be a geologist/knitter/beer snob at an undisclosed location.